Proficiency and mechanisms of perturbation of mature T-cell homeostasis by the TCL1 family of oncogenes

Inaugural-Dissertation

zur

Erlangung des Doktorgrades

der Mathematisch-Naturwissenschaftlichen Fakultät

der Universität zu Köln

vorgelegt von

Kathrin Warner

aus Düsseldorf

Köln, 2016

Berichterstatter: Prof. Dr. Jens Brüning

                      Prof. Dr. Björn Schumacher

Tag der mündlichen Prüfung: 18.01.2016

Table of Contents

List of Figures

List of Tables

Zusammenfassung

Die Gene der T-cell leukemia/lymphoma 1 (TCL1) Familie wurden erstmals aufgrund ihrer Beteiligung an spezifischen Chromosomenaberrationen in reifen T-Zell-Erkrankungen identifiziert. Bei Menschen besteht diese Familie aus den drei Genen TCL1A, MTCP1 und TCL1B (auch TML1 genannt). Normalerweise werden diese Gene in Lymphozyten während der frühen B- und T-Zell Entwicklung und während der frühen Embryogenese exprimiert. Überexpression von TCL1A wird in vielen reifen B-Zell- und T-Zell-Tumoren detektiert, einschließlich der chronisch lymphatischen Leukämie (CLL) und der T-Zell Prolymphozyten-Leukämie (T-PLL). Expression von TCL1A oder MTCP1 in T Zellen transgener Mäuse führt zur Entwicklung T-PLL-ähnlicher Erkrankungen nach einer langen Latenzzeit (>15 Monate). In diesen Untersuchungen wurden zwei unterschiedliche Promotoren für die T-Zell-spezifische Expression verwendet, die keinen direkten Vergleich dieser zwei Onkogene zulassen. Studien zum Transformationspotenzial von TML1 wurden bislang nicht veröffentlicht. Im ersten Teil dieser Arbeit wurde deshalb das onkogene Potenzial der TCL1 Gene verglichen, indem gamma-retrovirale Vektoren für humanes TCL1A, MTCP1 und TML1 in hämatopoetische Stammzellen/hämatopoetische Vorläuferzellen (HSC/HPC) von Wildtyp-Mäusen eingebracht und in Wildtyp-Empfänger transplantiert wurden. TCL1A und MTCP1 Empfängermäuse entwickelten überwiegend B-Zell-Tumore nach einer medianen Überlebenszeit von 388 Tagen, beziehungsweise 394 Tagen. Somit beweisen diese Daten, dass TCL1A und MTCP1 Onkogene mit vergleichbarem onkogenen Potenzial sind und zeigen zum ersten Mal, dass MTCP1 nicht nur ein T-Zell-Onkogen ist, sondern auch in der Lage ist, B Zellen zu transformieren. Das dritte Familienmitglied TML1 induzierte die Entwicklung von unreifen T-Zell-Malignitäten in wenigen Mäusen. Obwohl TML1 ein schwächeres Onkogen zu sein scheint, liefert diese Studie erste Hinweise für dessen onkogene Funktion. Jedoch besteht in diesem Modell das Risiko der Insertionsmutagenese, die möglicherweise zur Induktion oder Beschleunigung der Tumorentwicklung beigetragen hat.

Untersuchungen zur molekularen Funktion haben gezeigt, dass die Stimulierung des Antigenrezeptors (TCR) die Interaktion zwischen TCL1A und der Ser/Thr-Kinase AKT an der Zellmembran induziert, gefolgt von einer Kerntranslokalisation. Darauffolgende Studien zeigten, dass TCL1A auch mit anderen Signalmolekülen im Cytosol (p300, ATM) und im Kern (Jun, Fos) interagierte. Zusammen implizieren diese Daten, dass TCL1A Kompartiment-spezifische Funktionen hat. Aus diesem Grund wurde das

Transformationspotenzial von zwei Kompartiment-spezifischen TCL1A Varianten in dem zuvor beschriebenen Transplantationsmodell untersucht, indem eine myristoylierte (Membran-lokalisierende) Variante (myr-TCL1A) und eine Kern-lokalisierende Variante (nls-TCL1A) retroviral in HSC/HPC von Mäusen eingebracht wurden. Empfängermäuse von myr-TCL1A und nls-TCL1A transduzierten HSC/HPC entwickelten überwiegend B-Zell-Tumore nach einer medianen Überlebenszeit von 360 Tagen beziehungsweise 349 Tagen. Demnach zeigte sich eine signifikant kürzere Latenzzeit für nls-TCL1A im Vergleich zum zuvor beschriebenen generischen TCL1A. Die Genexpressionsanalyse dieser Tumore offenbarte größere Ähnlichkeiten zwischen den Expressionsprofilen von Tumoren, die durch TCL1A und nls-TCL1A induziert wurden. Zusammen implizieren diese Daten, dass die überwiegend onkogene Funktion von TCL1A auf dessen Vorkommen im Kern beruhen könnte.

Aufbauend auf publizierten in vitro Studien, die beschreiben, dass TCL1 die TCR-Signalisierung verstärkt (z.B. via AKT), wurde im zweiten Teil dieser Arbeit untersucht, ob und wie sich TCR Stimulation auf das Transformationspotenzial von TCL1A auswirkt. Hierfür wurden reife OT-1 T Zellen, dessen monoklonaler TCR spezifisch Ovalbumin (OVA) erkennt, retroviral mit TCL1A und seinen myr/nls Varianten transduziert und wiederholt in vivo mit OVA-Peptide stimuliert. TCR stimulierte Empfängermäuse von TCL1A transduzierten T Zellen zeigten eine signifikante Beschleunigung der Leukämie-Entwicklung und eine verringerte mediane Überlebenszeit von 305 Tagen im Vergleich zu unstimulierten TCL1A Empfängern (417 Tage). Stimulierte und unstimulierte Empfängermäuse zeigten vergleichbare Unterschiede in der Überlebenszeit für die Kompartiment-spezifischen TCL1A Varianten und seine generische Form. Diese Daten implizieren eine pro-leukämogene Zusammenarbeit von TCL1A und TCR Signalen, die möglicherweise in zukünftigen Therapiekonzepten berücksichtigt werden kann.

Abstract

The members of the T-cell leukemia/lymphoma 1 (TCL1) gene family were first identified through their involvement in specific chromosomal aberrations in mature T-cell malignancies. In humans this family consists of 3 genes: TCL1A, MTCP1, and TCL1B (also called TML1). Normally, these genes are expressed in lymphocytes during early B- and T-cell development and during initial embryogenesis. Overexpressed TCL1A is found in many mature B-cell and T-cell tumors, including chronic lymphocytic leukemia (CLL) and T-cell prolymphocytic leukemia (T-PLL). Transgenic mice expressing TCL1A or MTCP1 in T cells develop T-PLL-like diseases after a long latency period (>15months). These transgenes employ two different promoters to drive T-cell specific expression, which does not allow a direct comparison of the two oncogenes. Studies on the transforming potential of TML1 have not been published yet. Therefore, in the first part of this thesis, the oncogenic potential of TCL1 genes was comparatively evaluated by using gamma-retroviral vectors to introduce human TCL1A, MTCP1, and TML1 into hematopoietic stem cells/hematopoietic progenitor cells (HSC/HPC) of wild type mice that were transplanted into wild type recipients. TCL1A and MTCP1 recipient mice predominantly developed B-cell malignancies after a median survival of 388 days and 394 days, respectively. The presented data indicates that TCL1A and MTCP1 are oncogenes with comparable oncogenic potential and shows for the first time that MTCP1 is not only a T-cell oncogene, but is able to transform B cells as well. The third family member TML1 induced the development of immature T-cell malignancies in only a few mice. Although TML1 appeared to be a weaker oncogene, this study provides first evidence for its oncogenic function. However, there is a risk for insertional mutagenesis in this model that might have contributed to induction or acceleration of tumor development.

At the level of molecular function, it had been shown that engagement of the antigen receptor (TCR) induces the interaction of TCL1A with the ser/thr kinase AKT, initially at the cell membrane followed by nuclear translocation. Subsequent studies described TCL1A to engage with other signaling molecules in the cytosol (p300, ATM) and in the nucleus (Jun, Fos). Together, these data suggest that TCL1A has compartment-specific functions. Consequently, the transforming potential of compartment-targeted TCL1A variants was evaluated in the above described transplantation model by retroviral expression of a membrane localizing myristoylated (myr-TCL1A) and a nuclear localizing (nls-TCL1A) variant in murine HSC/HPC. Recipients of HSC/HPC transduced with myr-TCL1A and nls-TCL1A predominantly developed B-cell malignancies after a median survival of 360 days

and 349 days, respectively. There was a significantly shorter latency period for nls-TCL1A compared to the previously described generic TCL1A. Gene expression analysis of these tumors revealed higher similarities between expression profiles of tumors induced by TCL1A and nls-TCL1A. Together these data implicate that TCL1A's predominant oncogenic function might rely on its nuclear presence.

Expanding on previously reported in vitro observations of TCL1A to enhance TCR signaling (e.g. via AKT), the second part of this thesis aims to understand if and how TCR stimulation affects the transforming potential of TCL1A. Mature OT-1 T cells carrying monoclonal TCR's that specifically recognize ovalbumin (OVA) were retrovirally transduced with TCL1A and its myr/nls variants and repeatedly stimulated in vivo with OVA-peptides. TCR stimulated recipient mice of TCL1A transduced T cells showed a significantly accelerated leukemic outgrowth and a reduced median survival of 305 days, when compared to unstimulated recipients (417 days). Stimulated vs unstimulated recipient mice showed comparable differences in survival across the compartment-targeted TCL1A variants and its generic form. These data strongly implicate a pro-leukemogenic cooperation of TCL1A and TCR signals that might be actionable in upcoming interventional designs.

1.   Introduction

1.1   T lymphocytes

As part of the adaptive immune system, T lymphocytes are responsible for cell-mediated immune responses. They are able to recognize all kinds of foreign antigens through the expression of a highly variable antigen-receptor: the T-cell receptor (TCR). T cells cannot directly recognize pathogens. Their activation and function relies on other cells that display smaller fragments of processed proteins via a major histocompatibility complex (MHC) molecule. The majority of T cells have a TCR that consists of an α- and β-chain, whereas a minor population expresses γ/δ-TCRs. This thesis is focused on the more common α/β-T cells, which are generally referred to as T cells hereafter.

1.1.1   T-cell development

T lymphocytes originate from hematopoietic stem cells (HSC) in the bone marrow (BM). These stem cells differentiate into myeloid and lymphoid progenitors that give rise to the cellular components of the innate and adaptive immune system. For T-cell development (Figure 1-1), common lymphoid progenitors (CLPs) migrate to the thymus and pass through distinct developmental stages. As these progenitors still lack CD4 and CD8 co-receptor expression, they are referred to as double-negative (DN) thymocytes. Based on the expression of the adhesion molecule CD44 and the IL-2 receptor alpha-subunit CD25, DN thymocytes are subdivided into four stages: DN1 ($CD44^+$, $CD25^-$), DN2 ($CD44^+$, $CD25^+$), DN3 ($CD44^-$, $CD25^+$) and DN4 ($CD44^-$, $CD25^-$) (1). Expression of recombination-activating genes (RAG1 and RAG2) during the DN2 stage initiates rearrangement of the TCR β-chain (2,3). The TCR β-chain is then paired with a pre-Tα-chain to form a pre-TCR at the DN3 stage (4). Only thymocytes that signal through the pre-TCR will be able to transition to the DN4 stage (5). Rearrangement of the TCR α-chain in DN4 thymocytes results in expression of a mature αβ-TCR assembled with CD3/ζ proteins. These cells start to express CD4 and CD8, thereby forming a population of double-positive (DP) thymocytes. At this stage, different selection processes take place that only allow maturation of thymocytes that recognize presented MHC-bound self-peptides (spMHC) at the right strength: death by neglect, negative selection and positive selection.
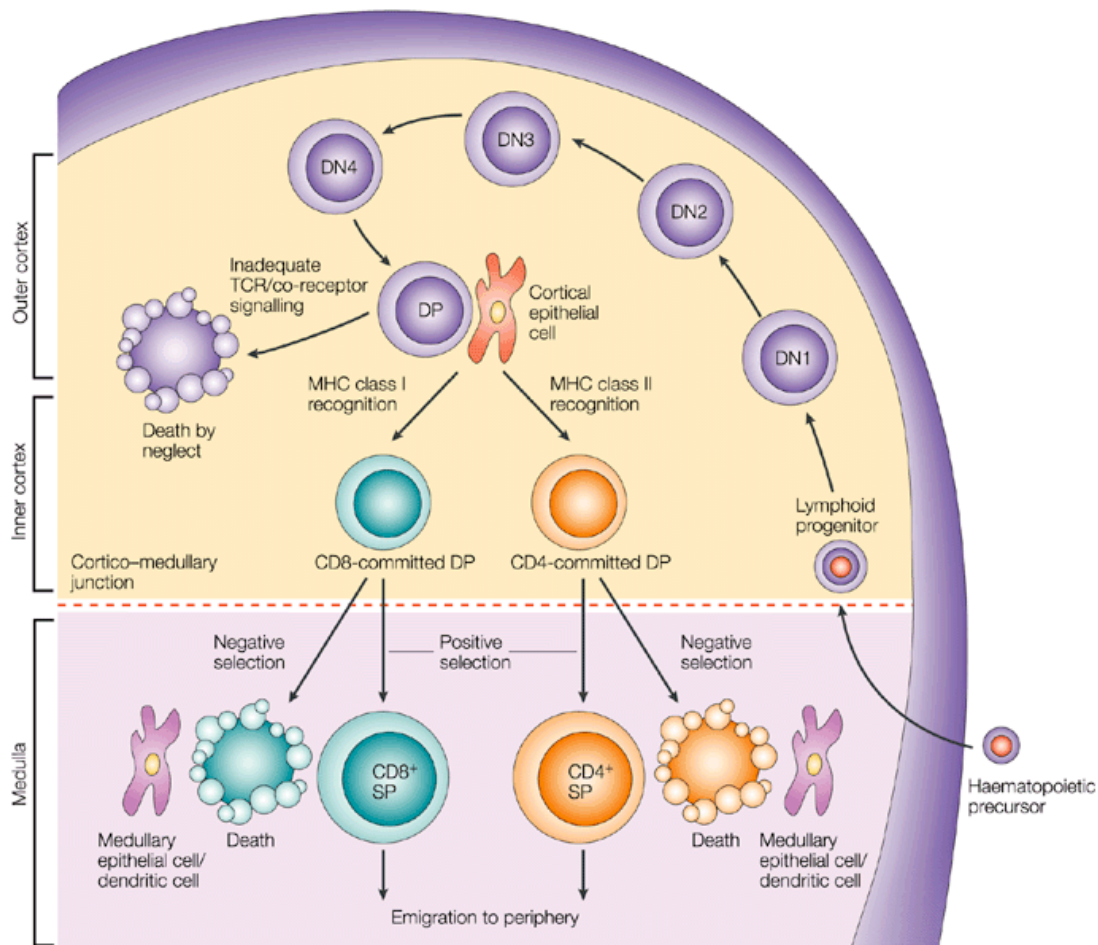
Figure 1-1: T-cell development in the thymus
HSCs give rise to CLPs that migrate to the thymus. There, they go through four different developmental stages as double-negative (CD4⁻/CD8⁻) thymocytes (DN1-4). Successful pre-TCR expression leads to transition into double positive (DP) (CD4⁺/CD8⁺) thymocytes and expression of a fully rearranged TCR. The fate of the DP thymocytes depends on their TCRs' affinity to MHC-bound self-peptides presented by cortical epithelial cells. Cells that bind too weakly will not receive a survival signal and die by neglect. DP thymocytes that interact with MHC class II molecules at the right strength develop into CD4+ cells, whereas an appropriate interaction with MHC class I molecules leads to maturation into CD8+ cells. These cells will receive apoptotic signals, if the interaction with these molecules is too strong. After successful maturation, naïve T cells migrate to the periphery. Adapted from Germain et al (6).

DP thymocytes that fail to interact with MHC-bound ligands will die by neglect, as they do not receive intracellular survival signals. A strong interaction between the TCR and the presented self-peptide on the other hand leads to induction of apoptosis (negative selection), thereby eliminating potentially self-reactive T cells. Only thymocytes that bind to self-peptide at low intensity receive signals that enable further maturation (positive selection). Depending on the recognition of MHC class I or MHC class II molecules, these cells develop into mature CD4 or CD8 single-positive (SP) T cells (7). Upon successful maturation and selection,

mature T cells leave the thymus and enter the peripheral blood to migrate to secondary lymphoid tissues.

1.1.2 T-cell subsets

Various mature T-cell subsets can be distinguished based on their function and expression of cell-surface markers. Co-receptor expression on these cells allows a broad division into two T-cell lineages: CD4 T-helper (Th) cells and cytotoxic CD8 T cells (CTL). CD4 T cells are mainly responsible for activating other immune cells through cytokine release. They recognize peptides presented by MHC class II molecules that are exclusively found on specialized antigen presenting cells (APCs), such as dendritic cells, macrophages and B cells (8). CD8 T cells are capable of killing infected cells and interact with MHC class I peptide complexes that are found on all nucleated cells (8). The functional status divides these lineages further into naïve, effector and memory cells (9). After their development in the thymus, naïve T cells circulate lymphoid tissue to screen for presented antigen. Upon antigen encounter, these cells proliferate and differentiate into effector T cells. Following the resolution of an immune response, most effector T cells die and only a small number of memory T cells remains that can quickly be reactivated at a second encounter with the same antigen (10). These basic functional groups can be distinguished based on specific marker expression. Differential isoform expression of the protein tyrosine phosphatase CD45 allows a general discrimination between naïve (CD45RA$^+$) and effector/memory (CD45RO$^+$) T cells in humans, but not in mice (11,12). In both species, the adhesion molecule CD62L and the chemokine receptor CCR7 are found on naïve and central memory T cells as these homing receptors enable migration within the lymphoid tissue (9). Effector T cells down-regulate these two markers and up-regulate E-selectin ligands, such as CD44, that enable migration to the site of infection (10). In addition, they up-regulate surface expression of CD69 and CD40 ligand (CD40L). The role of CD69 in activated T cells is still unclear. It was thought to act as a co-stimulatory molecule, but more recent studies argue with that perception and suggest roles in negative regulation and T-cell polarization (13). CD40L interacts with CD40 on APCs and induces up-regulation of the co-stimulatory proteins CD80 and CD86. Although the interaction between CD40L and CD40 plays a major role in the effector functions of CD4 T cells to activate APCs, it is also found on CD8 T cells (14). Moreover, activated CD8$^+$ CTLs are characterized by the production of perforin and granzyme (10). These cytolytic

proteins are required for inducing cell death in their target cells. Effector CD4$^+$ Th cells account for a heterogeneous group that can be further subdivided into Th1, Th2, Th9, Th17, Th22, Tfh (follicular Th) and Treg (regulatory T cells) based on their cytokine profile (15). Once an infection is cleared, most activation markers are down-regulated with exception of CD44. Subsequently, two populations of memory T cells remain: central memory (T_{CM}) and effector memory (T_{EM}) T cells. T_{CM} are CCR7+ CD62L+ and CD44+, reside in the lymph node (LN), produce IL-2 and proliferate extensively (13). T_{EM} lack CCR7 and CD62L expression and are found primarily in non-lymphoid tissue (16,17). They are less proliferative than T_{CM} and produce a variety of effector cytokines, such as IL-4, IL-5 and interferon-γ (IFN-γ) (16).

1.1.3   T-cell receptor engagement and signaling

The TCR consists of the two polypeptide chains TCRα and TCRβ. Each cell expresses a unique TCR that is generated during their development in the thymus by rearrangement of TCR gene segments. This process is called V(D)J recombination according to the involved variable (V), diversity (D) and joining (J) gene segments and has the potential to generate >10^{15} different TCRs in mice and >10^{18} TCRs in humans (18). Fully rearranged TCR chains are composed of a constant region and a variable region (Figure 1-2A). Complementarity determining regions (CDRs) within the variable region are primarily responsible for antigen binding. TCR diversity allows recognition of a broad range of different antigens presented by MHC molecules. Typically, MHC class I molecules present protein fragments of endogenous pathogens to CD8 T cells, whereas MHC class II molecules present peptides of exogenous pathogens taken up by APCs to CD4 T cells. However, some APCs are also able to present extracellular antigens via MHC class I molecules through a process called cross-presentation. MHC class I molecules have a closed binding groove and therefore bind short peptides with a length between 8-15 amino acids (19). In contrast, MHC class II molecules have an open binding groove that presents larger peptides with a length between 11-30 amino acids (19). The TCR is expressed on the cell surface in a complex with accessory molecules. In addition to the TCRα- and TCRβ-chain, this complex consists of one CD3γ, one CD3δ and two CD3ε chains, as well as one intracytoplasmic ζ homodimer (Figure 1-2B) (20).

Activation of naïve T cells requires two signals provided by APCs: a foreign antigen bound to a MHC molecule (signal one) and a co-stimulatory protein (CD80 or CD86) (signal two) (18). Signal one is recognized by the TCR and signal two by the co-receptor CD28 on T cells. Absence of either one of these signals leads to apoptosis or a state of anergy (18). In addition, the co-receptor CD4 or CD8 stabilizes the interaction between the TCR and MHC complex by binding to the respective MHC class (Figure 1-2B).

A

α chain   β chain

carbohydrate

variable region (V)

constant region (C)

hinge (H)

transmembrane region

cytoplasmic tail

disulfide bond

B

APC

MHC class I/II

Antigenic peptide

Co-receptor

TCR   α   β

T cell

γ ε   ε δ

ζ ζ

LCK

ITAM

CD3
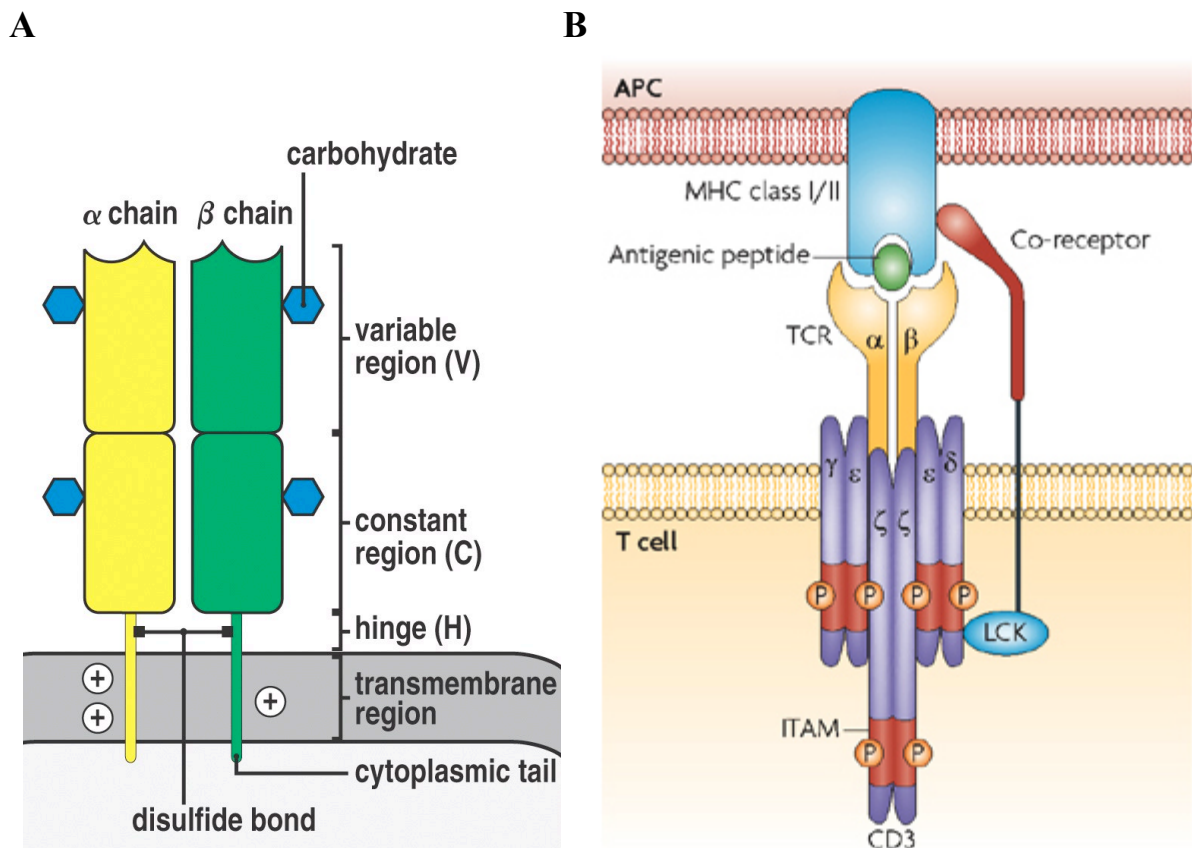
Figure 1-2: TCR structure and engagement
(A) The TCR consists of a TCRα- and TCRβ-chain. Each chain is composed of a variable and a constant region. Adapted from Murphy (21). (B) The TCR is expressed as a complex with CD3 and accessory chains on the cell surface. In association with the co-receptor, this complex is responsible for recognition of MHC-bound peptides and initiation of T-cell activation. Adapted from Gascoigne et al (22).

Upon antigen recognition, the src-family kinases Lck and Fyn are activated and subsequently phosphorylate immunoreceptor tyrosine-based activation motifs (ITAMs) within the cytoplasmic domains of the CD3 and accessory ζ chains. Phosphorylation of the ITAMs leads to recruitment and activation of the tyrosine kinase ZAP-70, which propagates the TCR

signal by phosphorylating two critical adaptor molecules: SH2 domain-containing leukocyte protein of 76 kDa (SLP-76) and the linker for activation of T cells (LAT) (Figure 1-3) (23). Together they form a membrane-associated signaling complex that recruits various adapter and effector molecules, including phospholipase-γ (PLCγ). PLCγ is phosphorylated within this complex. Subsequently, PLCγ cleaves membrane-bound phosphatidylinositol biphosphate (PtdInsP$_2$) into diacyl glycerol (DAG) and inositol trisphosphate (InsP$_3$) (24).
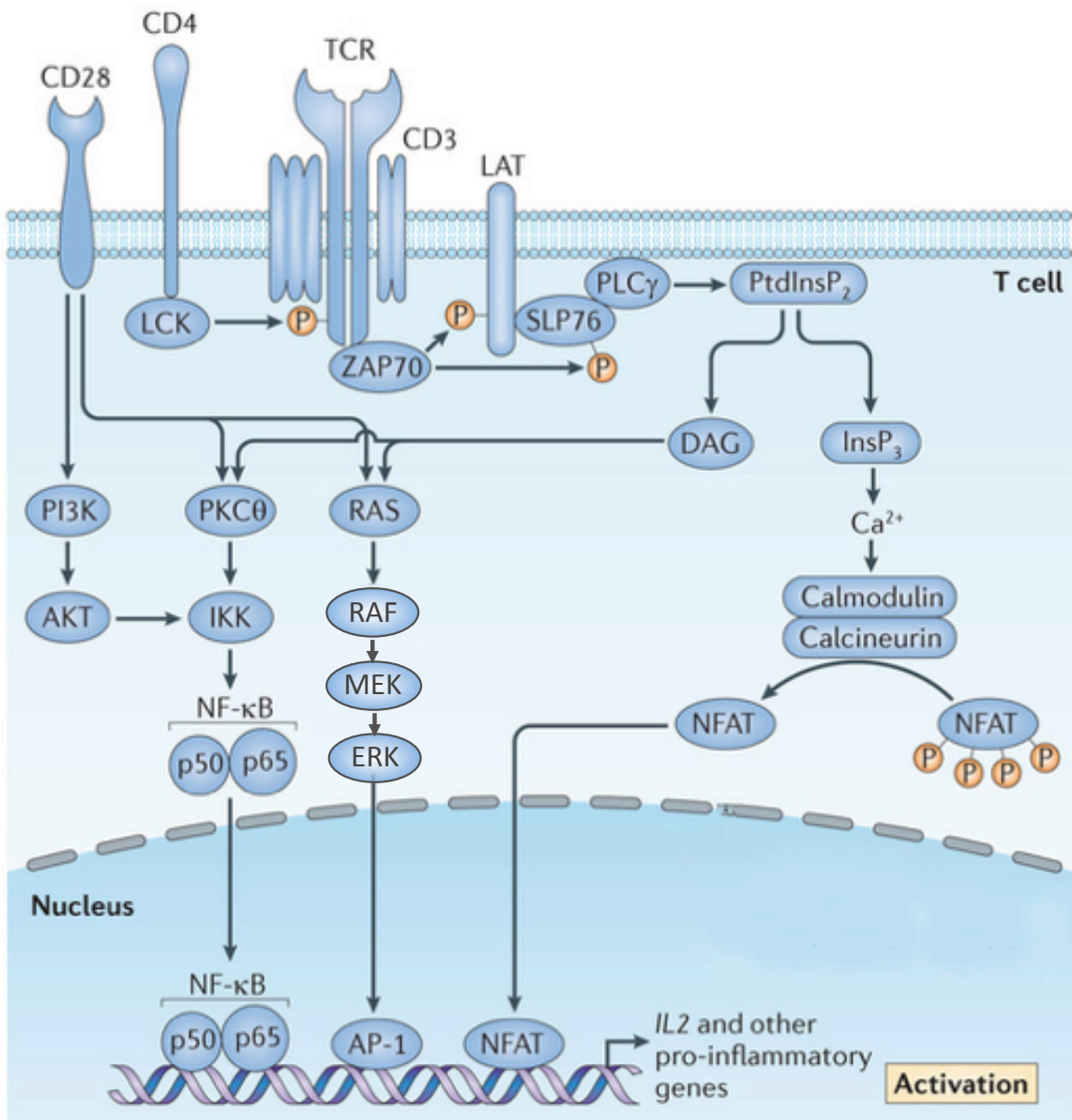
Figure 1-3: TCR signaling pathway
Engagement of the TCR leads to activation of the kinases Lck and ZAP-70, followed by formation of a multimolecular signaling complex at the membrane involving the two adapter proteins SLP70 and LAT. The resulting activation of PLCγ induces cleaving of PtdInsP2 into DAG and InsP3, which in turn activates various downstream signaling pathways, such as calcium signaling, MAPK signaling and NFκB signaling pathways. At the same time, co-stimulation through CD28 induces the PI3K/AKT signaling pathway. Ultimately, all pathways activate transcription factors that induce transcription of IL-2 and other pro-inflammatory genes. Adapted from Pollizzi et al (25).

InsP$_3$ binds to calcium channels on the endoplasmic reticulum (ER) membrane, thereby releasing stored calcium into the cytosol. Calcium induces conformational changes in the messenger protein calmodulin that lead to recruitment of serine/threonine protein phosphatase calcineurin. Activated calcineurin desphosphorylates the transcription factor nuclear factor of activated T cells (NFAT), allowing NFAT to enter the nucleus (26). In the nucleus, NFAT cooperates with other transcription factors to induce transcription of IL-2 and other pro-inflammatory genes. Parallel to calcium signaling, DAG recruits and activates the signaling molecules Ras and PKCΘ (27). Ras triggers the MAPK/ERK pathway, whereas PKCΘ activates the NF-κB pathway. The kinase cascade in the MAPK/ERK pathway follows successive activation of the mitogen-activated protein kinases (MAPK) Raf, MEK and ERK leading to activation of the transcription factor complex AP-1, which consists of Fos and Jun (28). The NF-κB pathway is blocked in resting T cells, as NF-κB transcription factors, such as p50 and p65, are associated with inhibitors of NF-κB (IκB) that prevent migration to the nucleus. Upon TCR stimulation, PKCΘ activates the IκB kinase (IKK), which induces degradation of IκB followed by translocation of NF-κB transcription factors to the nucleus (29,30). The MAPK/ERK and NF-κB pathways are also triggered through co-receptor CD28-mediated signaling (31,32). Additionally, CD28 initiates the PI3K/AKT signaling pathway. The phosphoinositide 3-kinase (PI3K) binds to the phosphorylated cytoplasmic tail of CD28, followed by recruitment and phosphorylation of the serine/threonine kinase AKT (33). The relative contribution of the TCR vs its coreceptors in the initiation of the PI3K/AKT signaling pathway remains unresolved (34). AKT is best known for its role in cell survival and growth by binding various substrates. The anti-apoptotic effect of AKT is the result of binding pro-apoptotic proteins directly, such as BAD, or the transcription factors that initiate transcription of pro-apoptotic genes, such as FOXO (35). AKT promotes cell growth through activation of the mammalian target of rapamycin (mTOR). Additionally, AKT directly interacts with the NF-κB pathway by phosphorylating IKK (36). Ultimately, all TCR- and CD28-initiated signaling pathways result in transcription of genes involved in cytokine production, differentiation and proliferation of effector T cells. One of these cytokines is IL-2, which plays an important role in enhancing activation of T cells. Activated T cells up-regulate expression of the IL-2 receptor and once IL-2 binds to this receptor, multiple signaling pathways are activated, including the MAPK/ERK pathway and the PI3K/AKT signaling pathway (37).

1.1.4 T-cell homeostasis

Homeostatic mechanisms regulate size and composition of the peripheral T-cell pool and maintain total T-cell number throughout life. These mechanisms differ for naïve, effector and memory T-cell populations. Naïve T cells can survive for long periods of time without being exposed to an antigen. However, they require survival signals provided by interleukin-7 (IL-7) and TCR interaction with spMHC molecules on APCs (Figure 1-4) (38). Naïve T cells compete for these survival signals based on the limited availability of cytokines and specific spMHC molecules. Several models have been proposed that aim to explain how these survival signals regulate size and diversity of the naïve T-cell pool. Some studies suggested that T cells with TCRs of the same peptide specificity compete with each other for access to the same spMHC molecules (intraclonal competition), whereas T cells with a different specificity are unaffected (39,40). Others proposed competition between T cells of different specificities as a mechanism for maintaining T-cell diversity (interclonal competition) that is either based on TCR promiscuity, TCR affinity and/or the ability to respond to other survival signals, such as cytokines, upon TCR interaction with spMHC molecules (41–43). Additionally, it was shown that mature TCR polyclonal, but not TCR monoclonal T cells are resistant to oncogene-induced transformation, suggesting a role of clonal competition in suppression of malignant outgrowth (44,45).

Upon activation, clonal expansion of antigen specific T cells is essential to generate a sufficient number of effector T cells to combat infection. Once a particular threat is eliminated, the large population of reactive T cells is not required any longer. Therefore, apoptosis is directly or indirectly induced in these cells through multiple mechanisms (Figure 1-4). An indirect mechanism is the withdrawal of survival signals such as co-stimulators and cytokines, resulting in a loss of anti-apoptotic gene expression and death by neglect (46,47). Regulatory mechanisms and components that actively terminate T-cell responses include activation-induced cell death (AICD), expression of cytotoxic T lymphocyte antigen 4 (CTLA-4) and the effect of Tregs. Repeated stimulation of the TCR triggers AICD by mediating the expression of the death receptor Fas (CD95) and its ligand FasL (48). Activated T cells also start to express CTLA-4, a second co-receptor besides CD28, that can bind the co-stimulatory molecules CD80 and CD86. Upon binding, CTLA-4 inhibits TCR downstream signaling, thereby blocking IL-2 production (49). Treg function is based on direct cell contact through binding of CTLA-4 on Tregs to CD80/CD86 on effector T cells,

the production of immunosuppressive cytokines, such as transforming growth factor–β1 (TGF-β1) and IL-10, as well as granzyme- and perforin-mediated cytolysis (50).
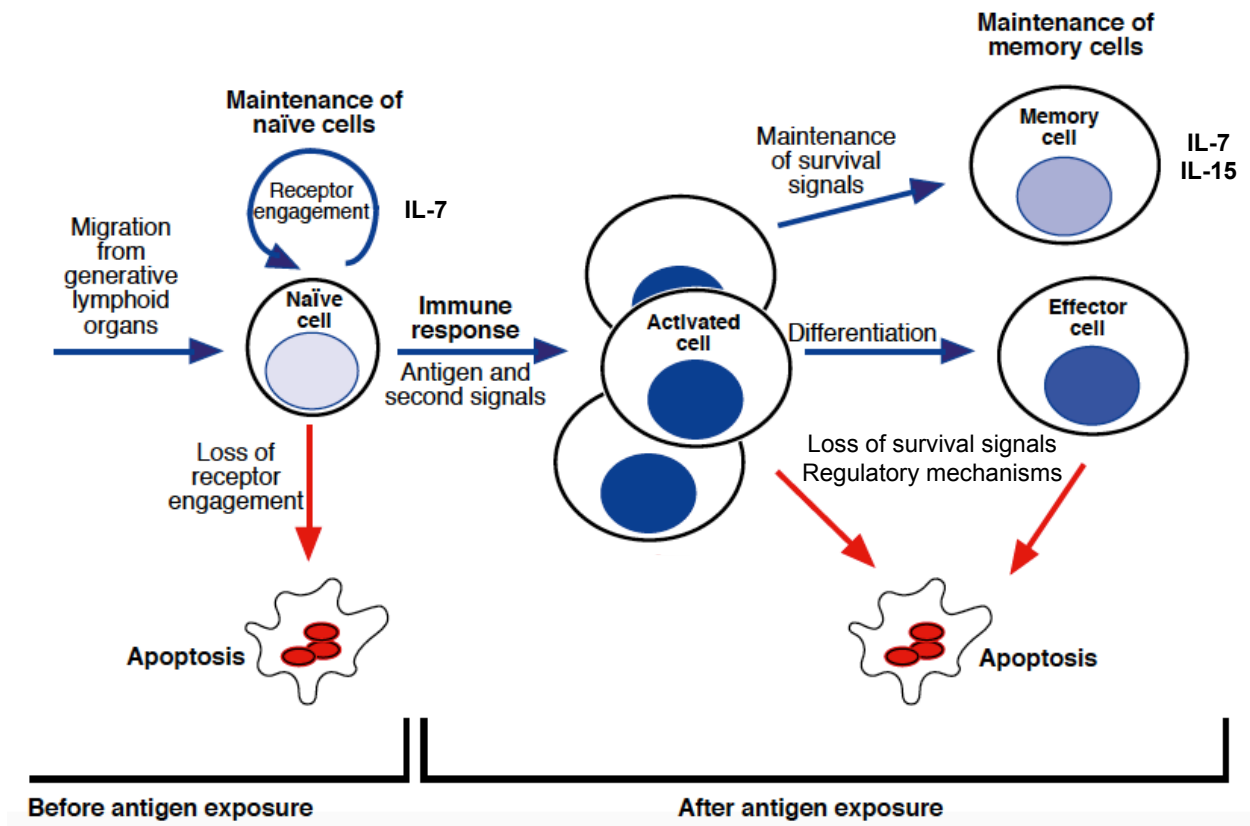
Figure 1-4: Homeostatic mechanisms during an immune response
Naïve T cells require IL-7 and TCR interaction with spMHC molecules for survival. Upon antigen exposure, activated T cells differentiate and expand into a large population of effector T cells. After clearance of an immune response, loss of survival signals and regulatory mechanism, such as AICD, CTLA-4 expression and immunosuppressive Tregs, induce apoptosis in most effector T cells to turn the immune system back to a responsive state. The remaining memory T cells are kept alive through cytokine signaling induced by IL-7 and IL-15. Adapted from Parijs et al (51).

The mechanisms that control survival and homeostasis of the remaining memory T cells in the absence of antigen stimulus are less well studied. Memory T cells seem to rely on survival signals mediated by the cytokines IL-7 and IL-15 (52–54). Thereby they compete with naïve T cells for the same resources. It remains controversial whether they require TCR-MHC interactions for survival as well (55–58).

1.2 Leukemia and Lymphoma

Malignant transformation of lymphocytes results in the development of leukemias and lymphomas. B- and T-cell malignancies can be divided into precursor B- and T-lymphoid neoplasms, mature neoplasms of B-, T-, and NK-cell lineage, and apart from these Non-Hodgkin Lymphomas, the category of Hodgkin lymphoma (59). The vast majority of lymphomas arise from B cells, as they are more susceptible to accumulate secondary mutations during their development than do T cells. Error-prone mechanisms like somatic hypermutation and immunoglobulin class switch recombination are necessary to generate a diverse antibody repertoire in B cells, but contribute significantly to lymphomagenesis (60,61).

1.2.1 Peripheral T-cell leukemia/lymphoma

Peripheral or mature T-cell leukemias/lymphomas (PTCL/MTCL) account for 5-10% of all Non-Hodgkin lymphomas and are often associated with a very poor prognosis (62). The World Health Organization (WHO) classifies these neoplasms based on their clinical presentation into primarily nodal, extranodal, cutaneous, and leukemic malignancies (59). These entities are heterogeneous in their clinico-pathologic presentation. Given their infrequent incidence, they represent a considerable diagnostic challenge. Generally, there is a high demand for better treatments in PTCL, as standard therapies show poor responses in these patients (63).

1.2.2 T-cell prolymphocytic leukemia (T-PLL)

1.2.2.1 Characteristics of T-PLL

T-cell prolymphocytic leukemia (T-PLL) represents the most frequent T-cell leukemia and incidences are estimated to be around 0.6 per million (64–66). Malignant T lymphocytes in T-PLL involve the peripheral blood (PB), LNs, BM, liver, spleen, and skin (59). Consequently, T-PLL patients commonly present with splenomegaly and elevated lymphocyte counts, and less frequently with lymphadenopathy, hepatomegaly, skin lesions, or serous effusions (67). T-PLL cells usually express the pan-T cell antigens CD2, CD3, CD5, and CD7 (68). The expression of CD4 and CD8 is variable. The most common

immunophenotype is CD4+/CD8- (60%), while cases with a CD4+/CD8+ (25%) and CD4-/CD8+ (15%) phenotype occur less frequent (68). Most T-PLL cells are morphologically characterized as medium-sized pro-lymphocytes with a single prominent nucleoli, basophilic cytoplasm, and cytoplasmic blebs (68). The nuclei are usually round to oval, but an irregular cerebriform shape is observed in less common variants of T-PLL as well. Molecular studies revealed two characteristic genetic aberrations involving chromosome 14. Most T-PLL cells carry either chromosomal inversion inv(14)(q11;q32) or translocation t(14;14)(q11;q32) (69). This leads in both scenario to juxtaposition of the T-cell leukemia 1 (TCL1A) gene locus at 14q32.1 to TCRα/δ regulatory elements (70). Consequently, overexpression of the TCL1A protein is observed in 70-80% T-PLL cases and is a hallmark of this entity (65,66,71–74). In 20% of patients the TCL1 family member mature T-cell proliferation 1 (MTCP1) is activated due to translocation t(X;14)(q28;q11) (68). While genetic abnormalities involving the TCL1 locus are regarded as initial transforming events, additional alterations, like those on chromosomes 11q (involving the tumor suppressor ataxia telangiectasia mutated (ATM)) or involving 8q are frequently observed as well (75,76).

1.2.2.2 T-cell receptor expression in T-PLL

The TCR is essential for normal T-cell survival and function. Transformed T cells of the different PTCL entities show diverse patterns of TCR expression and signaling activity, thereby suggesting a role in tumorigenesis (77). In T-PLL, most tumor cells express and signal through the TCR (65,74). TCR expression is associated with poorer patient survival compared to cases lacking TCR expression (Figure 1-5A) (74). TCL1A overexpression is a molecular hallmark for T-PLL and the result of chromosomal rearrangement involving TCRα/δ enhancer elements. Similar to TCR expression, TCL1A+ T-PLL cases correlate with poor outcome (Figure 1-5B). T-PLL cells with high expression of TCL1A have shown increased proliferation and AKT activation upon TCR engagement compared to tumor cells with low or absent TCL1A expression (74). A preferential usage of TCR-Vβ families, that would suggest an antigenic drive, has not been observed for this entity (78,79).
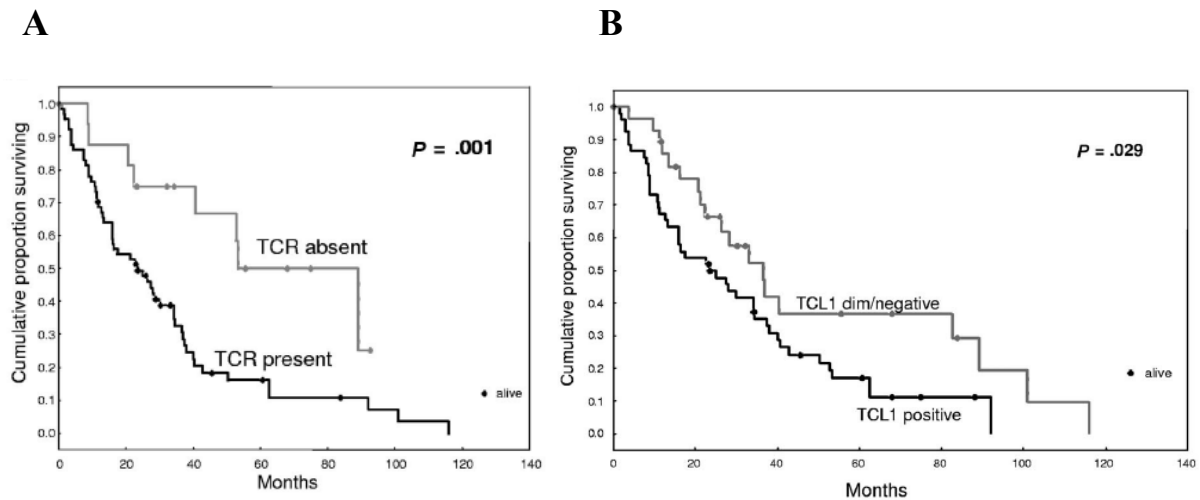
Figure 1-5: Correlation of TCR and TCL1A expression with patient survival in T-PLL
In T-PLL patients, expression of a surface TCR (A) and TCL1A (B) correlate with poor survival compared to cases lacking respective expression. Adapted from Herling et al (74).

1.2.2.3 Murine models for T-PLL

Murine models are widely used to study human cancer. Given the limited availability of primary material of rare entities like T-PLL, murine models are especially valuable to gain a better understanding of their pathogenesis. As T-PLL is characterized by overexpression of TCL1A, transgenic mice expressing TCL1A under a T cell-specific Lck promoter developed a monoclonal T-PLL-like disease between 15 and 20 months of age (80). These mice showed enlarged spleens, LNs and thymi, and elevated white blood counts (WBCs) (Figure 1-6E). In contrast to human T-PLL, malignant cells in these mice had a $CD4^-CD8^+$ immunophenotype. Another T-PLL model is the MTCP1^{p13}-transgenic mouse. The p13 oncogenic isoform of MTCP1 is expressed under a CD2 promoter in this model and induced a T-PLL-like disease to become clinically overt at 18-20 months of age (81). These mice frequently presented with enlarged spleens and lymphocytosis (Figure 1-6A-D). In most cases, leukemic cells showed a $CD4^-CD8^+$ immunophenotype.
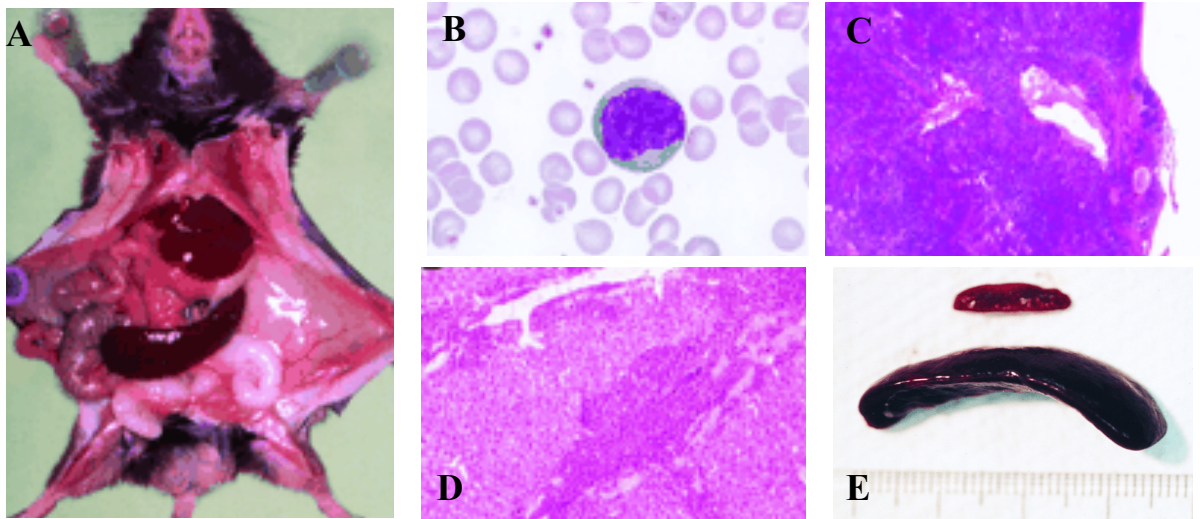
Figure 1-6: T-PLL-like disease in mice
MTCP1 (A-D) and TCL1A (E) transgenic mice develop a T-PLL like disease with enlarged spleens (A, E). T-cell prolymphocytes are found in the blood (B), spleen (C) and liver (D). Adapted from Virgilio et al and Gritti et al (80,81)

1.3 The T-cell leukemia/lymphoma 1 (TCL1A) family

The members of the T-cell leukemia/lymphoma 1 (TCL1A) family were first identified by their involvement in specific chromosomal rearrangements in mature T-cell malignancies. In humans this family consists of 3 genes: TCL1A, MTCP1, and TCL1B (also called TML1) (82–85). In mice, in addition to the 2 homologues of each TCL1A and MTCP1, there are five genes homologous to human TCL1B (Tcl1b1, Tcl1b2, Tcl1b3, Tcl1b4, Tcl1b5)(84).

1.3.1 TCL1A

1.3.1.1 Expression pattern of TCL1A in healthy tissues

The TCL1A gene encodes a 14kDa non-enzymatic protein with a closed antiparallel β-barrel structure, consisting of eight β-strands with a hydrophobic core (86,87). Structural studies revealed that the TCL1A protein contains a homodimerization domain (87).

In mice, TCL1A was shown to be expressed in embryonic stem cells and in fetal tissue, namely in liver, yolk sac, thymus and BM (88,89). In adult mouse tissue, TCL1A expression was found in spleen, thymus, BM, PB lymphocytes and testis, suggesting a functional role in lymphopoiesis (84,88,90). Murine TCL1A expression was detected in T cells at the DN4 and

DP stage (see section 1.1.1) and in B cells during all developmental stages in the BM, as well as in all subpopulations of the spleen and LN (90).

In human fetal tissues, TCL1A expression was detectable in liver, kidney, thymus and lung (91). In human adult tissues, it was found in spleen, LN, BM, thymus, and tonsil (91). Sorted B-cell populations from fetal BM showed TCL1A expression at the pro-B-cell, pre-B-cell and immature B-cell stage (70). High TCL1A transcript levels were also observed in naïve PB B cells and CD5$^+$ B cells sorted from healthy adult donors (92), whereas others reported TCL1A expression in PB lymphocytes only upon stimulation (70). Sorted thymocyte populations expressed TCL1A at the DN stage, but not at the DP stage (70). Additionally, TCL1 expression was found in plasmacytoid dendritic cells in reactive human LNs (93). The expression pattern of TCL1A in humans showed high similarities with the one in mice. It is therefore most likely that TCL1A plays a similar role in human embryonic development and early T- and B-cell development.

1.3.1.2 Oncogenic properties of TCL1A

TCL1A was first described based on its aberrant expression in T-cell malignancies (85). In humans, TCL1A overexpression is detected in many mature B-cell lymphomas, in the majority of T-PLL, in T-cell leukemias arising in patients with the condition of ataxia telangiectasia (A-T), blastic plasmacytoid dendritic cell neoplasms, germ cell tumors, hepatocellular carcinoma, and adenocarcinoma of the esophagus (65,70,93–100). TCL1A expression has also been described for various human lymphoma/leukemia cell lines: Burkitt's lymphoma cell lines Raji, Daudi, CA-46, P3HR-1 and AKUA; EBV transformed lymphoblastic cell lines Ado-1701 and Ado-2199; acute lymphoblastic cell lines 697, ALL380, ALL-1 and BV173; T-lymphoblastic leukemia/lymphoma cell line Sup-T11 (70,84,91).

In mice, the TCL1 locus is found on chromosome 12, whereas in humans the TCL1 locus is located on chromosome 14, band q32.1 (101). In humans, rearrangements involving the TCL1 locus are commonly found in T-PLL (see section 1.2.2.1) and lead to abnormal expression of TCL1A. The TCL1 locus rearranges either with the TCRα/δ locus on chromosome 14 by inversion inv(14)(q11;q32) or translocation t(14;14)(q11;q32) (Figure 1-7), or with the TCRβ locus on chromosome 7 by translocation t(7;14)(q35;q32) (101). In all of these scenarios the TCL1 locus is juxtaposed to TCR enhancer elements, most likely

causing aberrant (prolonged) activation of TCL1A (101) as opposed to its physiological post-thymic silencing.
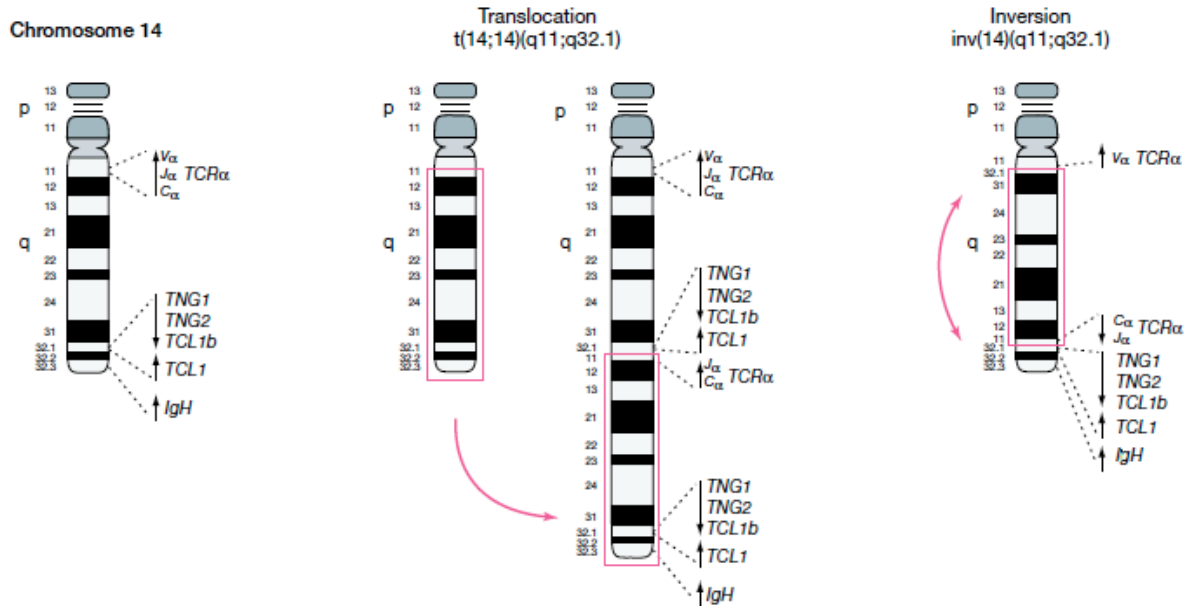
Figure 1-7: Chromosomal rearrangements involving the TCL1 locus
The TCL1 locus is located on chromosome 14, band q32.1 (left). Chromosomal rearrangements that lead to overexpression in mature T-cell leukemias involve the TCRα/δ locus on chromosome 14, band q11. These rearrangements juxtapose TCL1A to the TCR locus either by translocation t(14;14)(q11;q32) (middle) or inversion inv(14)(q11;q32) (right). Adapted from Pekarsky et al (102).

The majority of cases of human chronic lymphocytic leukemia (CLL) are associated with TCL1A expression as well (103). However, TCL1A expression levels vary between these patients. High TCL1A expression was associated with an unmutated IGHV gene status, high ZAP-70 expression, and chromosome 11q22–23 deletions in these patients (103). In contrast to T-PLL, CLL patient samples do not show rearrangements involving the TCL1 locus (104). Alternative mechanisms leading to abnormal expression of TCL1A in B-cell malignancies have been proposed, including those that involve transcriptional activation by Sp1, external signals provided by cells in the microenvironment that are either TCL1A suppressive (T cell-mediated) or activating (stromal cell-mediated), and decreased levels of TCL1A-targeting micro-RNAs (103,105–109). Gene expression profiling revealed comparable TCL1A transcript levels in CLL cells and mature B-cell populations (naïve B cells and CD5^{+} B cells) from healthy donors, suggesting that CLL cells either inherited or adopted high TCL1 expression from their histogenetically related healthy B-cell populations (92).

As described in section 1.2.2.3, overexpression of TCL1A in T cells of transgenic mice causes cellular transformation, thereby providing functional proof for its oncogenic potential (80). Although originally identified as an oncogene in T cells, TCL1A also plays a role in the transformation of mature B cells. Transgenic mice that expressed TCL1A in B and T cells predominantly developed Burkitt-like lymphoma (BLL) and diffuse large B-cell lymphoma (DLBCL) starting at the age of 4 months (110). These mice presented with variable splenomegaly, lymphadenopathy, and macroscopic lesions of the liver, lung, kidney, and intestines. Tumor cells in most cases were $IgM^+B220^{lo}CD5^{lo}$ B cells. Splenocytes isolated from these transgenic mice before tumor development showed prolonged cell survival and increased proliferation compared to control mice. When TCL1A expression was driven by a B cell-specific IgH Eµ enhancer element, transgenic mice developed a CLL-like malignancy (111). These mice showed enlarged spleens, LNs and livers associated with elevated WBCs. Tumor cells were characterized as $CD5^+IgM^+$. This system has been widely used as a model for human CLL (112).

1.3.1.3 Functional aspects of TCL1A

The functional role of TCL1A as extrapolated by its expression patterns and as identified by its interaction partners and subcellular localization, is most likely determined in a cell and tissue specific manner. In embryonic stem cells, TCL1A enhanced proliferation and suppressed differentiation, implicating a functional role in self-renewal and maintenance of pluripotency (89,113–115). Its importance in embryonic development was also supported by studies of TCL1A deficient mice that showed reduced fertility in females caused by an impaired pre-implantation embryo development (95). TCL1A seems to function similarly in adult stem cells of the hair follicle as these cells showed reduced proliferation and loss of the stem-cell marker CD34 in TCL1A deficient mice (116). Loss of TCL1A also led to a significant decrease in the number of pre-B cells, immature B cells and thymocytes at the DN and DP stages, as well as splenic T-and B-cell populations (90).

The first protein that was identified to co-precipitate and specifically (directly) interact with TCL1A in human B-cell lines is the serine/threonine kinase AKT (117). The PI3K/AKT signaling pathway has been described in section 1.1.3 as one of the major downstream signaling pathways involved in T-cell activation. TCL1A was described to interact with AKT at the membrane by binding to its N-terminal pleckstrin homology (PH) domain, a functional

domain that mediates protein-protein and protein-lipid interactions (117,118). Aberrant AKT activation by TCL1A resulted in augmented phosphorylation of downstream AKT target proteins promoting cellular survival and proliferation (117,119,120).

Moreover, it was described that TCL1A activates the NF-κB pathway by interacting with the transcriptional activator p300, a known co-activator of NF-κB, in the Burkitt's lymphoma cell line Daudi (121). In the same study, they showed that TCL1A also binds the AP-1 components Jun and Fos in the nucleus, thereby inhibiting AP-1 transcriptional activity. In CLL cells, up-regulation of TCL1A was associated with down-modulation of Fos and Jun proteins (107). Although the AP-1 complex was described as an activator of proliferation in section 1.1.3, it is also known to be involved in induction of apoptosis in lymphoid cells after growth factor withdrawal (122).

Another interaction partner of TCL1A is the serine/threonine protein kinase ATM that normally induces cell cycle arrest, DNA repair and/or apoptosis upon DNA damage (123,124). This interaction resulted in the activation of NF-κB by inducing degradation of IκB, allowing translocation of NF-κB transcription factors to the nucleus. Similar to AP-1, NF-κB transcription factors are required for T-cell activation (see section 1.1.3), but have been associated with initiation of apoptosis in response to cellular stress (125).

AKT and ATM modulate important cellular signaling pathways and deregulation of these genes alone results in cellular transformation. Transgenic mice expressing myristoylated or constitutively active AKT developed lymphoblastic lymphomas (126). These tumors also arose in ATM-deficient mice (127). The oncogenic function of TCL1A is therefore mostly likely based on the combined deregulation of several different pathways, as it is associated with induction of mature T- and B-cell malignancies.

As described before, the majority of T-PLL cells express a functional TCR (see 1.2.2.2). Engagement of the TCR in these cells led to TCL1A and AKT recruitment to the cell membrane (Figure 1-8A) and formation of TCR-signalosomes with other signaling kinases, such as Lck (Figure 1-8B) (74). Eventually TCL1A and AKT co-localized to the nucleus (74). Similarly, B-cell receptor (BCR) engagement in TCL1 expressing CLL cells led to recruitment of TCL1A and AKT to BCR membrane complexes (128). In mice, abnormal TCL1A expression enhanced cytokine secretion and proliferation of mature T cells upon TCR or pharmacologic activation through enhanced phosphorylation of PKCΘ and ERK (71). This is in contrast with a study of activated human T cells that showed impaired PKCΘ and ERK phosphorylation in the presence of TCL1A leading to an inhibition of AICD (129). However, it is unclear how TCL1A interferes with these signaling molecules.

The previously described interactions of TCL1A with other proteins were detected in the cytosol (AKT, p300, ATM) and the nucleus (AKT, Jun, Fos) (74,86,119,121,123). Thus, TCL1A protein localization is not restricted to a particular cellular compartment, but rather determines its function through compartment-specific interaction partners.
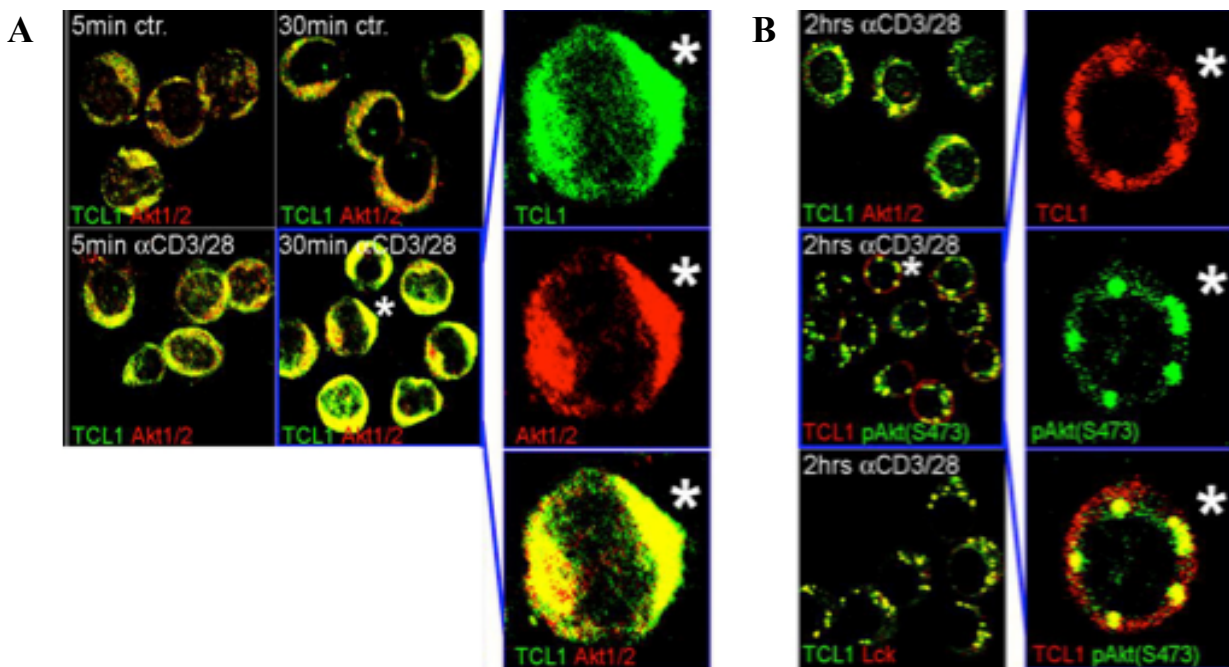
Figure 1-8: TCL1A recruitment to the membrane upon TCR engagement in T-PLL cells
(A) In unstimlulated T-PLL cells, TCL1A and AKT are found in the cytosol without co-localizing (ctr, top panel). However, upon TCR stimulation with CD3/28 beads, TCL1A and AKT co-localize at the cell membrane (middle panel). (B) Continuous TCR engagement leads to accumulation of TCL1A and AKT in distinct membrane complexes (top and middle panel) together with the signaling kinase Lck (bottom panel). Adapted from Herling et al (74).

1.3.2 MTCP1

MTCP1 was discovered by involvement in t(X;14) translocations in two mature T-cell proliferations (82). Normally, the gene is localized on Xq28 (82) and encodes two different proteins: the mitochondrial protein p8 (130) and the protein p13 (131). These proteins share no similarity with each other, but the p13 isoform shows 39% amino acid identity with TCL1A and 95% identity with murine p13Mtcp1 (131). As only the p13MTCP1 protein is part of the TCL1 family, it is generally referred to as MTCP1 in this thesis. Although this 13kDA protein lacks a dimerization surface, it has been shown that it interacts with AKT (K_d of 537µM), however, with much lower affinity than TCL1A (K_d of 5.7µM) (87,117,132).

The fact that MTCP1 is oncogenic suggests other relevant executioners than / in addition to AKT or that it likely requires additional bridging molecules (132). Other interaction partners have not been described for this protein. In mice, normal Mtcp1 expression is found in early fetal tissues (liver, yolk sac); in liver, kidney and spleen in adult tissue (88) and in mature T cells after infection (133). The human MTCP1 oncoprotein showed low expression in most tissues (82) and was not detected in normal resting or activated lymphocytes (131). Therefore, MTCP1 expression was limited to mature T-cell proliferations with t(X;14) translocations in humans (82,131). Transgenic mice for human MTCP1 developed mature T-cell leukemia similar to human T-PLL after a long latency period (>15months) (81), thereby directly demonstrating its oncogenic properties. Sick mice often presented with splenomegaly and elevated WBC. Further examination revealed infiltrations of lymphoid cells into all lymphoid organs, liver and lungs. In 23 cases tumor cells were phenotypically characterized as $CD3^+$, $CD8^+$, $CD4^-$, $CD25^-$, $B220^-$ and in one case as $CD3^+$, $CD4^+$, $CD8^-$, $CD25^-$, $B220^-$.

1.3.3   TCL1B/TML1

Human TCL1B/TML1 (TCL1A/MTCP1-like 1) is the third member of the TCL1 family and was identified by screening the frequently rearranged region on chromosome 14q32.1 for affected genes other than TCL1A (83,91). The amino acid sequence of TML1 shows over 30% identity and 60% similarity with TCL1A and MTCP1, and has a 14 amino acid insertion compared to human TCL1A (84,91). Similar to MTCP1, this 15kDA protein does not contain a dimerization domain and interacts with AKT with lower affinity than TCL1A (83,117). Human TML1 is normally expressed in fetal liver, kidney, heart, spleen and thymus (91). In adult tissue very low expression levels are found in placenta, testis, kidney, spleen, LNs, tonsil and PB lymphocytes (83,91). In human cancer cell lines, TML1 expression is detected in Burkitt's lymphomas, EBV-transformed lymphoblastoid B-cell lines and T-cell leukemia with a translocation at 14q32.1 (83,91). In mice, five genes (Tcl1b1-Tcl1b5) were found in the TCL1 locus that are homologous to human TML1 (84). The five proteins showed a 30-40% similarity to human TML1. Expression was high in mouse oocytes and two-cell embryos, but low in adult tissues and lymphoid cell lines (84). TML1 is the least studied family member and it is unknown whether it has oncogenic properties by itself.

1.4   Objectives

Deregulated expression of the TCL1 family genes TCL1A, MTCP1 and TML1 was first described in T-cell malignancies. In transgenic mice, overexpression of TCL1A and MTCP1 causes outgrowth of mature T- and B-cell tumors. Different promoters were used in these studies to target gene expression to T and/or B cells, making it difficult to compare oncogenic properties of the two family members directly. Studies describing the oncogenic potential of TML1 in vivo have not been described yet. Therefore, the first aim of this thesis is to determine and characterize tumorigenicity of the TCL1 family genes in vivo by using gamma-retroviral vectors to introduce human TCL1A, MTCP1 and TML1 into HSC/hematopoietic progenitor cells (HPC) of wild type mice that are transplanted into wild type recipients. TCL1A is expressed in the cytoplasm and the nucleus, thereby targeting different signaling molecules. To examine if enforced TCL1A localization influences its downstream effects, allowing inferences on a preferred/differential oncogenic potential, a myristoylated (membrane localizing) variant (myr-TCL1A) and a nuclear-site directed variant (nls-TCL1A) of the TCL1A construct are additionally used in the previously described mouse model.

TCL1A overexpression is detected in the majority of T-PLL. These tumor cells usually express a TCR. The oncogenic function of TCL1A is based on the modulation of various signaling pathways by interacting with key signaling molecules, especially in the context of TCR activation. This suggests a cooperation of TCL1A and TCR signals in the development of T-PLL. However, it is unknown how and to what extend TCR signaling plays a role in TCL1-driven lymphomagenesis/leukemogenesis. The second part of this thesis aims to understand the combined action of TCR signals and TCL1A oncogenes in perturbation of T-cell homeostasis and in cellular transformation. Therefore, TCR-transgenic monoclonal OT-1 T cells are retrovirally transduced with vectors encoding TCL1A, myr-TCL1A, and nls-TCL1A, and then transplanted into RAG1-deficient ($RAG1^{-/-}$) mice. Recipient mice are injected with the OVA peptide SIINFEKL every two weeks to specifically stimulate the TCR of OT-1 donor cells and to study the impact of repeated TCR engagement on TCL1-driven transformation.

2. Materials and Methods

2.1 Materials

2.1.1 Antibodies

Antibody Specificity	Clone	Conjugate	Reactivity	Manufacturer	Application
CD3ε	145-2C11	Purified	Mouse	BD, Franklin Lakes, New Jersey, USA	T-cell stimulation
CD3ε	145-2C11	PE	Mouse	Miltenyi Biotec, Bergisch Gladbach, Germany	FC
CD4	GK1.5	APC	Mouse	Miltenyi Biotec, Bergisch Gladbach, Germany	FC
CD4	GK1.5	APC-Cy7	Mouse	Biolegend San Diego, California, USA	FC
CD5	53-7.3	PE	Mouse	eBioscience, San Diego, California, USA	FC
CD8	53-6.7	VioBlue	Mouse	Miltenyi Biotec, Bergisch Gladbach, Germany	FC
CD19	6D5	APC	Mouse	Miltenyi Biotec, Bergisch Gladbach, Germany	FC
CD19	1D3	PE-Cy7	Mouse	eBioscience, San Diego, California, USA	FC
CD28	37.51	Purified	Mouse	BD, Franklin Lakes, New Jersey, USA	T-cell stimulation
CD44	IM7.8.1	VioBlue	Mouse	Miltenyi Biotec, Bergisch Gladbach, Germany	FC
CD45.1	A20	PE	Mouse	BD, Franklin Lakes, New Jersey, USA	FC
CD45.2	104	V450	Mouse	BD, Franklin Lakes, New Jersey, USA	FC
CD45R/B220	RA3-6B2	APC	Human, Mouse	Biolegend, San Diego, California, USA	FC
CD62L	MEL-14	APC	Mouse	BD, Franklin Lakes, New Jersey, USA	FC
CD69	H1.2F3	PE-Cy7	Mouse	BD, Franklin Lakes, New Jersey, USA	FC
CD117 (c-Kit)	3C11	PE, APC	Mouse	Miltenyi Biotec, Bergisch Gladbach, Germany	FC
CD197 (CCR7)	4B12	PE	Mouse	BD, Franklin Lakes, New Jersey, USA	FC
IgG2b, κ	MPC-11	Alexa Fluor 647	Human	Biolegend San Diego, California, USA	ICFC
IgM	Il/41	APC	Mouse	eBioscience, San Diego, California, USA	FC

MTCP1	-	-	Human	Abcam, Cambridge, UK	WB
Phospho- AKT (S473)	M89-61	PE	Mouse	BD, Franklin Lakes, New Jersey, USA	ICFC
Phospho-ERK1/2 (pT202/pY204)	20A	PE	Mouse	BD, Franklin Lakes, New Jersey, USA	ICFC
Phospho-STAT5 (pY694)	47	PE	Mouse	BD, Franklin Lakes, New Jersey, USA	ICFC
Sca-1	D7	PE	Mouse	Miltenyi Biotec, Bergisch Gladbach, Germany	FC
Streptavidin	-	APC	Mouse	BD, Franklin Lakes, New Jersey, USA	FC
TCL1A	1-21	Alexa Fluor 647	Human	Biolegend, San Diego, California, USA	ICFC
TCL1A	-	-	Human	Provided by Dr. M. Herling	WB
TML1	-	-	Human	Provided by Dr. M. Herling	WB
Vα2 TCR	B20.1	APC	Mouse	eBioscience, San Diego, California, USA	FC
Vβ5 TCR	MR9-4	PE	Mouse	BD, Franklin Lakes, New Jersey, USA	FC

Table 2-1: Antibodies
FC: Flow Cytometry, ICFC: Intracellular Flow Cytometry, WB: Western Blot.

2.1.2 Bacteria

One Shot TOP10 chemically competent Escherichia coli (E.coli) (Invitrogen, Life Technologies, Darmstadt, Germany)

Genotype: F- mcrA Δ(mrr-hsdRMS-mcrBC) Φ80lacZΔM15 Δ lacX74 recA1 araD139 Δ(araleu)7697 galU galK rpsL (StrR) endA1 nupG

2.1.3 Buffer and Solution Compositions

Buffer	Composition
Annealing buffer (5x)	0.5 M Tris (pH 7.4-7.5), 0.35 M MgCl$_2$
Bovine serum albumine BSA (10%)	10% (m/v) BSA in ddH$_2$O, sterile-filtered and stored at 4°C
Bind and wash buffer (2x)	10mM Tris (pH 7.5), 1mM EDTA, 2M NaCl
BSA/PBS 10% stock solution	10g BSA in 100ml PBS

Chloroquine	25µM in ddH$_2$O, sterile-filtered and stored at 4°C
FACS Fixation Solution	2% Paraformaldehyde in PBS
FACS-buffer	PBS, 2% FCS, 0.05% NaN$_3$ stored at 4°C
HEPES (2x)	281mM NaCl, 100mM HEPES, 5mM Na$_2$HPO$_4$ in ddH$_2$O, pH 7.0, stored at -20°C
MSA blocking solution 0.1%	25mg MSA in 25ml PBS, sterile filtered and stored at 4°C
PBS-T	0.05% Tween-20 in PBS
SDS, 10%	25g SDS in 250ml ddH$_2$O
SDS loading buffer, 6x	60% (v/v) glycerin, 18% (w/v) SDS, 0.3% (v/v) bromophenol blue, 600mM Tris-HCl, 12% (v/v) β-mercaptoethanol
Transfer/Blotting Buffer	20% (v/v) Methanol, 10% (v/v) TOWBIN Buffer
TOWBIN Buffer	144g Glycin, 30.29g Tris, 250mg SDS

Table 2-2: Buffer Compositions

2.1.4 Chemicals and Reagents

Chemical/Reagent	Manufacturer
4-(2-Hydroxyethyl)piperazine-1-ethanesulfonic acid (HEPES)	Sigma-Aldrich, St.Louis, Missouri, USA
Ampicillin, sodium salt	Roth, Karlsruhe, Germany
Amplification buffer (10x) (Buffer A)	Segenetic, Borken, Germany
β-mercaptoethanol	Gibco, Life Technologies, Darmstadt, Germany
BSA (bovine serum albumin)	Sigma-Aldrich, St.Louis, Missouri, USA
Bromophenol Blue	Sigma-Aldrich, St.Louis, Missouri, USA
CaCl$_2$	Merck, Darmstadt, Germany
CellTrace Violet Cell Proliferation Kit	Life Technologies, Darmstadt, Germany
Chloroquine	Sigma-Aldrich, St.Louis, Missouri, USA
Dimethyl sulfoxide (DMSO)	Serva, Heidelberg, Germany
Distilled Water	Gibco, Life Technologies, Darmstadt, Germany
D-Luciferin	PerkinElmer, Waltham, Massachusetts, USA
DNA ExitusPlus IF	AppliChem, Darmstadt, Germany
DNA Ladder (100bp, 1kb)	New England Biolabs, Ipswich, Massachusetts, USA

DNA loading dye (6x)	New England Biolabs, Ipswich, Massachusetts, USA
dNTPs (10mM)	Fermentas, Thermo Fisher Scientific, Waltham, Massachusetts, USA
Dulbecco's Modified Eagle Medium (DMEM)	Gibco, Life Technologies, Darmstadt, Germany
Dulbecco's Phosphate Buffered Saline (PBS)	PAA Laboratories, Pasching, Austria
Ethylenediaminetetraacetic acid (EDTA)	Sigma-Aldrich, St.Louis, Missouri, USA
Ethanol	Roth, Karlsruhe, Germany
Ethidium bromide	Bio-Rad, Hercules, California, USA
Extensor High Fidelity Master Mix	ABgene, Thermo Fisher Scientific, Waltham, Massachusetts, USA
FcR Blocking Reagent, mouse	Miltenyi Biotec, Bergisch Gladbach, Germany
Fetal bovine serum (FBS)	PAA Laboratories, Pasching, Austria
Freund's Adjuvant, Incomplete (IFA)	Sigma-Aldrich, St.Louis, Missouri, USA
Formaldehyde (37%)	Roth, Karlsruhe, Germany
Glycerol	Roth, Karlsruhe, Germany
Glycin	Sigma-Aldrich, St.Louis, Missouri, USA
Hanks balanced salt solution (HBSS)	Sigma-Aldrich, St.Louis, Missouri, USA
Human interleukin-2 (IL-2) (10000U/ml)	Novartis, Basel, Switzerland
Hydrochloride (HCl)	Merck, Darmstadt, Germany
Isopropanol	Merck, Darmstadt, Germany
Iscove's Modified Dulbecco's Medium (IMDM)	Gibco, Life Technologies, Darmstadt, Germany
Isoflurane	Abbvie, Ludwigshafen, Germany
Kanamycin-sulfate	Roth, Karlsruhe, Germany
LB Broth	Roth, Karlsruhe, Germany
LE Agarose	Bio-Rad, Hercules, California, USA
L-Glutamine	Gibco, Life Technologies, Darmstadt, Germany
Lyse/Fix Buffer (5X)	BD, Franklin Lakes, New Jersey, USA
Lysing Buffer (10x)	BD, Franklin Lakes, New Jersey, USA
Methanol	Roth, Karlsruhe, Germany
Magnesium Chloride $MgCl_2$	Merck, Darmstadt, Germany
Mouse Serum Albumin (MSA)	EMD Millipore, Billerica, USA

Non-essential amino acids (NEAA)	Gibco, Life Technologies, Darmstadt, Germany
NuPAGE MES SDS Running Buffer (20X)	Life Technologies, Darmstadt, Germany
NuPAGE Novex 4-12% Bis-Tris Protein Gels, 1.0 mm, 15 well	Life Technologies, Darmstadt, Germany
NuPAGE Novex 12% Bis-Tris Protein Gels, 1.0 mm, 15 well	Life Technologies, Darmstadt, Germany
OVA (257-264)	Eurogentec, Seraing, Belgium
PCR Primers	Eurofins MWG Operon, Ebersberg, Germany
Penicillin/Streptavidin	Gibco, Life Technologies, Darmstadt, Germany
Perm Buffer III	BD, Franklin Lakes, New Jersey, USA
Phosphatase Inhibitor Cocktail Tablets, PhosSTOP	Roche Diagnostics, Mannheim, Germany
Phusion High-Fidelity DNA Polymerase	Finnzymes, New England Biolabs, Ipswich, Massachusetts, USA
Protease Inhibitor Cocktail Tablets, cOmplete Mini	Roche Diagnostics, Mannheim, Germany
Retronectin	Takara/Clontech, Mountain View, California, USA
Restriction Endonucleases	New England Biolabs, Ipswich, Massachusetts, USA
Roswell Park Memorial Institute (RPMI) 1640	Gibco, Life Technologies, Darmstadt, Germany
Roti-Block	Roth, Karlsruhe, Germany
RNase (DNase free)	Roche, Basel, Switzerland
S.O.C. medium	Invitrogen, Life Technologies, Darmstadt, Germany
Sodium Chloride (NaCl)	Roth, Karlsruhe, Germany
Sodium Dodecyl Sulfate (SDS)	AppliChem, Darmstadt, Germany
Sodium Fluoride (NaF)	Fluka, Sigma-Aldrich, St.Louis, Missouri, USA
Sodium Hydroxide (NaOH)	Merck, Darmstadt, Germany
Sodium Orthovanadate (Na_3VO_4)	Sigma-Aldrich, St.Louis, Missouri, USA
Sodium Phosphate (Na_3PO_4)	Sigma-Aldrich, St.Louis, Missouri, USA
Sodium Pyruvate	Gibco, Life Technologies, Darmstadt, Germany
StemSpan SFEM	STEMCELL Technologies, Vancouver, Canada
T4 DNA Ligase	New England Biolabs, Ipswich, Massachusetts, USA
Taq Polymerase	Segenetic, Borken, Germany
Tris-(Hydroxymethyl)-Aminomethane (Tris)	AppliChem, Darmstadt, Germany
Tris-Hydrogen Chloride Buffer (Tris-HCl)	Bio-Rad, Hercules, California, USA

Trypan Blue	Sigma-Aldrich, St.Louis, Missouri, USA
Trypsin-EDTA solution (0.05%)	Invitrogen, Life Technologies, Darmstadt, Germany
Tween-20	Merck, Darmstadt; Germany

Table 2-3: Chemicals and Reagents

2.1.5 Commercial Kits

Kit	Manufacturer
Calcium Phosphat Transfektion Kit	Sigma-Aldrich, St.Louis, Missouri, USA
DNeasy Blood & Tissue Kit	Qiagen, Hilden, Germany
Dynabeads M-280 Strepavidin	Invitrogen, Life Technologies, Darmstadt, Germany
Dynabeads M-450 Epoxy	Invitrogen, Life Technologies, Darmstadt, Germany
ECL-Plus Western Blot Kit	Amersham, GE Healthcare Life Sciences, Freiburg, Germany
Fix&Perm Cell Permeabilization Kit	Life Technologies, Darmstadt, Germany
Gel and PCR Clean-up	NucleoSpin, Macherey-Nagel, Düren, Germany
Lineage Cell Depletion Kit	Miltenyi Biotec, Bergisch Gladbach, Germany
MinElute Reaction Cleanup Kit	Qiagen, Hilden, Germany
peqGold Cycle Pure Kit	peqLab, Erlangen, Germany
Qiagen Plasmid Maxi Kit	Qiagen, Hilden, Germany
QIAquick PCR Purification Kit	Qiagen, Hilden, Germany
RNAlater	Qiagen, Hilden, Germany
RNeasy Mini Kit	Qiagen, Hilden, Germany
TOPO TA Cloning Kit	Invitrogen, Life Technologies, Darmstadt, Germany

Table 2-4: Commercial Kits

2.1.6 Laboratory Equipment and Instruments

Equipment / Instrument	Manufacturer
Analytical balance, BP61	Sartorius Stedim Biotec, Göttingen, Germany
Autoclave, VX-95	Systec, Wettenberg, Germany
Blotting system, Criterion	Bio-Rad, Hercules, California, USA

Cell freezing container, Mr. Frosty	Nalgene, Thermo Fisher Scientific, Waltham, Massachusetts, USA
Cell Sorter, BD FACSAria II	BD, Franklin Lakes, New Jersey, USA
Centrifuge Heraeus Fresco 21, tabletop	Heraeus, Thermo Fisher Scientific, Waltham, Massachusetts, USA
Centrifuge, tabletop	Hettich, Tuttlingen, Germany
Centrifuge, Biofuge 15R, tabletop	Thermo Fisher Scientific, Waltham, Massachusetts, USA
Centrifuge, Minifuge RF	Heraeus, Thermo Fisher Scientific, Waltham, Massachusetts, USA
Centrifuge Megafuge 1.0R	Heraeus, Thermo Fisher Scientific, Waltham, Massachusetts, USA
Clean bench HERAsafe KS	Thermo Fisher Scientific, Waltham, Massachusetts, USA
CO_2 Incubator HERAcell 150i	Thermo Fisher Scientific, Waltham, Massachusetts, USA
Flow Cytometer, MACS Quant Analyzer	Miltenyi Biotec, Bergisch Gladbach, Germany
Fluorescence Microscope, Axioskop 2	ZEISS, Oberkochen, Germany
Horizontal Electrophoresis Systems	Bio-Rad, Hercules, California, USA
Hot Air Sterilizer, T12	Heraeus, Thermo Fisher Scientific, Waltham, Massachusetts, USA
Imaging System, Fusion-SL	peqLab, Erlangen, Germany
In Vivo Imaging System, IVIS Lumina Series II	PerkinElmer, Waltham, Massachusetts, USA
MACS MultiStand	Miltenyi Biotec, Bergisch Gladbach, Germany
MACS Separators	Miltenyi Biotec, Bergisch Gladbach, Germany
Magnetic Particle Concentrator, MPC-S	Invitrogen, Life Technologies, Darmstadt, Germany
Magnetic Stirrer, RCT basic	IKA, Staufen, Germany
Microplate Reader Infinite M200 Pro	Tecan, Männedorf, Switzerland
Microscope Olympus IX70	Olympus, Tokyo, Japan
Mini-Cell Electrophoresis System, XCell SureLock	Life Tehnologies, Darmstadt, Germany
Nano-Drop ND 1000 spectrometer	peqLab, Erlangen, Germany
pH-Meter	Knick, Berlin, Germany
Pipettes	Eppendorf, Hamburg, Germany
Pipetus	Hirschmann, Eberstadt, Germany
Pipet Stepper	Eppendorf, Hamburg, Germany
Power supply PowerPac	Bio-Rad, Hercules, California, USA
Scil Vet ABC (Animal Blood Counter)	Scil animal care company, Viernheim, Germany

Shaking Incubator	Edmund Bühler LabTec, Hechingen, Germany
Thermal Cycler Mastercycler Pro	Eppendorf, Hamburg, Germany
Thermomixer	Eppendorf, Hamburg, Germany
UV-Lamp	Konrad Benda, Wiesloch, Germany
Vacuum Pump	Integra Biosciences, Fernwald, Germany
Vortex	Roth, Karlsruhe, Germany
Water Bath	GFL, Burgwedel, Germany
XGI-8 anesthesia system	PerkinElmer, Waltham, Massachusetts, USA

Table 2-5: Laboratory Equipment and Instruments

2.1.7 Laboratory Supplies and Consumables

Supply / Consumable	Manufacturer
Blotting Sandwich Immobilon-P	Merck Millipore, Billerica, Massachusetts, USA
Combitips Advanced (1, 5 and 10ml)	Eppendorf, Hamburg, Germany
Conical Centrifuge Tubes (15 and 50ml)	Greiner Bio-One, Frickenhausen, Germany
C-Chip Disposable Hemocytometer, Neubauer improved	NanoEnTek, Seoul, Korea
Cryogenic Tubes (2ml)	Thermo Fisher Scientific, Waltham, Massachusetts, USA
Filter Cap Cell Culture flasks (25, 75 and 175cm^2)	Greiner Bio-One, Frickenhausen, Germany
Microvette CB 300 µl, K2 EDTA	Sarstedt, Nümbrecht, Germany
Nitril Gloves	Braun, Melsungen, Germany
Non-tissue culture plates (6 and 24 well)	Falcon, Corning, New York, USA
Pasteur Pipettes	Corning, New York, USA
Petri Dishes	Greiner Bio-One, Frickenhausen, Germany
Pipette tips (10, 100, 200 and 1000µl)	peqLab, Erlangen, Germany
Pipette tips (10, 100, 200 and 1000µl) aerosol-resistant	peqLab, Erlangen, Germany
Polystyrene Round-Bottom Tube (5ml)	Falcon, Corning, New York, USA
Reaction tubes (0.1, 0.2, 1.5 and 2ml)	Eppendorf, Hamburg, Germany
Scalpels	mediware Servoprax, Wesel, Germany
Serological pipettes (2, 5, 10 and 25ml)	Costar, Corning, New York, USA

Sterile cell strainer	BD, Franklin Lakes, New Jersey, USA
Sterile filters (0.22 and 0.45μm)	Merck Millipore, Billerica, Massachusetts, USA
Syringes (5,10 and 20ml)	Braun, Melsungen, Germany
Tissue culture dishes (10cm)	Greiner Bio-One, Frickenhausen, Germany
Tissue culture plates (6, 12, 24 and 96 well)	Costar, Corning, New York, USA
Tube 5ml, 75x12mm, PS	Sarstedt, Nümbrecht, Germany

Table 2-6: Laboratory Supplies and Consumables

2.1.8 Plasmids and Vectors

Plasmid name	Description	Reference
Eco-env	Expression plasmid for ecotropic envelope protein from MLV	Stitz, J., et al (134)
MP91-EGFP	Retroviral vector with a modified leader region MP91 (MPSV-LTR and MESV-leader), coding for IRES-EGFP with a 5' packaging signal	Schambach, A., et al (135)
MLV gag-pol	Expression plasmid for MLV Gag-Pol with SV40-Promotor	C.Baum (MHH)
MP91-TCL1A-EGFP	Retroviral vector containing human TCL1A-IRES-EGFP.	Cloned for this study.
MP91-myr-TCL1A- EGFP	Retroviral vector coding for human myristoylated (myr) TCL1A-IRES-EGFP.	Cloned for this study.
MP91-nls-TCL1A-EGFP	cDNA for human TCL1A, containing a nuclear localization sequence (nls), cloned into MP91-EGFP.	Cloned for this study.
MP91-MTCP1-EGFP	Retroviral vector coding for human MTCP1-IRES-EGFP.	Cloned for this study.
MP91-TML1-EGFP	Retroviral vector coding for human TML1-IRES-EGFP.	Cloned for this study.
MP91-T-Sapphire-Luc	Retroviral vector coding for T-Sapphire-IRES-Luc.	K.Cornils (University of Hamburg)
MP91-TCL1A-Luc	Retroviral vector coding for human TCL1A-IRES-Luc.	K.Cornils (University of Hamburg)

Table 2-7: Plasmids and Vectors

The used retroviral vectors are flanked by 5' and 3' long terminal repeats (LTR), responsible for gene expression, reverse transcription and viral integration. Furthermore, the internal ribosome entry site (IRES) allows co-expression of multiple genes, e.g. a reporter gene and a gene of interest. In the presented model, enhanced green fluorescent protein (EGFP) or firefly luciferase (luc) were used as reporter genes and TCL1 oncogenes were genes of interest. The

Woodchuck hepatitis virus posttranscriptional regulatory element (WPRE) further enhances gene expression. For plasmid maps, see Figure 5-1 in section 5.2.

2.1.9   Primary Cells and Cell Lines

Cells	Media	Description
Murine Splenocytes	RPMI 1640 Mouse Special	Isolated from spleen and LNs of OT-1 donor mice.
Murine HSCs/HPCs	StemSpan SFEM complete	Isolated from femur and tibia of B6 SJL donor mice.
HEK 293T	DMEM complete	Human embryonic kidney 293 cells containing the SV40 T-antigen (136).
SC1	DMEM complete	Mouse embryonic fibroblasts (137)
CTLL-2	IMDM CTLL-2	Mouse cytotoxic T-lymphocyte (138)

Table 2-8: Primary Cells and Cell Lines

2.1.10 Primer Sequences

Name	Sequence 5' → 3'	Application
A1 RV Biotin	(biotin) CTG GGG ACC ATC TGT TCT TGG CCC T	LM-PCR
A2 RV	AAC CTT GAT CTG AAC TTC TC	LM-PCR
A3 RV	CCA TGC CTT GCA AAA TGG C	LM-PCR
OC1 FW	GTA ATA CGA CTC ACT ATA GGG C	LM-PCR
OC2 FW	ACT ATA GGG CAG GCG TGG T	LM-PCR
Linker1 FW	GTA ATA CGA CTC ACT ATA GGG CAC TAT AGG GCA CGC GTG GT	LM-PCR
Linker2 RV	(phosphate) ACC ACG CGT GCC CTA TAG T	LM-PCR
M13_for (-40)	GTT TTC CCA GTC ACG AC	Colony PCR
M13_for (-20)	GTA AAA CGA CGG CCA G	Sequencing after Colony PCR
M13_rev	CAG GAA ACA GCT ATG AC	Colony PCR
Clonecheck FW	GTC TTG TCT GCT GCA GCA TC	Control PCR
Clonecheck RV	GCT TCG GCC AGT AAC GTT AG	Control PCR
TCL1A FW	ATC GGC GGC CGC ATC GCA TGG CCG AGT GCC CGA C	Vector cloning
TCL1A RV	ATC GGA ATT CAT CGG GCC GCC ACT GTG CTG GA	Vector cloning

myr-TCL1A FW	TGC AGC GGC CGC TGC AGG AGA CCC AAG CTG GCT AGT T	Vector cloning
myr-TCL1A RV	GCC ACT GTG CTG GAT ATC TGC	Vector cloning
nls-TCL1A FW	GAC TGC GGC CGC GAC TGG GAG ACC CAA GCT GGC TAG	Vector cloning
nls-TCL1A RV	GTC ATC TGG CAG CAG CTG GG	Vector cloning

Table 2-9: Primer Sequences

2.1.11 Media

Media	Composition
DMEM complete	DMEM with 10% Fetal bovine serum (FBS), 2% L-glutamine, 1% Penicillin/Streptomycin
RPMI 1640 complete	RPMI 1640 with 10% Fetal bovine serum (FBS), 2% L-glutamine, 1% Penicillin/Streptomycin
RPMI 1640 Mouse Special	RPMI 1640 with 10% Fetal bovine serum (FBS), 2% L-glutamine, 1% Penicillin/Streptomycin, 1% Non-essential amino acids, 1% Sodium pyruvate, 0,1% β-mercaptoethanol
StemSpan SFEM complete	StemSpan SFEM with 10% Fetal bovine serum (FBS), 2% L-glutamine, 1% Penicillin/Streptomycin, 10ng/ mIL3, 50ng/ml mIL-6, 50ng/ml mSCF.
IMDM CTLL-2	IMDM with 10% Fetal bovine serum (FBS), 2% L-glutamine, 1% Penicillin/Streptomycin, 0,1% β-mercaptoethanol, 300U IL-2/ml.

Table 2-10: Media

2.1.12 Mouse Strains

Name	Common Name	Distributor
C57BL/6J	Black 6 or B6	The Jackson Laboratory, Bar Harbor, Maine, USA
B6.SJL-Ptprc[a] Pepc[b]/BoyJ	B6 CD45.1 or B6 SJL	The Jackson Laboratory, Bar Harbor, Maine, USA
B6.129S7-Rag1tm1Mom/J	RAG1^{-/-}	The Jackson Laboratory, Bar Harbor, Maine, USA
C57BL/6-Tg (TcraTcrb) 1100Mjb/j	OT-1	The Jackson Laboratory, Bar Harbor, Maine, USA

Table 2-11: Mouse Strains

2.1.13 Tools and Software for Data Analysis

Tool / Software	Provider/Producer
DNAstar Lasergene SeqMan / EditSeq / SeqBuilder	DNASTAR, Inc., Madison, Wisconsin, USA
Expression Console™ Software	Affymetrix, Santa Clara, California, USA
FlowJo	TreeStar Inc, Ashland, Oregon, USA
GraphPad Prism	GraphPad Software Inc., La Jolla, California, USA
Living Image Software 4.0	PerkinElmer, Waltham, Massachusetts, USA
MACSQuantify Software	Miltenyi Biotec, Bergisch Gladbach, Germany
Mavric (Methods for analyzing viral integration clusters)	Departments of Haematology and Bioinformatics, Erasmus MC
PANTHER Classification System	Thomas et al, 2003 (139)
Transcriptome Analysis Console 3.0 Software	Affymetrix, Santa Clara, California, USA

Table 2-12: Tools and Software for Data Analysis

2.2   Methods

2.2.1   Molecular Biology

2.2.1.1   DNA digestion

Digestion of DNA with endonucleases was performed according to the manufacturer's protocol (New England Biolabs, Ipswich, Massachusetts, USA). Unless otherwise stated, reactions were incubated for 1 hour at 37°C in a total volume of 25μl.

2.2.1.2   Agarose gel electrophoresis

Standard agarose gel electrophoresis was carried out to separate DNA fragments. For preparation of the gel, agarose was dissolved in 1xTAE (Tris-acetate-EDTA) buffer by heating the agarose/buffer mixture in a microwave. Agarose concentration in the gel was typically between 1-2% (w/v). Afterwards, ethidium bromide (EtBr) was added to the mixture at a concentration of 2μg/ml to allow visualization of DNA under UV light exposure. The polymerized gel was then placed into an electrophoresis system with 1xTAE buffer, followed by loading of DNA samples mixed with 6x loading dye. DNA fragments were separated by running the gel at 100-120V for 30-60min, depending on the size of the desired fragments. These fragments were then visualized and documented in a Multi-Imaging System (Fusion-SL, peqLab, Erlangen, Germany).

2.2.1.3   Isolation of DNA fragments from agarose gels

Single DNA fragments were excised from agarose gels with a clean scalpel. DNA was isolated using a NucleoSpin Gel and PCR Clean-up Kit (Macherey-Nagel, Düren, Germany) by following the manufacturer's instructions.

2.2.1.4   Ligation of DNA-fragments with T4 DNA ligase

Ligation of insert-DNA into vector-DNA was performed according to the manufacturer's protocol using a molar ratio of 1:3 recipient vector to insert fragment. The reaction volume was increased to 25μl and incubated at 16°C overnight.

2.2.1.5   Baterial Transformation

For amplification, plasmid DNA was transformed into chemically competent *E.coli* TOP10 (Invitrogen). One vial of bacteria (50µl) was thawed and mixed with 100ng of plasmid DNA. The mix was kept on ice for 30min, followed by a short incubation at 42°C for 1min and another 2min on ice. Subsequently, 500µl LB medium was added to the bacteria and incubated at 37°C in a shaking incubator (200rpm) for 45min. Finally, 30-70µl of the bacteria mix were spread on LB plates supplemented with ampicillin and incubated at 37°C overnight. LB plates were examined for colony formation on the following day.

2.2.1.6   Preparation of plasmid DNA from bacteria cultures

After bacterial transformation, single colonies were picked from LB plates with a pipet tip and inoculated in 3ml LB medium supplemented with ampicillin. Bacterial cultures were kept in a shaking incubator (200rpm) at 37°C overnight. For small-scale DNA preparation, DNA was isolated from the overnight cultures using a JETquick Plasmid Miniprep Spin Kit (Genomed, Löhne, Germany) according to the manufacturer's protocol. For large-scale DNA preparation, 200µl from the overnight cultures were added to 200ml LB medium supplemented with ampicillin. The cultures were kept in a shaking incubator (200rpm) at 37°C overnight. DNA was isolated from these cultures using a Qiagen Plasmid Maxi Kit (Qiagen, Hilden, Germany) following the manufacturer's instructions. Finally, DNA concentrations were determined using a NanoDrop (peqLab, Erlangen, Germany).

2.2.1.7   DNA isolation from cell suspensions

For DNA isolation from single cell suspensions, $1x10^6$ to $5x10^6$ cells were pelleted and processed using a DNeasy Blood and Tissue Kit (Qiagen, Hilden, Germany) according to the manufacturer's protocol. DNA was eluted with 50µl H_2O and DNA concentration was determined using a NanoDrop (peqLab, Erlangen, Germany).

2.2.1.8   DNA sequencing

For DNA sequencing at an external sequencing facility (Eurofins Genomics, Ebersberg, Germany), a sequencing reaction mix was prepared using 50-100ng/µl plasmid DNA or 2-10ng/µl purified PCR product in a total volume of 15µl and adding 2µl primer (10µM). This

facility performs Sanger sequencing using an Applied Biosystems 3730xl DNA Analyzer (Life Technologies, Darmstadt, Germany).

2.2.1.9   Polymerase chain reaction (PCR)

For DNA amplification, PCR reactions were prepared using a Taq Polymerase (Table 2-13). The reaction tubes were transferred to a thermocycler. The used thermocycler program is shown in Table 2-14. Annealing temperature was adjusted to the melting temperatures of the forward and reverse primer.

Amplification buffer (10x) (Buffer A)	5µl
Forward Primer (10µM)	1µl
Reverse Primer (10µM)	1µl
Taq Polymerase	0.4µl
dNTPs (10mM)	1.5µl
H_2O	40.1µl
DNA template (50-100ng/µl)	1µl

Table 2-13: PCR Reaction

95°C	3min	Initial Denaturation	
95°C	30sec	Denaturation	
45-68°C	30sec	Annealing	30 cycles
72°C	1min	Elongation	
72°C	3min	Final Elongation	

Table 2-14: Thermocycling Conditions

2.2.1.10   Ligation-mediated PCR (LM-PCR)

Ligation-mediated PCR was performed to determine retroviral integration sites. Therefore, DNA was isolated from single cell suspensions of developed tumors (see section 2.2.1.7). The genomic DNA (250-1000ng) was then digested with the restriction enzyme Tsp5091 (New England Biolabs, Ipswich, Massachusetts, USA) that cuts upstream from the LTR within the proviral sequence. Afterwards, the digestion mix was cleaned up using a MinElute

Reaction Cleanup Kit (Qiagen, Hilden, Germany). Next, the fragments containing LTR-genomic DNA junctions were tagged with a biotinylated LTR-specific primer using a high fidelity DNA polymerase (Finnzymes, New England Biolabs, Ipswich, Massachusetts, USA). The product was cleaned up using a MinElute Reaction Cleanup Kit (Qiagen, Hilden, Germany), followed by incubation with streptavidin-coated beads (Invitrogen, Life Technologies, Darmstadt, Germany) at room temperature for 60min. Afterwards, the mix was washed several times using a magnetic particle concentrator to remove unbound DNA fragments. To be able to specifically amplify the isolated DNA fragments, an adapter oligonucleotide cassette of known sequence was ligated to the fragments using a T4 DNA ligase (New England Biolabs, Ipswich, Massachusetts, USA). After washing the reaction mix, a PCR and a nested PCR (Extensor Hi-Fidelity PCR Master Mix 1, Thermo Fisher Scientific, Waltham, Massachusetts, USA) were performed with oligonucleotides that specifically bind to the adaptor region. PCR products were analyzed by gel electrophoresis (see section 2.2.1.2). Single bands were cut out of the gel and cleaned up (see section 2.2.1.3). The product was then subcloned into a pCR2.1 TOPO vector (Life Technologies, Darmstadt, Germany) following the manufacturer's protocol. Finally, the product was transformed into TOP10 *E.coli* bacteria (see section 2.2.1.5).

2.2.1.11   Colony PCR

After LM-PCR and transformation of subcloned DNA fragments into bacteria, single colonies were picked and incubated in 50μl PCR reaction mix for 2min. During the following PCR, primers specifically bind to the TOPO plasmid and allow amplification of a single DNA fragment isolated during LM-PCR. Typically, 10 clones were picked per sample. Finally, the PCR reaction was cleaned up using NucleoSpin Gel and PCR Clean-up Kit (Macherey-Nagel, Düren, Germany) and send to an external sequencing facility for DNA sequencing (see section 2.2.1.8).

2.2.1.12   Integration Site Analysis

During the previously described LM-PCR and colony PCR, retroviral integration sites within the murine genome were isolated and amplified. The resulting DNA sequences contain parts of the proviral LTR on one side and the ligated adapter molecule on the other side. These

sequences were removed from the amplicon using Lasergene's DNAStar SeqMan tool. The remaining sequence was then uploaded to the online tool Mavric (Departments of Haematology and Bioinformatics, Erasmus MC) to analyze the retroviral integration site in terms of exact integration locus, chromosomal location, surrounding genes, distance to surrounding genes and orientation. Thereby, genes 250kb up- and downstream of the integration site were included in this analysis. To further analyze these genes, 'Entrez Gene' IDs were entered into the online PANTHER Gene Ontology database (version 10.0) and characterized in terms of pathways, biological processes and molecular functions. As a reference dataset the 'NCBI build 37 mouse genome' was used.

2.2.1.13 Western Blot

For protein expression analysis by Western Blot, $1x10^6$ cells were resuspended in 100µl cell lysis buffer (including protease inhibitors). The mix was kept at 99°C for 10min. Afterwards, samples were loaded onto 4-12% or 12% Bis-Tris Protein Gels (NuPage, Life Technologies, Darmstadt, Germany), depending on protein size. Gel electrophesis was performed at 40mA for 90min. Subsequently, proteins were eletrophoretically transferred from the polyacrylamide gel onto a polyvinylidene fluoride (PVDF) membrane (Immobilon, Merck Millipore, Billerica, Massachusetts, USA). The membrane was blocked with 1x Roti-Block (Roth, Karlsruhe, Germany) for one hour at room temperature to reduce nonspecific antibody binding. Afterwards, the membrane was incubated with the primary antibody at 4°C overnight. On the following day, the membrane was washed and then incubated with the secondary antibody for 2 hours. For chemiluminescent protein detection, the membrane was treated with the ECL-Plus Western Blot Kit (GE Healthcare Life Sciences, Freiburg, Germany) according to the manufacturer's protocol and analyzed with a Multi-Imaging System (Fusion-SL, peqLab, Erlangen, Germany).

2.2.1.14 Gene Expression Analysis

For gene expression analysis, RNA was isolated from $2x10^5$ cells using the RNeasy Mini Kit (Qiagen, Hilden, Germany). After transcription into cDNA, samples were hybridized onto Mouse Gene 1.0 ST Arrays (Affymetrix, Santa Clara, California, USA). Data normalization

and quality control was done using the Affymetrix Expression Console Software. The Affymetrix Transcriptome Analysis Console 3.0 Software was used for data analysis.

2.2.2 Cell culture

2.2.2.1 Cell line culture

The adherent cells lines HEK 293T and SC-1 were cultured in DMEM complete medium (see section 2.1.11). HEK293T cells were passaged when 80% confluent to a ratio of 1:5, typically every 2-3 days. Similarly, SC-1 were subcultured at a 1:10 ratio. Both adherent cell lines were detached from the culture flask by using Trypsin-EDTA. The suspension cell line CTLL-2 was cultured in IMDM CTLL-2 medium (see section 2.1.11). Cultures were maintained at a density of $1x10^5$ to $1x10^6$ cells/ml by replacement of medium every 2-3 days. All cell lines were kept in an incubator at 5.9% CO_2 and 37°C.

2.2.2.2 Primary single cell suspensions

Primary cells were isolated from murine spleen, LN, BM, liver and thymus by squeezing the tissue through a 100μm cell strainer with a syringe plunger. Erythrocytes were removed from cell suspensions using 1x lysing buffer (BD, Franklin Lakes, New Jersey, USA). Cells were washed with PBS before further use.

2.2.2.3 Primary murine HSC / HPC culture

Primary hematopoietic stem cells (HSC)/hematopoietic progenitor cells (HPC) were isolated from tibias and femurs of B6 SJL mice (see section 2.2.2.2). After lysis and washing, BM cells were depleted of lineage-committed cells using a Lineage Cell Depletion Kit (Miltenyi Biotec, Bergisch Gladbach, Germany) according to the manufacturer's instructions. Enriched lineage negative cells were resuspended in StemSpan SFEM complete at a density of $1x10^6$ cells per ml (see section 2.1.11).

2.2.2.4   Primary murine OT-1 T-cell culture

Primary murine mononuclear cells were isolated from spleen and LNs of OT-1 mice as described before (see section 2.2.2.2). After washing with PBS, cells were resuspended in RPMI mouse special medium (see section 2.1.11) at a density of $2.5x10^6$ cells per ml. Medium was additionally supplemented with ovalbumin (OVA) peptide (257-264) (10ng/ml) and IL-2 (10U/ml).

2.2.2.5   Flow Cytometry

Fluorescence activated cell sorting (FACS) was performed to either sort specific cell populations or analyze extra- and intracellular marker expression. Typically, $1\text{-}3x10^7$ cells were used for cell sorting and $0.5\text{-}1x10^6$ cells for flow cytometric analysis. For extracellular staining, $1x10^6$ cells were resuspended in 100µl PBS with 1µl FcR Blocking Reagent and 0.05-0.5ug antibody. Samples were incubated in the dark for 15min and washed twice with PBS. Cells were analyzed or sorted in PBS with 2% FCS and at a density of $1x10^7$ per ml. For intracellular staining, $1x10^6$ cells were treated with the Fix&Perm Cell Permeabilization Kit (Life Technologies, Darmstadt, Germany) following the manufacturer's protocol.

For intracellular staining of phosphorylated protein, $1\text{-}2x10^6$ cells were resuspended in 1x pre-warmed lyse/fix buffer (BD, Franklin Lakes, New Jersey, USA) and incubated at 37°C for 10min. Afterwards cells were washed with stain buffer (500ml PBS, 2,2ml sodium azide, 15ml FCS). Cells were then incubated with Perm Buffer III (BD, Franklin Lakes, New Jersey, USA) on ice for 30min. Subsequently cells were washed twice with stain buffer and then stained with 5µl phospho-antibody. After another 30min of incubation, cells were washed once with stain buffer before analysis.

Antibodies used for FACS staining are shown in Table 2-1. Flow cytometric analysis was performed on a MACSQuant Analyzer (Miltenyi Biotec, Bergisch Gladbach, Germany) and cell sorting on a BD FACSAria II (BD, Franklin Lakes, New Jersey, USA).

2.2.2.6   Retroviral vector production

For production of replication-defective retroviral vectors, a split packaging approach was followed. Genes encoding for the gene of interest, envelope proteins (Env) and structural and enzymatic proteins (Gag/Pol) were kept on separate plasmids. Only the plasmid encoding the

gene of interest contained the packaging signal Ψ that allowed packaging into the viral capsid during replication. Consequently, the produced retroviral vectors lacked Env and Gag/Pol genes that are necessary for further replication.

One day before transfection, 5×10^6 cells of the packaging cell line HEK293T were seeded in a 10cm tissue culture dish. The following day, 75µM chloroquine was added to the medium and cells were transfected using a Calcium Phosphate Transfection Kit (Sigma-Aldrich, St.Louis, Missouri, USA). Therefore, 7.5µg transfer vector, 12.5µg packaging plasmid (Gag/Pol) and 1µg envelope (Env) plasmid in 450µl H_2O were mixed with 50µl $CaCl_2$ (2.5M) and added dropwise to 500µl 2x HEPES buffer while bubbling. The DNA mix was kept at room temperature for 20min and then added to the cells. After 6 hours of incubation the medium was replaced with 5ml DMEM complete medium. Supernatant was collected 24, 36 and 48 hours after transfection, filtered through a 0.45µm syringe filter and stored at 4°C (short-term) or -20°C (long-term).

2.2.2.7   Retroviral vector titration

For titration of retroviral supernatants, 5×10^4 SC1 cells were seeded in a 24-well tissue culture treated plate. The next day, supernatant was added to the cells using dilutions from 1:1 to 1:100. The culture plate was centrifuged at 2000rpm and 31°C for 1hour. Transduction efficiencies were determined by flow cytometry 2 days later. The viral titer per ml was calculated as follows: (Percentage of fluorescent cells/100) x number of seeded cells x dilution factor.

2.2.2.8   Retroviral transduction on retronectin-coated plates

Transduction of cell lines and primary cells was performed on retronectin-coated 6- or 24-well plates. Therefore, 1ml (6-well) or 0.4ml (24-well) retronectin (50µg/ml) were added to each well and incubated at room temperature for 2 hours or at 4°C overnight. Afterwards, plates were blocked with 2% BSA in PBS at room temperature for 30min. Plates were washed once with 1x HBSS and once with PBS. Subsequently, 1-5ml retroviral supernatant was added to the treated wells and centrifuged at 3100rpm and 31°C for 90min. Supernatant was removed before adding cells to the wells. For transduction of HSCs/HPCs (see section 2.2.2.3), 1×10^6 cells were added to each 24-well the day after cell isolation. These cells were

only transduced once. OVA-stimulated OT-1 T cells (see section 2.2.2.4) were transduced in 3ml medium on a retronectin-coated 6-well plate at a density of 1.5×10^6 cells per ml. Transduction was repeated 24 hours after the first transduction. For transduction of the murine cell line CTLL-2, 3ml cell suspension was added to a coated 6-well plate at a density of 2×10^5 cells per ml.

2.2.3 Animals experiments

2.2.3.1   Animal use

Laboratory mice were kept in the animal facility of the Georg-Speyer-Haus (Frankfurt am Main) in individually ventilated cages (IVC). All animal use was approved by the regional authority (Regierungspräsidium, Darmstadt, Germany/Tierversuchsnummer: F21/03; FK/1050), and animals were maintained and killed in accordance with the guidelines of the Federation of European Laboratory Animal Science Associations (FELASA).

2.2.3.2   Transplantation of HSCs/HPCs

After isolation (see section 2.2.2.3) and transduction (see section 2.2.2.8) of HSCs/HPCs, cells were analyzed for transduction efficiency and HSC/HPC marker expression (Sca-1, c-Kit) before transplantation into recipient mice. C57BL6 (CD45.2) recipient mice were irradiated with a split dose of 5.5Gy each, with 24 hours between doses, using a BIOBEAM 2000 Cs-137 chloride gamma irradiator (Eckert & Ziegler, Berlin, Germany). One hour after the last dose, 1×10^6 cells were transplanted into each recipient mouse.

2.2.3.3   Transplantation of OT-1 T cells

After isolation (see section 2.2.2.4) and two rounds of transduction (see section 2.2.2.8), OT-1 T cells were analyzed for transduction efficiency and lymphocyte marker expression (CD3, CD4, CD8, CD19, Vα2 TCR, Vβ5 TCR). Afterwards, 5×10^6 cells were injected intravenously into each RAG1$^{-/-}$ recipient.

2.2.3.4 Blood collection from mice

Blood samples were taken from recipient mice of transduced HSCs/HPCs or OT-1 T cells to monitor for repopulation and lymphoma/leukemia development. Therefore, the lateral tail vein was gently nicked with a clean scalpel and 25-100µl blood were collected using EDTA-coated microvettes (Sarstedt, Nümbrecht, Germany). Blood samples were prepared for flow cytometric analysis by lysing erythrocytes using 1x lysing buffer (BD, Franklin Lakes, New Jersey, USA).

2.2.3.5 In vivo proliferation assay

To analyze proliferation of OT-1 T cells upon OVA stimulation in vivo, freshly isolated OT-1 splenocytes (CD45.2) were stained with CellTrace Violet (Life Technologies, Darmstadt, Germany) according to the manufacturer's protocol and $1x10^6$ cells transplanted into B6 SJL (CD45.1) mice. After transplantation, mice were injected with 25µg OVA/IFA or PBS/IFA (see section 2.2.3.6). Two and five days later mice were sacrificed. Single cell suspensions of the spleen were stained with CD3 and CD45.2 and analyzed by flow cytometry.

2.2.3.6 Stimulation of OT-1 T-cell recipient mice

For specific OT-1 T-cell stimulation, OT-1 T-cell recipient mice (see section 2.2.3.2) were injected intraperitoneally (i.p.) with 25µg OVA (257-264) in PBS mixed in a 1:1 ratio with incomplete Freund's adjuvant (IFA) every two weeks. Control mice received PBS/IFA (1:1) injections.

2.2.3.7 Necropsy of mice

Mice were anesthetized with isoflurane prior to euthanasia by cervical dislocation. The thoracic cavity was opened immediately afterwards to allow blood collection via cardiac puncture. The mouse abdomen was opened through midline incisions of the skin and peritoneum. The organs were examined for macroscopic abnormalities. Spleen, liver, lung, LNs (inguinal, axillary, mesenteric), kidney, femur and tibia were isolated for flow cytometric and/or histological analysis.

2.2.3.8   Histological analysis

For histological analysis, organs were fixed in 4% formaldehyde solution overnight. Fixed tissue was then placed into embedding cassettes, dehydrated and finally embedded in paraffin. Paraffin blocks were cut with a microtome into 5-10μm thick sections. Sections were stained with hematoxylin/eosin (HE) and TCL1A. Sample processing and staining was done in the Senckenberg Institute of Pathology, Frankfurt am Main, Germany. Histological examination was performed by Prof. Dr. Dr. h.c. Martin-Leo Hansmann and Dr. Sylvia Hartmann.

2.2.3.9   Bioluminescence Imaging

In vivo imaging was performed for recipient mice of OT-1 T cells transduced with luciferase vectors four weeks after transplantation and repeated every four weeks. Therefore, mice were placed in a XGI-8 anesthesia system (PerkinElmer, Waltham, Massachusetts, USA) flooded with isoflurane gas. Anesthetized mice were shaved and injected i.p. with 150μl D-Luciferin (15mg/ml). Mice were then moved to the IVIS Imaging System Lumina II (PerkinElmer, Waltham, Massachusetts, USA) and imaged 10min after i.p. injection of D-Luciferin. Images were taken in ventro-dorsal and latero-lateral position and acquired after an exposure time of 2 and 5 minutes using binning 4. Signal intensity was quantified as average radiance of photons emitted per second and area (p/s/cm²/sr) within a region of interest (ROI) using the Living Image Software 4.0 (PerkinElmer, Waltham, Massachusetts, USA).

3.   Results

Syngeneic mouse models using genetically manipulated grafts, offer a valuable method to study and compare cellular transformation in vivo. Therefore, a transplantation model established by Newrzela et al using gamma retroviral vectors to introduce oncogenes into HSCs/HPCs and T cells (44) was utilized in this thesis to study oncogenic properties of TCL1 family members (section 3.2.2) and variants (sections 3.2.3-3.2.6) in HSCs/HPCs, and the cooperation of TCL1 and TCR signaling in monoclonal T cells (section 3.3).

3.1   Cloning of retroviral vectors and validation

For retroviral gene transfer of the different TCL1 family members and variants, gamma-retroviral vectors encoding human TCL1A, TML1, MTCP1, myr-TCL1A and nls-TCL1A were generated (Figure 3-1). Therefore, all cDNAs were cloned in front of the IRES of the previously described gamma retroviral vector MP91-EGFP using the restriction sites EcoRI and NotI (44). The cDNA of human TCL1A and variants were obtained from Michael Teitell, MD (UCLA, USA). The cDNAs of human MTCP1 and human TML1 were purchased from Life Technologies (Darmstadt, Germany) and Source BioScience (Nottingham, UK), respectively. MP91-EGFP was used as a control vector and referred to as "EGFP only" hereafter. For in vivo imaging experiments, EGFP was replaced with a firefly luciferase reporter and either T-Sapphire or human TCL1A were cloned in front of the IRES. Luciferase vectors were cloned and provided by Kerstin Cornils, PhD (University of Hamburg). Figure 3-1 shows the design of retroviral vectors used in this thesis.

Successful cloning of retroviral vectors was verified by sequence analysis (data not shown). Additionally, protein expression of our genes of interest was confirmed by Western Blot analysis (Figure 3-2). Comparison of the protein expression level induced by the different TCL1A variants showed that myr-TCL1 was slightly higher expressed than generic TCL1A and nls-TCL1A (Figure 3-2C).
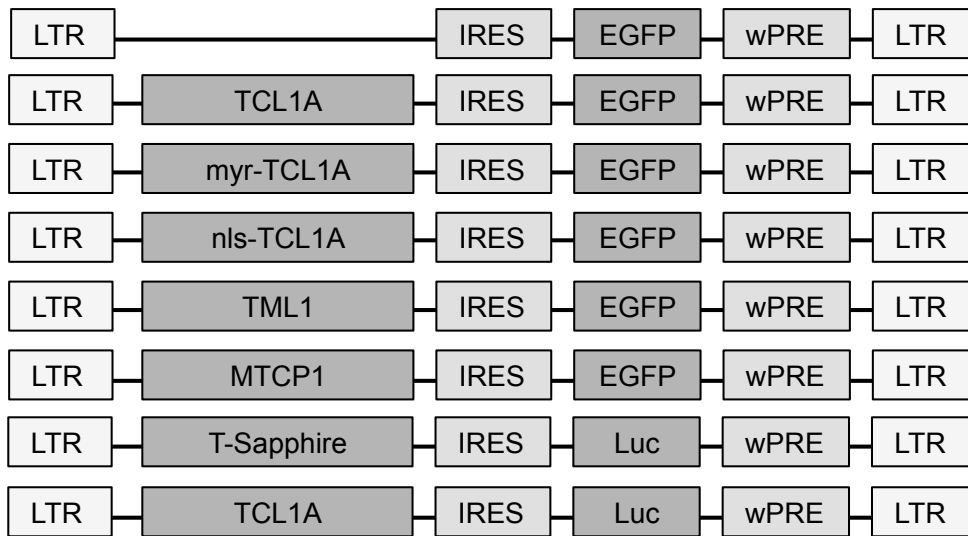
Figure 3-1: Design of retroviral vectors
cDNAs of human TCL1A, myr-TCL1A, nls-TCL1A, MTCP1 and TML1 were cloned into the gamma retroviral vector MP91-EGFP / MP91-Luc. LTR: long terminal repeats. IRES: internal ribosomal entry site. wPRE: Woodchuck hepatitis virus posttranscriptional regulatory element.
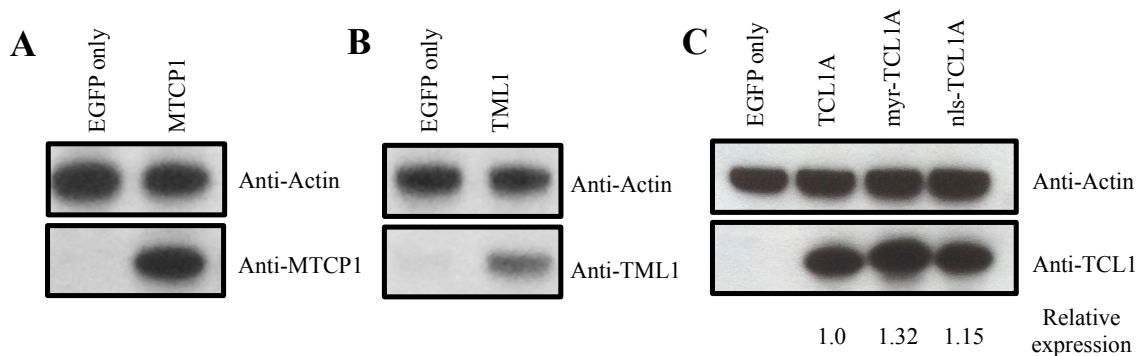
Figure 3-2: Protein expression of transgenes
Western blot analysis of transgene expression in SC-1 cells transduced with MTCP1 (A), TML1 (B), TCL1A and its variants myr-TCL1A and nls-TCL1A (C).

3.2 Targeted expression of TCL1 family members and variants in HSCs/HPCs

3.2.1 Transgene expression in mice

To introduce TCL1 family members and variants into HSCs/HPCs, BM cells from C57BL/6 mice (CD45.1) were depleted of lineage-committed cells (Lin⁻ BM cells), transduced and 1×10^6 cells were then transplanted into C57BL/6 (CD45.2) recipient mice (Figure 3-3).
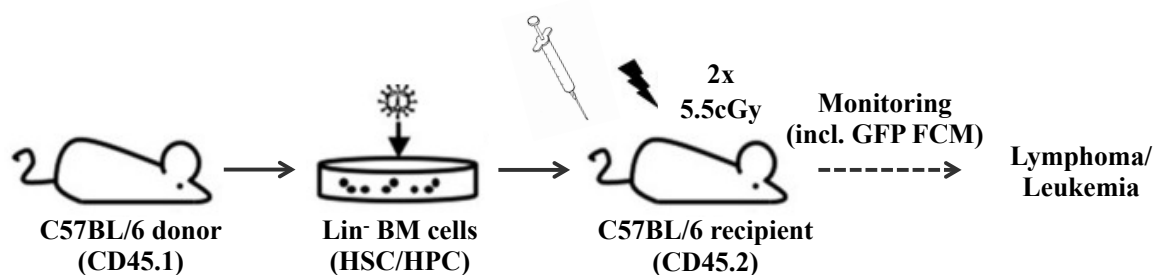
Figure 3-3: Experimental design of the HSC/HPC transplantation model
C57BL/6 (CD45.1) mice were used as donors for Lin⁻ depleted BM cells. These isolated cells were retrovirally transduced and kept in culture for 2 days followed by transplantation into lethally irradiated C57BL6 (CD45.2) mice. Mice were monitored by blood sampling and analyzed after lymphoma/leukemia development.

Before transplantation into mice, cells were analyzed for transduction efficiency (Figure 3-4A). For all constructs, the HSC/HPC culture showed comparable transduction efficiencies (52-65%). To monitor repopulation of donor HSC/HPC-derived lymphocytes, blood samples were taken from recipient mice six weeks after transplantation and analyzed by flow cytometry. Blood samples were stained with the T-cell marker CD3 and the B-cell marker CD19. Transgene (EGFP) expressing T and B cells were detectable in the PB of recipient mice as shown in Figure 3-4B.
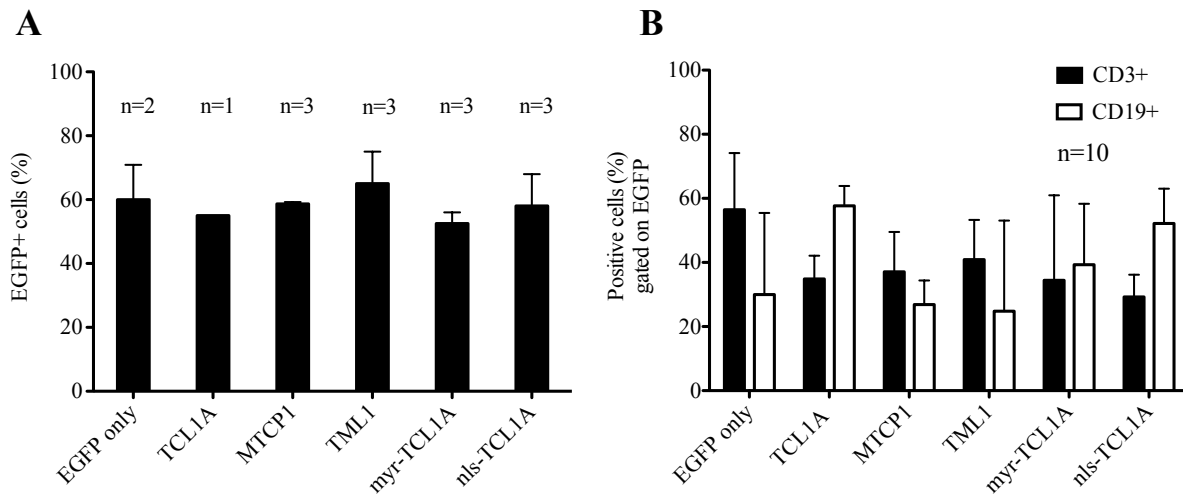
Figure 3-4: Transduction efficiency and repopulation of HSCs/HPCs
(A) Percentage of EGFP+ cells within HSC/HPC transplants transduced with TCL1 family members (TCL1A, MTCP1, TML1) and TCL1A variants (myr-TCL1A, nls-TCL1A). (B) Blood samples from HSC/HPC recipient mice were analyzed by flow cytometry for EGFP expressing CD3+ T cells and CD19+ B cells six weeks after transplantation. Error bars represent SD.

3.2.2 TCL1A and MTCP1 are oncogenes with similar oncogenic potential

After transplantation of TCL1A, MTCP1, and TML1 transduced HSCs/HPCs, recipient mice developed lymphoid malignancies after latencies between seven and 18 months (Figure 3-5, Table 3-1).

TCL1A HSC/HPC recipient mice developed lymphoma / leukemia after a median latency of 388 days (Figure 3-5). These mice showed an enlarged liver and spleen as well as enlarged mesenteric, inguinal, and/or axillary LNs (Table 3-1, Figure 3-7). All TCL1A mice displayed a leukemic WBC higher than $15x10^6$ cells per µl peripheral blood (Table 3-1).
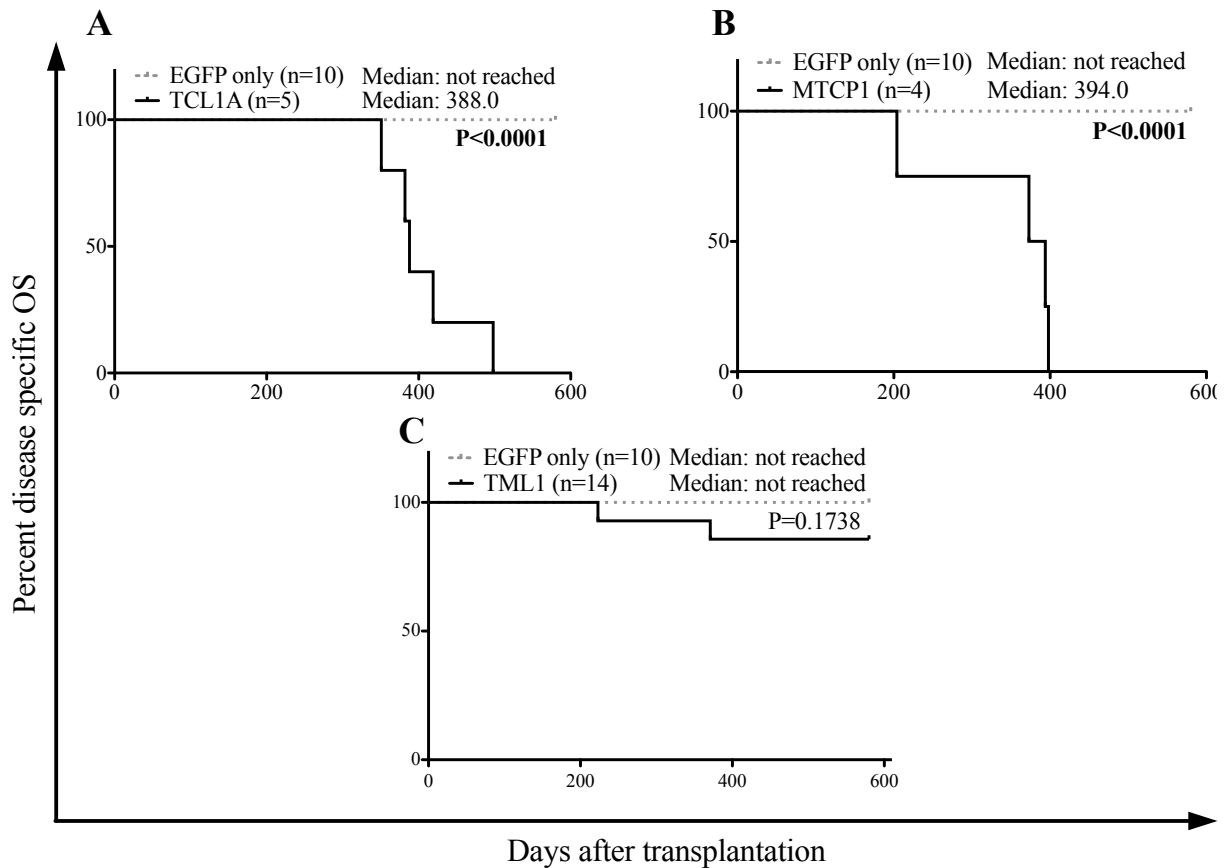
Figure 3-5: Survival of TCL1 family mice
Animals that received human TCL1A (A), MTCP1 (B) and TML1 (C) transduced HSCs/HPCs developed lymphoma/leukemia after indicated latencies (black solid line, A-C). Control animals (EGFP only) did not show any signs of disease during the observation time (grey dotted line, A-C).

The phenotype of these tumors was determined by flow cytometric analysis, staining for the basic lymphocyte markers CD3, CD4, CD8, and CD19. Additionally, the leukocyte markers CD45.1 and CD45.2 were analyzed to differentiate between recipient-derived (CD45.2) and donor-derived (CD45.1) cells. All tumor cells isolated from TCL1A recipient mice were positive for CD19 and CD45.1. This B-cell phenotype was further characterized using the following markers: CD5, IgM, CD21/35, B220, and CD138 (Table 3-2). The tumor cells did not express the plasma cell marker CD138 and the splenic marginal zone B-cell markers CD21/35. Positive staining was observed for B220 and surface IgM. Tumor cells in most mice expressed CD5 as well (Table 3-2).

Oncogene	Gross-anatomic features	Elevated PB leukocyte count (15×10^6 cells/µl)	CD4/8 DP	CD19
TCL1A	Hepatomegaly, Splenomegaly, Lymphadenopathy.	5/5	0/5	5/5
MTCP1	Thymoma (CD4/8DP). Hepatomegaly, Splenomegaly, Lymphadenopathy (CD19).	4/4	1/4	3/4
TML1	Thymoma	2/2	2/2	0/2

Table 3-1: Phenotypes and WBC of tumors induced by TCL1 family genes
DP=double positive.
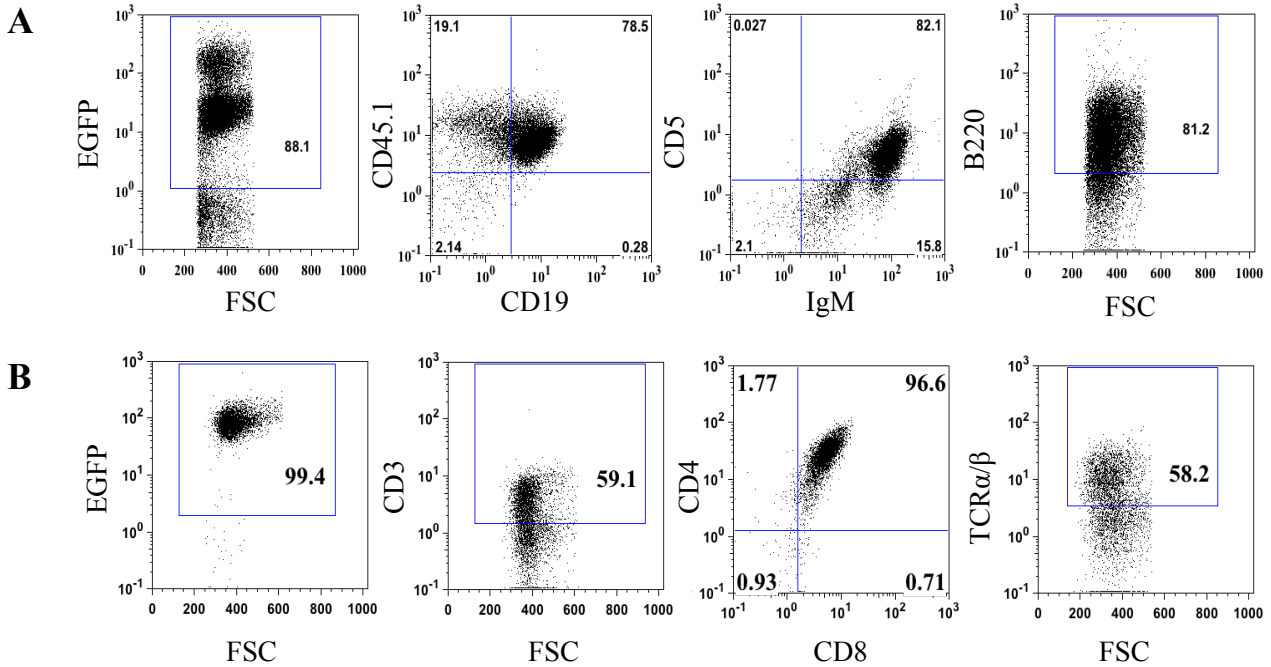
Figure 3-6: Flow cytometric analysis of tumors induced by TCL1 family genes
Representative FACS plots of analyzed B-cell tumors (A) and T-cell tumors (B) gated on EGFP positive cells.

MTCP1 HSC/HPC recipient mice developed lymphoma/leukemia after a median latency of 394 days (Figure 3-5). Similar to TCL1A recipient mice, mice developed mostly B-cell malignancies (CD19$^+$, B220$^+$, IgM$^+$, CD5$^-$) with elevated WBC and enlarged liver, spleen and LNs (Table 3-1). Only one recipient showed an enlarged thymus with a CD3$^+$ and CD4/CD8 DP phenotype.

Only two out of 14 TML1 recipient mice developed lymphoma/leukemia, becoming overt at 223 and 371 days after transplantation (Figure 3-5). Therefore, no median survival was reached. The diseased mice displayed enlarged thymi with a CD4/8 DP phenotype, and varying CD3$^+$ and TCR$\alpha\beta^+$ expression (Table 3-1, Figure 3-6B).

Oncogene	CD19	B220	IgM	CD5	CD138	CD21/35
TCL1A	5/5	5/5	5/5	4/5	0/5	0/5
MTCP1	4/4	4/4	3/4	0/4	0/4	0/4

Table 3-2: Phenotype of B-cell tumors induced by TCL1 family members

Sick mice with B-cell malignancies presented with variable hepatomegaly, splenomegaly and lymphadenopathy. Round lymphoblasts with scant cytoplasm were visible in spleen, LN, and liver (Figure 3-7A,B), and were also abundant in blood (Figure 3-8A). Additionally, macroscopic lesions and microscopic infiltrations were often visible in lung and kidney of mice with B-cell malignancies (not shown). Mice with immature T-cell malignancies showed enlarged thymi and mostly no other macroscopic visible abnormalities (Figure 3-7C). Tumor cells had a round lymphoblastoid morphology in thymus (Figure 3-7C) and blood (Figure 3-8B), similar to the one seen in B-cell tumors.

TCL1A-induced tumors were further analyzed for expression of TCL1A by flow cytometry (Figure 3-9A) and by immunohistochemical stainings (Figure 3-9B). All tumors expressed TCL1A and signals were observed in the cytoplasmic and nuclear compartments (Figure 3-9B). A representative plot/image is shown in Figure 3-10.

A Spleen / LN

B Liver

C Thymus
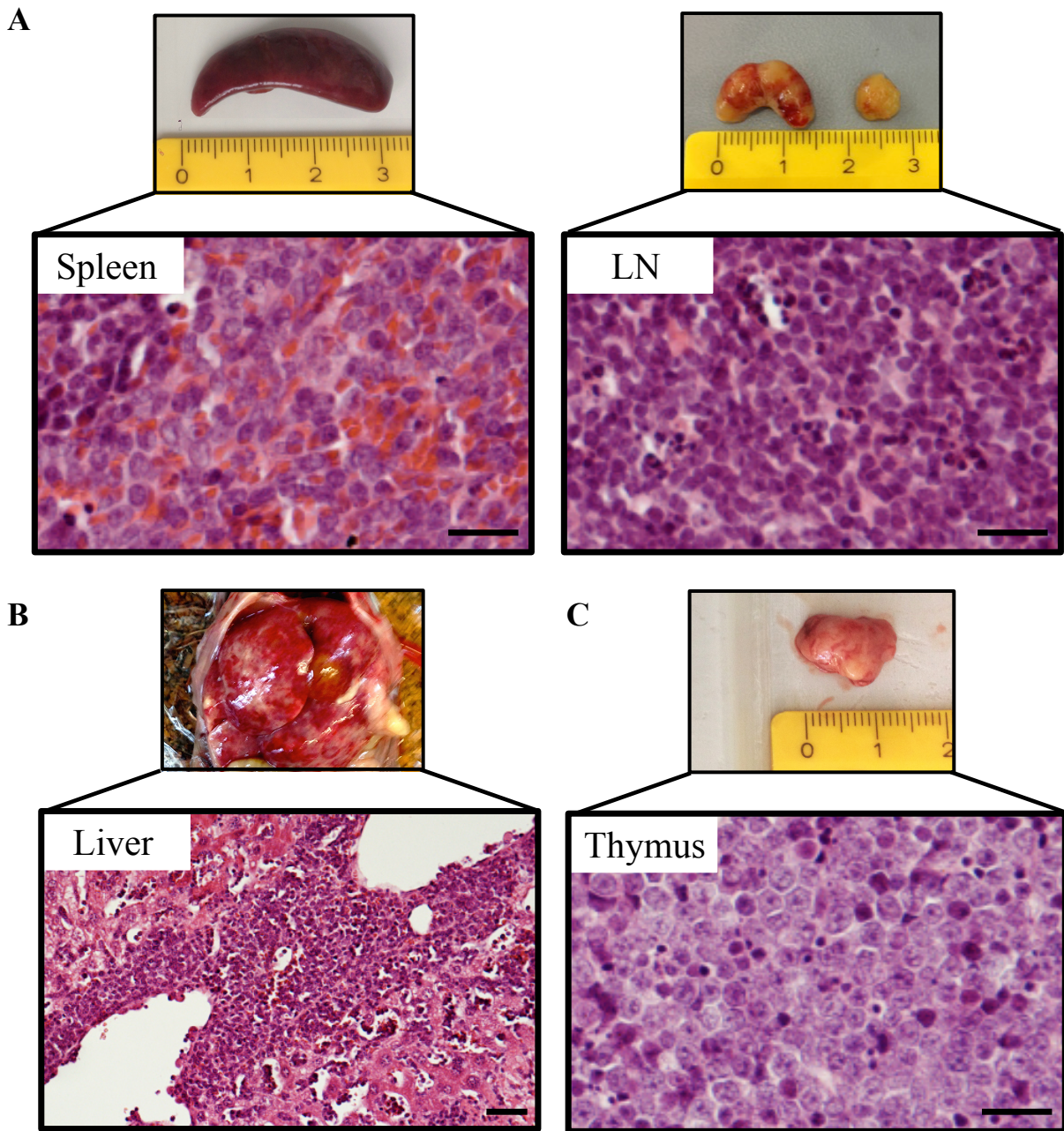
Figure 3-7: Gross-anatomic and histological features of B-cell and immature T-cell malignancies induced by TCL1 family genes

Representative macroscopic images and H&E stained histological sections of animals with B-cell malignancies showing enlarged spleens, LNs (A) (original magnification 20x) and livers (B) (original magnification 10x); and animals with immature T-cell malignancies showing enlarged thymi (C) (original magnification 20x). Scale bar: 20µm.

A PB

B PB
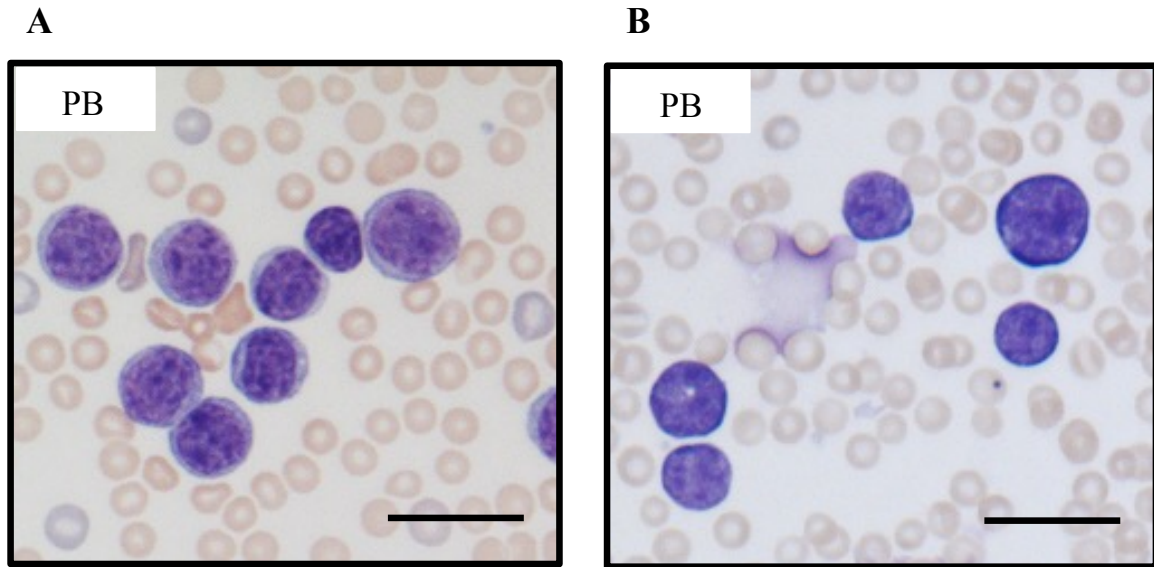
Figure 3-8: Cytological features in blood smears of TCL1A recipient mice upon tumor development
Representative blood smears of animals with B-cell malignancies (A) and with immature T-cell malignancies (B). Original magnification: 40x. Scale bar: 20µm.

A

B
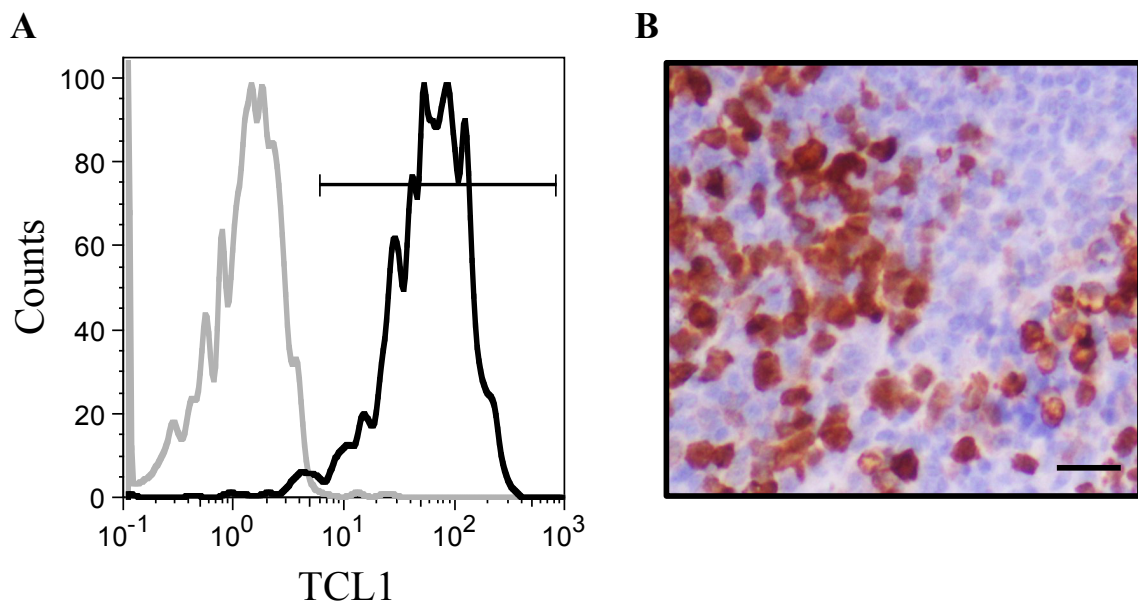
Figure 3-9: TCL1A expression in TCL1A-induced tumors
Intracellular TCL1A staining of the blood gated on EGFP+ cells (black line) and EGFP- cells (grey line) (A). Representative immunohistochemical staining for TCL1A of tumor bearing LN (original magnification: 20x, scale bar: 20µm) (B).

3.2.3 Targeted expression of TCL1A to the membrane and the nucleus

Engagement of the TCR in T-PLL cells leads to TCL1A recruitment to the cell membrane and later to the nucleus (22). The changing localization of TCL1A during TCR signaling suggests that the protein participates in this process by interacting with different proteins along the signaling cascade. To address the functional impact of TCL1A localization on its oncogenic potential, retroviral vectors containing modified TCL1A transgenes were used to target protein expression to the membrane (myr-TCL1A) or the nucleus (nls-TCL1A).
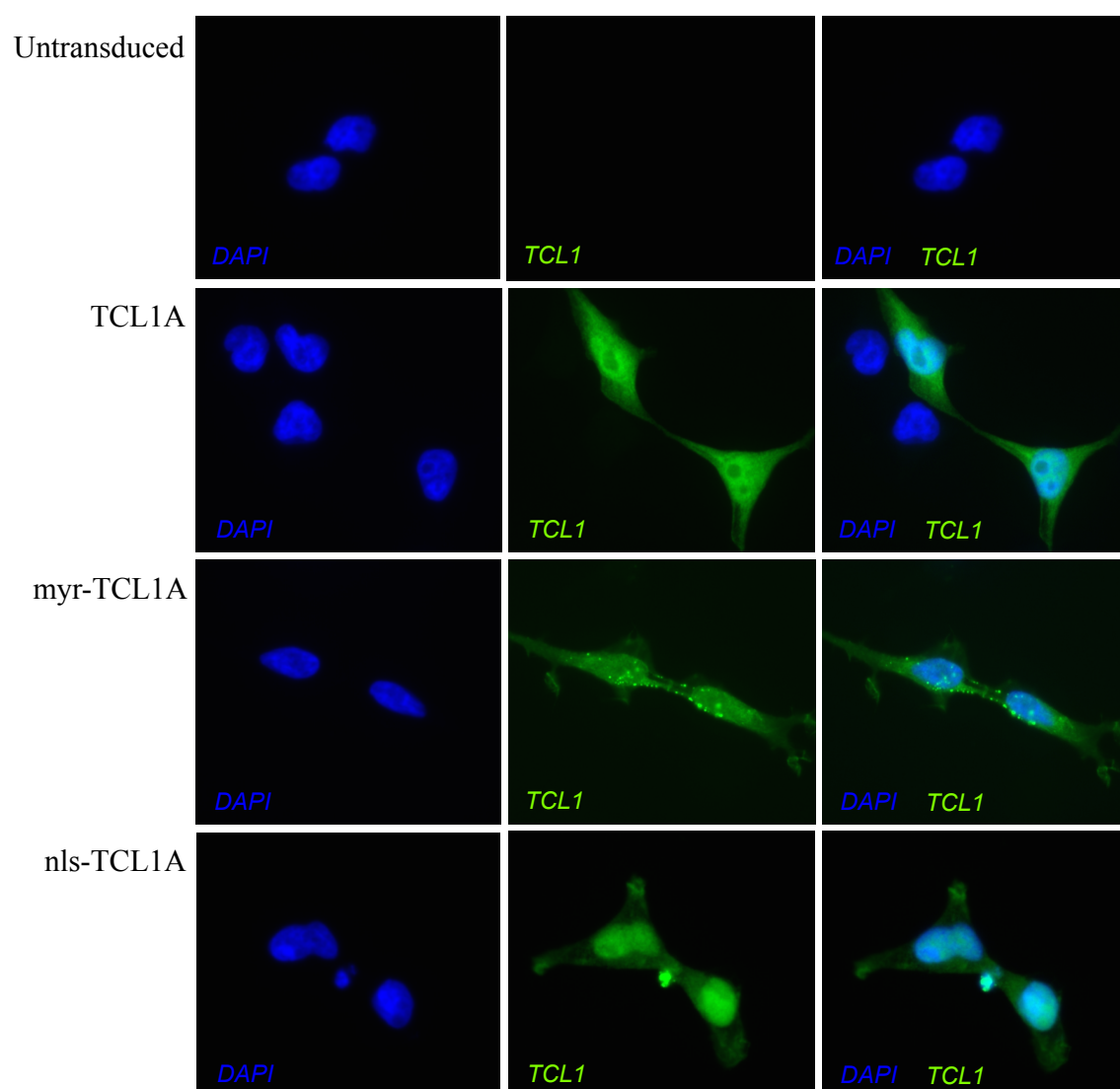
Figure 3-10: TCL1A protein localization in HEK293T cells after transduction with different TCL1A variants
Fluorescence microscopy on TCL1A (second row), myr-TCL1A (third row) and nls-TCL1A (fourth row) transduced HEK293T cells. Non-transduced HEK293T cells were used as a negative control (first row). Staining was done using DAPI (blue, left column) and anti-TCL1A (green, middle column). Merged pictures are shown in the right column.

For membrane localization, a DNA sequence for an N-terminal myristoylation signal was added to the transgene sequence. This signal allows cotranslational modification resulting in the attachment of a myristic acid to the N-terminus of TCL1A (myr-TCL1A). Myristic acid is hydrophobic and anchors the protein into the lipid bilayer of the cell's membrane. For nuclear localization, a DNA sequence for an N-terminal nuclear localization signal (nls) was added to the transgene sequence. This peptide motif tags the protein for traffic through nuclear pores into the nucleus. To validate targeted TCL1A expression, HEK293T cells were transduced with retroviral vectors for TCL1A, myr-TCL1A and nls-TCL1A, and analyzed by fluorescence microscopy for TCL1A expression (Figure 3-10). For this analysis, HEK293T cells were chosen as their larger size allowed studying protein distribution in cellular compartments. HEK293T cells expressing the generic TCL1A showed an even distribution of the protein in the cytoplasm and nucleus (Figure 3-10, second row). Myr-TCL1A expressing cells showed condensed protein localization at the membrane (Figure 3-10, third row). A nuclear accumulation of TCL1A was observed for nls-TCL1A transduced HEK293T cells (Figure 3-10, fourth row). Therefore, targeted expression of TCL1A to the membrane and nucleus with myr-TCL1A and nls-TCL1A was validated.

3.2.4   Localization of TCL1A influences its oncogenic potential

Transplantation of myr-TCL1A and nls-TCL1A transduced HSCs/HPCs resulted in lymphoma/leukemia development in recipient mice after latencies between five and 20 months. Survival was compared to the previously described cohort of generic TCL1A recipient mice (see section 3.2.2). TCL1A HSC/HPC recipient mice developed lymphoma/leukemia after a median latency of 388 days. Similarly, myr-TCL1A recipient mice had a median survival of 372 days (Figure 3-11A). However, survival was significantly reduced in nls-TCL1A recipients compared to recipient mice of TCL1A HSCs/HPCs with a median latency of 349 days (Figure 3-11B). Despite a reduced latency in nls-TCL1A mice, no striking difference in phenotype was observed between tumors induced by the generic TCL1A and its variants. Similar to TCL1A-induced tumors, most myr-TCL1A and nls-TCL1A mice developed tumors with a B-cell phenotype and presented with enlarged liver, spleen and LNs (Table 3-3). The remaining mice, showed enlarged thymi with a DP or DN T-cell phenotype (Table 3-3). An elevated WBC ($>15 \times 10^6$ cells/µl blood) was detected in the majority of myr-TCL1A and nls-TCL1A recipient mice upon tumor development (Table 3-3).

Flow cytometric analysis of B-cell tumors induced by myr-TCL1A and nls-TCL1A showed expression of CD19, surface IgM, and B220, except for one nls-TCL1A tumor that lacked surface IgM expression (Table 3-4). None of the B-cell tumors expressed CD138 or CD21/35 (Table 3-4). CD5 expression was only detected in half of the tumors induced by myr-TCL1A tumors and nls-TCL1A, whereas most tumors derived from overexpression of generic TCL1A expressed this marker (Table 3-4). A representative flow cytometric analysis is shown in Figure 3-6A.
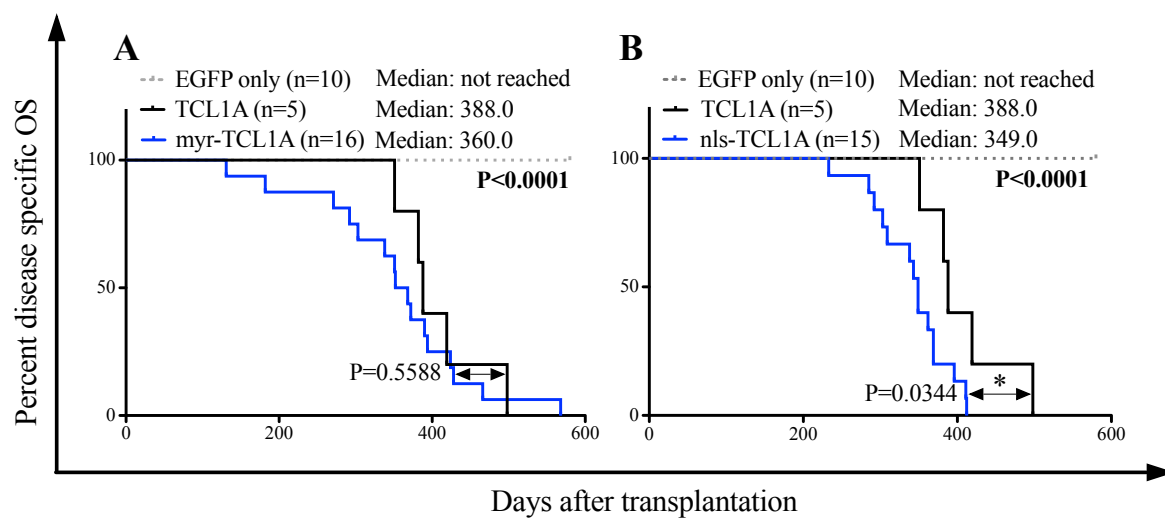
Figure 3-11: Survival of TCL1A variants mice
Animals that received TCL1A variants myr-TCLA (A) and nls-TCL1A (B) transduced HSCs/HPCs developed lymphoma/leukemia after indicated latencies (blue solid line, A-B). Survival of the previously described recipient mice of generic TCL1A is shown as black solid line in each graph. Control animals (EGFP only) did not show any signs of disease during the observation time (grey dotted line, A-B).

Myr-TCL1A and nls-TCL1A HSC/HPC recipient mice that developed T-cell malignancies displayed enlarged thymi with a CD4/8 DP phenotype and varying expression of CD3 and TCRαβ. A representative flow-cytometric analyses is shown in Figure 3-6B. Only one T-cell tumor induced by myr-TCL1A was negative for CD4 and CD8 expression (CD4/8 DN) (Table 3-3), but showed TCRαβ$^+$ expression (data not shown).

Representative images of macroscopic and histological/cytological analyses of B- and T-cell malignancies are shown in Figure 3-7 and Figure 3-8, as they had the same cytomorphologic features as tumors induced by non-compartment targeted TCL1A overexpression.

Oncogene	Gross-anatomic features	Elevated PB leukocyte count (15×10^6 cells/μl)	CD4/8 DP	CD4/8 DN	CD19
TCL1A	Hepatomegaly, Splenomegaly, Lymphadenopathy.	5/5	0/5	0/5	5/5
myr-TCL1A	Thymoma (CD4/8DP). Hepatomegaly, Splenomegaly, Lymphadenopathy (CD19).	13/16	3/16	1/16	12/16
nls-TCL1A	Thymoma (CD4/8DP). Hepatomegaly, Splenomegaly, Lymphadenopathy (CD19).	12/15	2/15	0/15	13/15

Table 3-3: Phenotype of tumors induced by TCL1A variants

Oncogene	CD19	B220	IgM	CD5	CD138	CD21/35
TCL1A	5/5	5/5	5/5	4/5	0/5	0/5
myr-TCL1A	12/12	12/12	12/12	6/12	0/12	0/12
nls-TCL1A	13/13	13/13	12/13	5/13	0/13	0/13

Table 3-4: Phenotype of B-cell tumors induced by TCL1A variants

3.2.5 The primary oncogenic function of TCL1A depends on its nuclear presence

A comparative gene expression analysis of the TCL1A variants was performed to identify differently expressed genes in target cells at overt leukemic phases. These analyses were performed on an Affymetrix Mouse Gene 1.0 ST Array, whose 764885 probes cover a total of murine 28869 genes. Differently expressed genes were filtered using a fold-change of 2 (up and down) and an ANOVA p-value lower than 0.05.

For tumor cell analysis, cell suspensions from spleens of mice with B-cell malignancies were used with at least 70% tumor cell content. Gene expression profiles of tumor samples from TCL1A, myr-TCL1A and nls-TCL1A recipient mice were compared to CD19⁺EGFP⁺ B cells sorted from spleen and LNs of EGFP only control mice 100 days after transplantation (Figure 3-12).
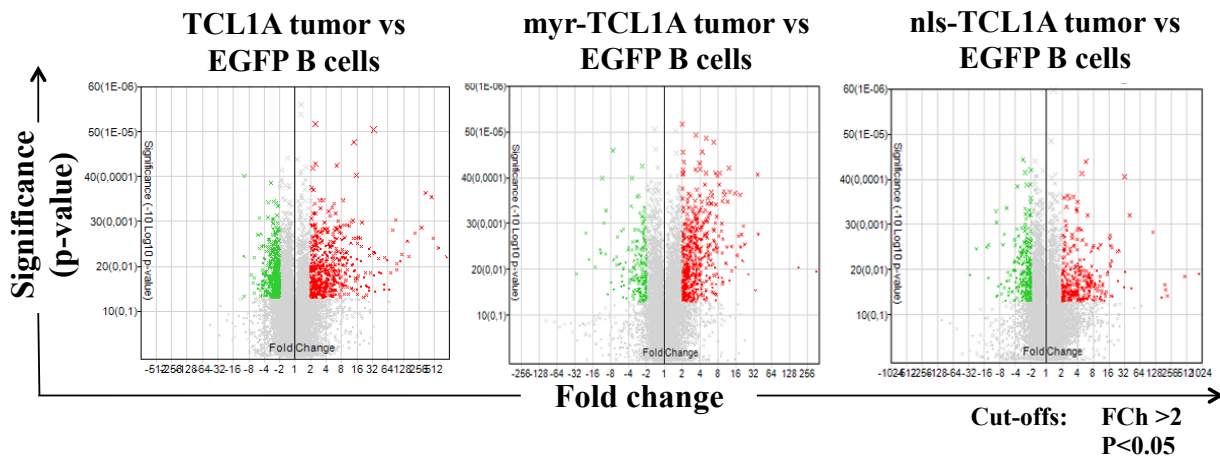
Figure 3-12: Differently expressed genes in TCL1A-, myr-TCL1A- and nls-TCL1A-induced tumors compared to control B cells
Volcano plots of up-regulated (red) and down-regulated (green) genes with a fold change (FCh) of 2. Genes in grey did not match the filter criteria (FCh>2, P<0.05) and were excluded from further analysis.

A pathway enrichment analysis was performed to characterize the functional role of differently expressed genes. There was a large overlap within the ten most affected pathways in TCL1A-, myr-TCL1A-, and nls-TCL1A-induced tumors including chemokine, cell cycle, PI3K/AKT, p53, and MAPK signaling pathways (Figure 3-13). Interestingly, a lot of receptor-induced signaling pathways were deregulated in these tumors involving the BCR, cytokine receptors, chemokine, and other G protein–coupled receptors (GPCRs). A list of genes that are up-regulated or down-regulated in at least two of three cohorts are shown in Table 5-1 in the supplementary section 5.3.
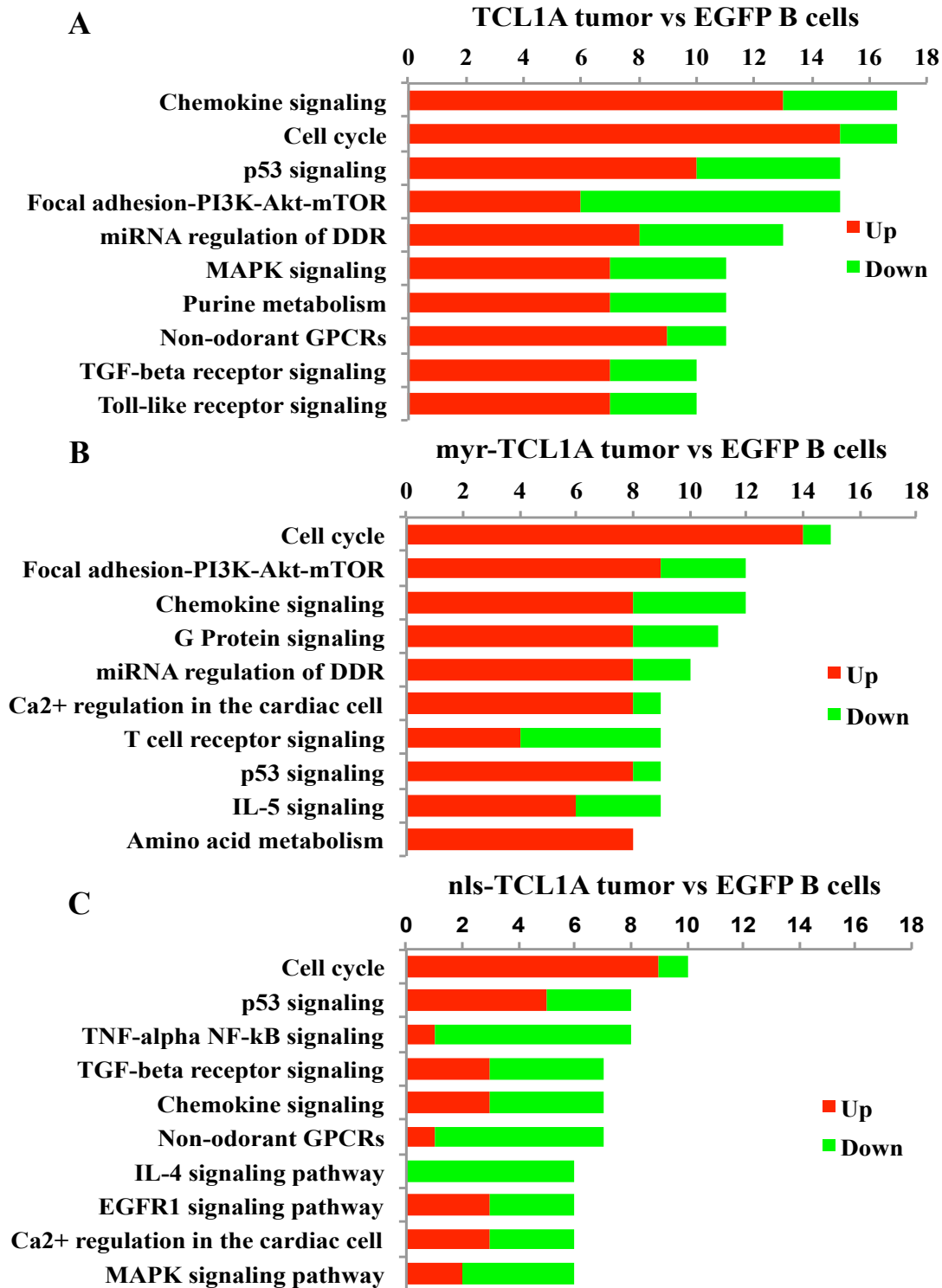
***Figure 3-13: Top 10 pathways affected in TCL1A-, myr-TCL1A- and nls-TCL1A-induced tumors
compared to control B cells***

*Pathway enrichment analysis of differently expressed genes in TCL1A- (A), myr-TCL1A- (B), and nls-
TCL1A-induced (C) tumors compared to control B cells.*

Next, the relation of compartment-targeting variants of TCL1A to unmodified TCL1A was characterized. The numbers of overlapping genes that are differently expressed in the three TCL1A cohorts are shown in Figure 3-14. The largest overlap was observed between the generic TCL1A and its nuclear variant nls-TCL1A.
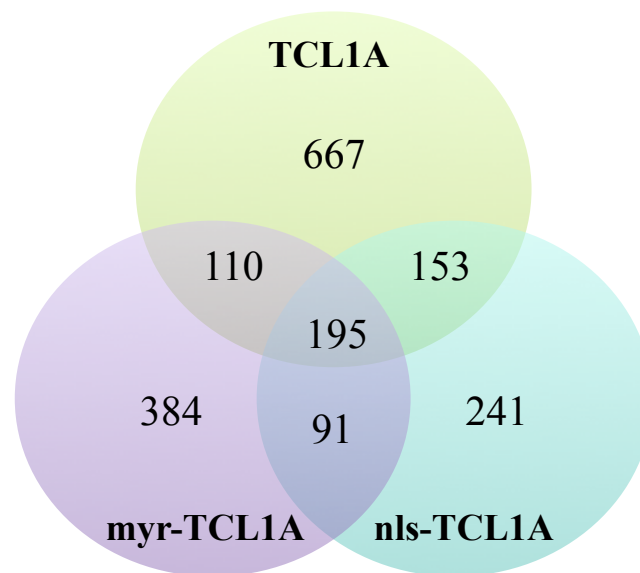
Figure 3-14: Overlap of differently expressed genes in TCL1A-, myr-TCL1A- and nls-TCL1A-induced tumors
Venn diagram showing the number of differently expressed genes in B-cell tumors induced by TCL1A, myr-TCL1A and nls-TCL1A.

This overlap was further supported by a pathway enrichment analysis of deregulated genes in TCL1A-induced tumors compared to tumors induced by myr-TCL1A and nls-TCL1A (Figure 3-15). There was no significant enrichment within the top ten pathways between tumors of TCL1A and nls-TCL1A recipient mice.

Noteworthy is also the more than 2-fold down-regulation of the TCL1 family gene Mtcp1 in TCL1A-induced tumors (data not shown). Expression of the murine TML1 isoforms was not affected.

A

TCL1A tumor vs myr-TCL1A tumor

Ca2+ regulation in the cardiac cell
Focal adhesion-PI3K-Akt-mTOR
Chemokine signaling
Purine metabolism
Odorant GPCRs
Insulin signaling
mRNA processing
G Protein signaling
EGFR1 signaling pathway
BCR signaling

■ Up
■ Down

B

TCL1A tumor vs nls-TCLA tumor

Androgen receptor signaling
Cytoplasmic ribosomal proteins
Insulin signaling
Focal adhesion-PI3K-Akt-mTOR
Folic acid network
Selenium micronutrient network
Focal adhesion
Tryptophan metabolism
Amino acid metabolism
Integrin-mediated cell adhesion

■ Up
■ Down

Figure 3-15: Top 10 pathways affected in tumors induced by TCL1A compared to tumors induced by compartment-targeting TCL1A variants
Pathway enrichment analysis of differently expressed genes in TCL1A-induced tumors compared to myr-TCL1A-induced tumors (A) and nls-TCL1A-induced tumors (B).

3.2.6 TCL1A-induced changes in gene expression are more prominent in B cells than in T cells at pre-leukemic stages

To characterize TCL1A-induced changes in gene expression of lymphocytes at pre-leukemic phases, CD19$^+$ EGFP$^+$ B and CD3$^+$ EGFP$^+$ T cells were sorted from spleen and LNs of EGFP only, TCL1A, myr-TCL1A and nls-TCL1A HSC/HPC mice 100 days after transplantation. This time point was chosen based on tumor latencies that showed that the earliest tumor arose 131 days after transplantation (Figure 3-11). Analyses were performed on the previously described Affymetrix Mouse Gene 1.0 ST Array. Due to the low number of differently expressed genes in T cells, results were filtered using a fold-change of 1.5 (up and down) and

an ANOVA p-value lower than 0.05. Gene expression in sorted B and T cells from TCL1A, myr-TCL1A and nls-TCL1A recipient mice, was compared to sorted B and T cells from EGFP only control mice (Figure 3-16). Interestingly, a significant higher number of genes were differently expressed in B cells (more than 400 genes per cohort) than in T cells (less than 400 genes per cohort) at the pre-leukemic phase (Figure 3-16).
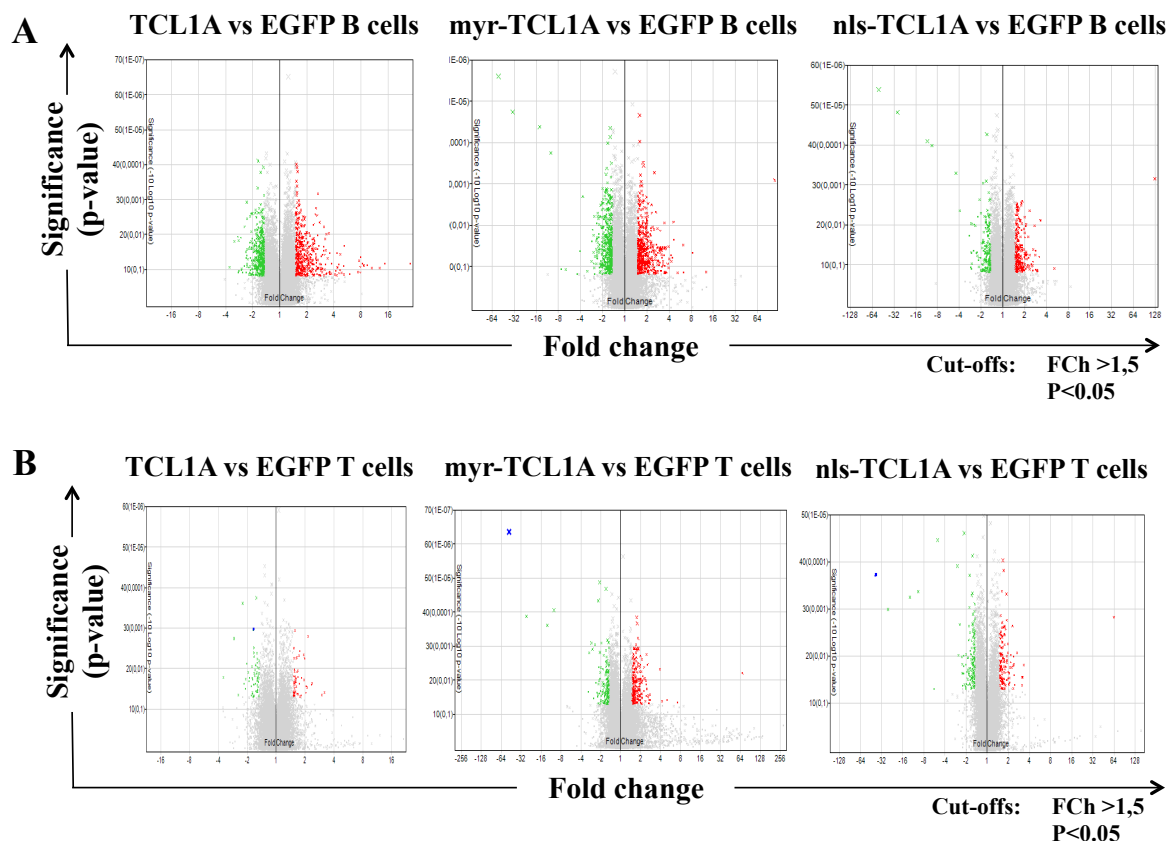
Figure 3-16: Differently expressed genes in TCL1A, myr-TCL1A and nls-TCL1A expressing B and T cells compared to control cells
Volcano plots of up-regulated (red) and down-regulated (green) genes with a fold change (FCh) of 1.5. Genes in grey did not match the filter criteria (FCh>1.5, P<0.05) and were excluded from further analysis.

To further classify the functional role of differently expressed genes, a pathway enrichment analysis was performed. Genes involved in chemokine, PI3K/AKT, and MAPK signaling pathways were differently expressed in pre-leukemic B and T cells (Figure 3-17, Figure 3-18). Additionally, pre-leukemic B cells showed a deregulation of genes involved in cell cycle and p53 signaling. A list of genes that are up-regulated or down-regulated in pre-leukemic B and

T cells from at least two of three cohorts are shown in Table 5-2 and Table 5-3 in the supplementary section 5.3.

A TCL1A vs EGFP B cells

Pathways: Cell cycle, MAPK signaling pathway, Adipogenesis genes, Focal adhesion-PI3K-Akt-mTOR, Non-odorant GPCRs, mRNA processing, p53 signaling, Purine metabolism, Regulation of actin cytoskeleton, Prostaglandin regulation

B myr-TCL1A vs EGFP B cells

Pathways: MAPK signaling pathway, Cell cycle, Insulin signaling, B cell receptor signaling pathway, EGFR1 signaling pathway, T cell receptor signaling pathway, p53 signaling, Focal adhesion-PI3K-Akt-mTOR, miRNA regulation of DDR, Focal adhesion

C nls-TCL1A vs EGFP B cells

Pathways: Focal adhesion-PI3K-Akt-mTOR, Adipogenesis genes, MAPK signaling pathway, p53 signaling, IL-5 signaling pathway, mRNA processing, Purine metabolism, Cell cycle, Circadian regulation, Regulation of actin cytoskeleton

Legend: ■ Up ■ Down

Figure 3-17: Top 10 pathways affected in TCL1A, myr-TCL1A and nls-TCL1A pre-leukemic B cells compared to control B cells
Pathway Enrichment Analysis of differently expressed genes in TCL1A (A), myr-TCL1A (B) and nls-TCL1A (C) B cells 100 days after transplantation compared to control B cells.

A

TCL1A vs EGFP T cells

- Chemokine signaling pathway
- EGFR1 signaling pathway
- MAPK signaling pathway
- Kit receptor signaling pathway
- Translation factors
- Mecp2 and associated Rett syndrome
- Focal segmental glomerulosclerosis
- Androgen receptor signaling pathway
- Peptide GPCRs
- miRNAs involved in DNA damage

■ Up
■ Down

B

myr-TCL1A vs EGFP T cells

- MAPK signaling pathway
- Cell cycle
- Focal Adhesion-PI3K-Akt-mTOR
- Purine metabolism
- G1 to S cell cycle control
- IL-3 signaling pathway
- Androgen receptor signaling pathway
- TNF-alpha NF-kB signaling pathway
- Apoptosis
- Focal adhesion

■ Up
■ Down

C

nls-TCL1A vs EGFP T cells

- Focal adhesion-PI3K-Akt-mTOR
- MAPK signaling pathway
- IL-6 signaling pathway
- B Cell receptor signaling pathway
- Cytoplasmic ribosomal proteins
- Tryptophan metabolism
- G1 to S cell cycle control
- Kit receptor signaling pathway
- Chemokine signaling pathway
- GPCRs, class A Rhodopsin-like

■ Up
■ Down

Figure 3-18: Top 10 pathways affected in TCL1A, myr-TCL1A and nls-TCL1A pre-leukemic T cells compared to control T cells

Pathway Enrichment Analysis of differently expressed genes in TCL1A (A), myr-TCL1A (B) and nls-TCL1A (C) T cells 100 days after transplantation compared to control T cells.

The numbers of overlapping genes that are differently expressed in pre-leukemic B and T cells of the three TCL1A cohorts are shown in Figure 3-19 to study the relation of different TCL1A variants. In pre-leukemic B cells, the biggest overlap was observed between B cells expressing the generic TCL1A and B cells expressing myr-TCL1A (Figure 3-19A). In T cells, the biggest overlap was found in T cells expressing myr-TCL1A and T cells expressing nls-TCL1A (Figure 3-19B).

Similar to the gene expression in TCL1A B cells at the tumor stage, day 100 B cells showed a 1.5-fold down-regulation of a TCL1 family member, in this case Tcl1b4 (data not shown).
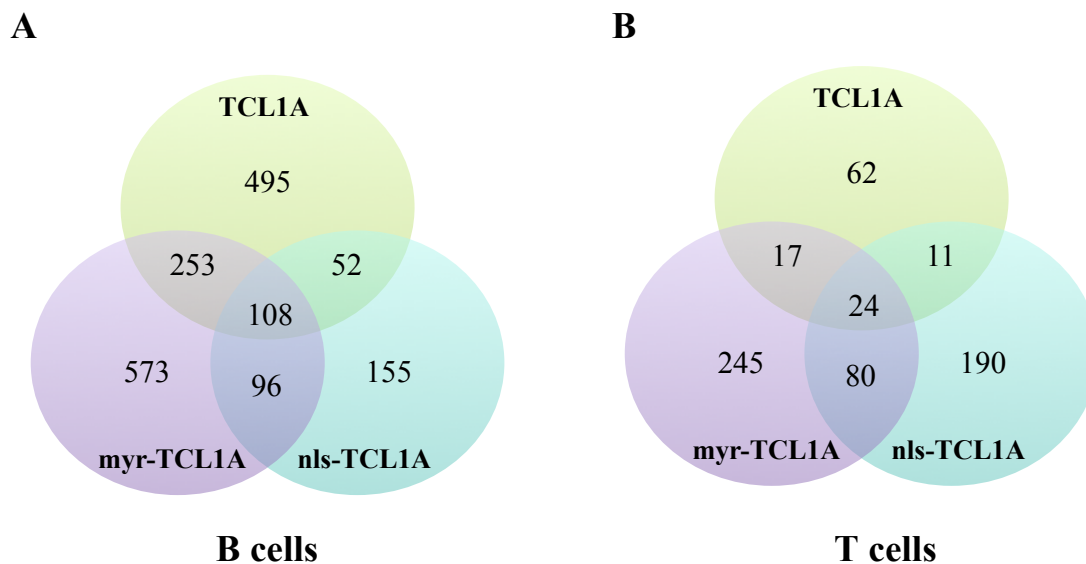
Figure 3-19: Overlap of differently expressed genes in TCL1A, myr-TCL1A and nls-TCL1A B and T cells
Venn diagrams showing the number of differently expressed genes in pre-leukemic B cells (A) and T cells (B) of TCL1A, myr-TCL1A and nls-TCL1A HSC/HPC recipient mice.

3.3   Targeted expression of TCL1A variants in monoclonal T cells

3.3.1   Specific TCR stimulation in vivo

For the second aim of this thesis, the chimeric model was modified using transplanted T cells as target cells instead of reconstitution by HSCs/HPCs. Single cell suspensions from spleens and LNs of OT-1 transgenic TCR mice were retrovirally transduced with TCL1A and its variants myr-TCL1A and nls-TCL1A. Subsequently, 5×10^6 transduced cells were transplanted into RAG1$^{-/-}$ recipient mice (no irradiation) that lack mature T and B cells (Figure 3-20). CD8 T cells from OT-1 mice exclusively express a monoclonal TCR that specifically recognizes the OVA peptide (amino acids 257-264) and is composed of a Valpha2 (Vα2) and a Vbeta5 (Vβ5) chain. Therefore, the TCR of transgenic OT-1 T cells can be stimulated specifically, which allows to study the impact of chronic TCR engagement on TCL1A-driven transformation. In the presented model, TCR stimulation was initiated by injecting recipient mice i.p. with OVA (257-264) in PBS mixed with the adjuvant IFA every two weeks. This mix was prepared to generate water-in-oil emulsions that serve as antigen depots at the injections site. Control mice were injected with a PBS/IFA mix.
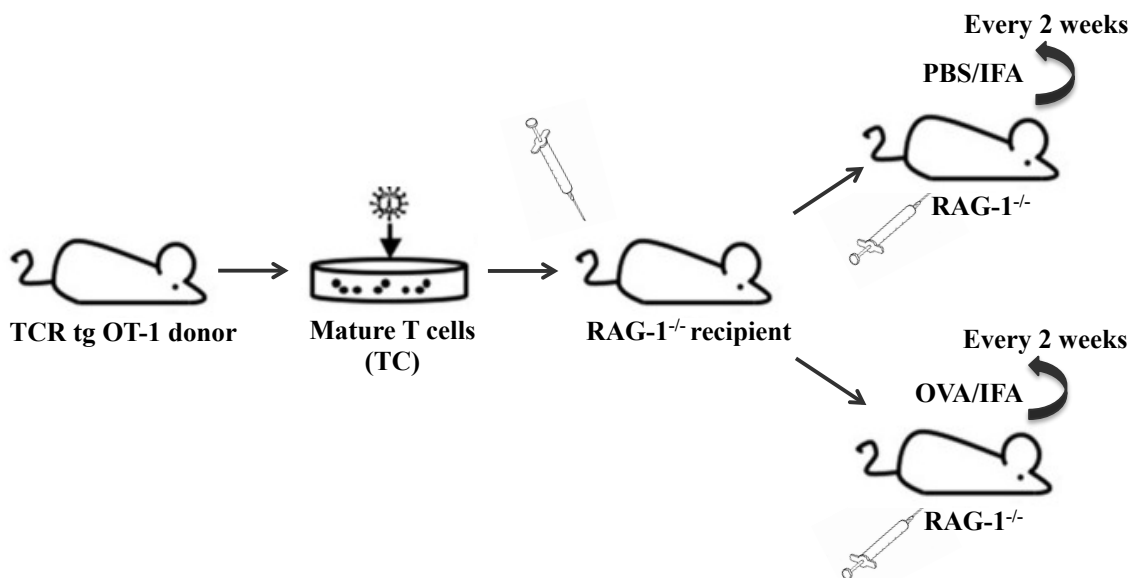
Figure 3-20: Experimental design of the T-cell transplantation model
TCR transgenic (tg) OT-1 mice were used as donors for mature T cells. These cells were retrovirally transduced and kept in culture for 3 days followed by transplantation into RAG1$^{-/-}$ recipient mice. Every two weeks, mice were injected with an OVA/IFA or PBS/IFA mix. Mice were monitored by blood sampling and analyzed after lymphoma/leukemia development.

Before using OVA/IFA injections in the described transplantation model, the responsiveness of OT-1 T cells to OVA stimulation was first analyzed in vivo. For that, OT-1 splenocytes (CD45.2) were stained with the proliferation marker CellTrace Violet and transplanted into B6 SJL WT (CD45.1) mice. WT mice were used as recipients for this experiment instead of RAG1$^{-/-}$ mice, as T cells undergo spontaneous proliferation in lymphopenic mice without the presence of a TCR stimulus, thereby not allowing to study the effect induced by the injection of OVA. After transplantation, mice were injected with OVA/IFA or PBS/IFA. Spleen suspensions were analyzed two and five days after transplantation for proliferation within the donor cell population (CD45.2$^+$, CD3$^+$) (Figure 3-21). Donor splenocytes in OVA/IFA-injected mice showed distinct inductions of proliferation after two days, whereas donor splenocytes in PBS/IFA-injected mice did not show any proliferative activity at this time point (Figure 3-21, left panel). After five days, the CellTrace Violet fluorescent signal had mostly disappeared within the high proliferating donor cell population of OVA stimulated mice, but was still detectable in slow proliferating donor cells of PBS control mice (Figure 3-21, right panel). OT-1 T cells responded to OVA/IFA injections and were thus applicable for chronic TCR engagement in the T-cell transplantation model.
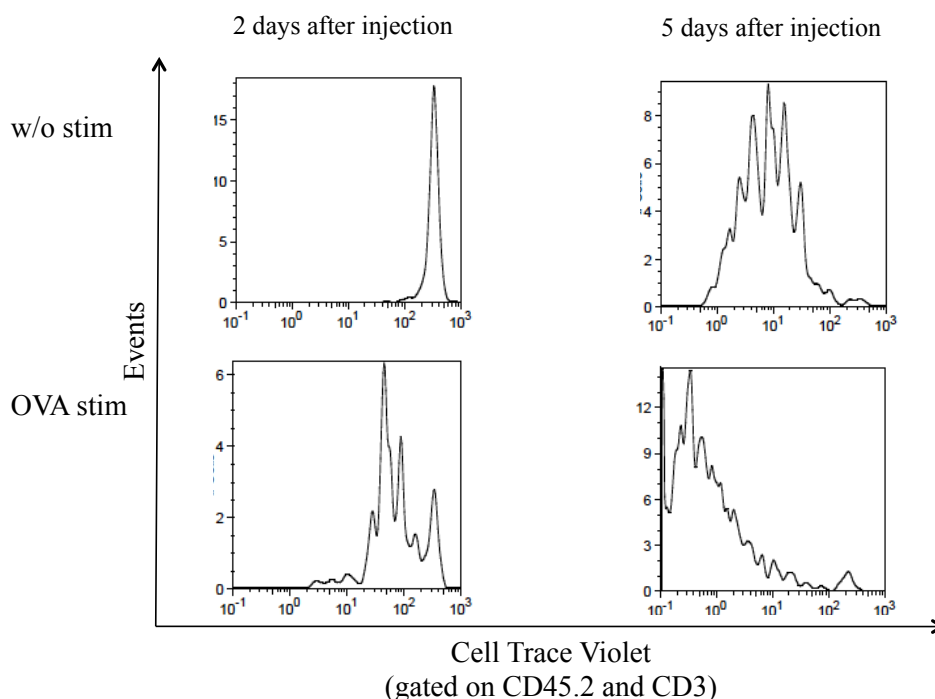
Figure 3-21: Proliferation of OT-1 T cells in vivo
B6 SJL WT mice were injected with PBS/IFA (w/o stim) or PBS/OVA (OVA stim) after transplantation of CellTrace Violet stained OT-1 splenocytes. Mice were sacrificed two and five days later. Spleen suspensions were analyzed by flow cytometry for CellTrace labeled generations of proliferating, donor derived (CD45.2, CD3) OT-1 T cells.

Next, the transplantation model as shown in Figure 3-20 was set up. Phenotype and transduction efficiency of OT-1 T-cell cultures were analyzed by flow cytometry before transplantation into recipient mice (Figure 3-22A). All retrovirally transferred constructs showed comparable transduction efficiencies (35-50%). Phenotypically, transgenic CD8$^+$ Vα2/Vβ5 DP T cells made up >95% of the cells in this culture. The remaining cells were comprised of CD19$^+$ B cells (<4%) and CD4$^+$ T cells (<1%).
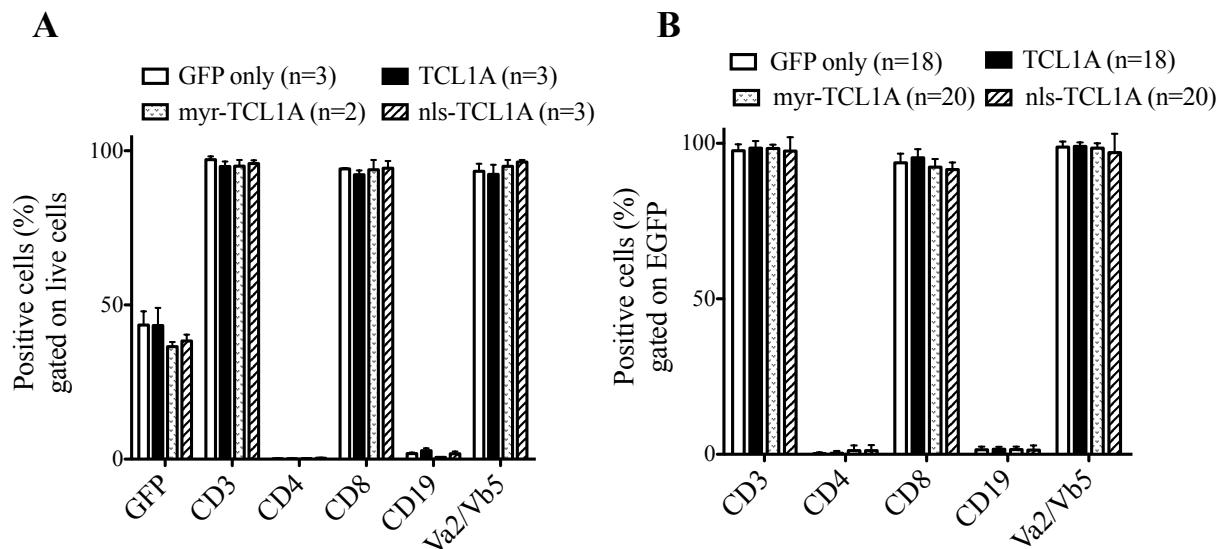
Figure 3-22: Transduction efficiency and repopulation of OT-1 T cells
(A) Percentage of EGFP+ T cells transduced with TCL1A variants (TCL1A, myr-TCL1A, nls-TCL1A). (B) Blood samples from OT-1 T cells recipient mice were analyzed by flow cytometry for EGFP expressing T cell populations (CD3+, CD4+, CD8+ and Vα2/Vβ5 DP) and CD19+ B cells two weeks after transplantation. Error bars represent SD.

To monitor repopulation of OT-1 T cells, blood samples were drawn from recipient mice two weeks after transplantation and analyzed by flow cytometry. Blood samples were stained with the B-cell marker CD19, transgenic TCR markers Vα2 and Vβ5, as well as the T-cell markers CD3, CD4, and CD8. CD8 and Vα2/Vβ5 DP T cells accounted for around 98% of the transgenic (EGFP$^+$) lymphocytes in PB (Figure 3-22B). CD19$^+$ B cells and CD4+ T cells made up less than 2% of the EGFP+ population. Blood analysis was repeated every four weeks until mice developed lymphoma/leukemia (Figure 3-23).
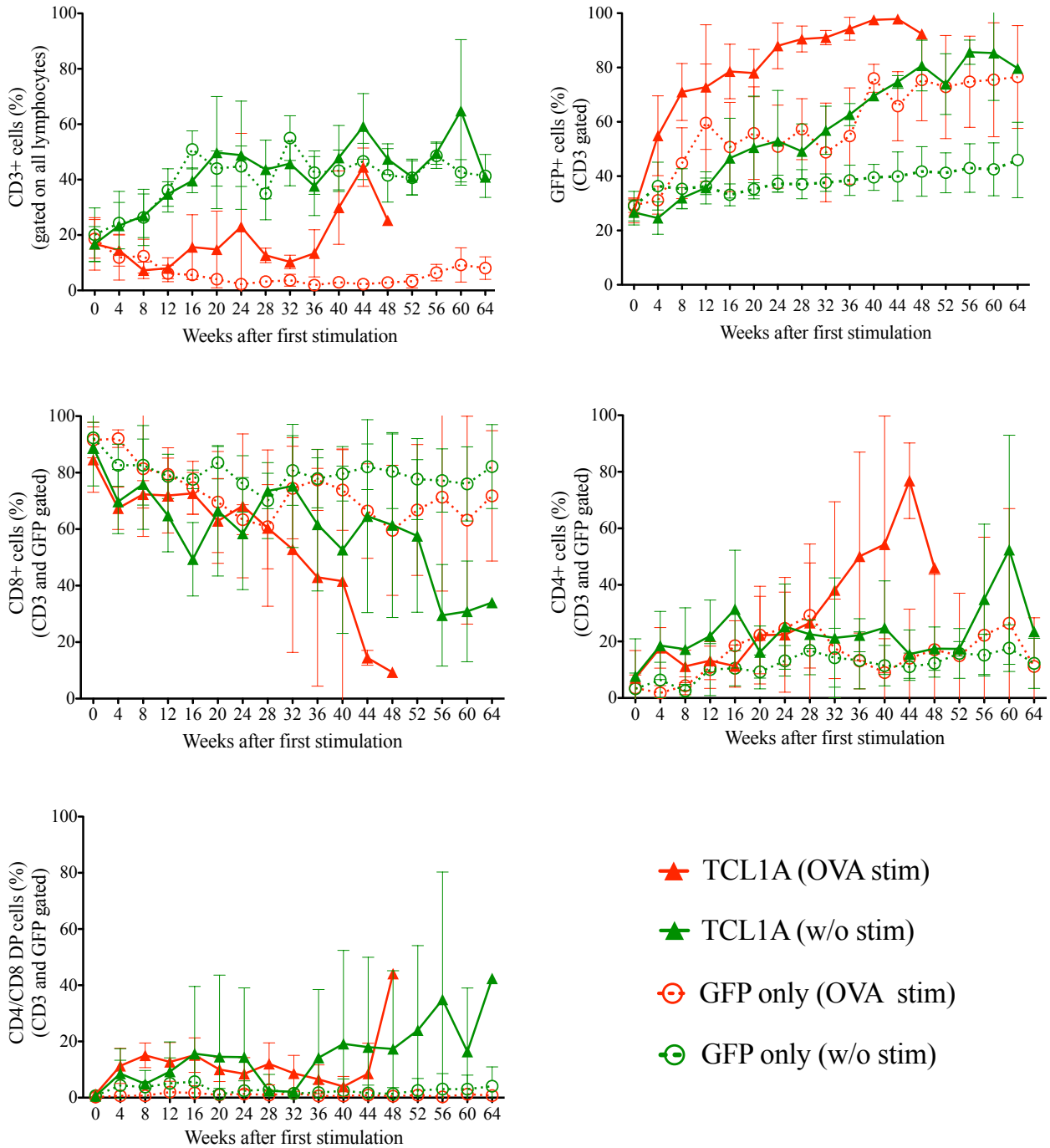
Figure 3-23: Monitoring of transduced OT-1 T cells in the PB over time
Blood samples were taken from unstimulated (green, w/o stim) and stimulated (red, OVA stim) EGFP only (circle) and TCL1A (triangle) OT-1 T-cell recipient mice every four weeks and analyzed by flow cytometry. Mean percentage of CD3^{+} cells gated on live cells (top left), EGFP^{+} cells gated on CD3^{+} cells (top right), CD8^{+} (middle left), CD4^{+} (middle right) and CD4/8 DP (bottom left) cells gated on CD3^{+} and EGFP^{+} cells was compared between different cohorts throughout the whole observation time. Experiment was started with five mice per group. Symbols represent mean values and error bars represent SD.

In OVA stimulated EGFP and TCL1A cohorts, the percentage of CD3$^+$ T cells dropped within the first 12 weeks after the first injection (Figure 3-23). Interestingly, stimulated TCL1A mice showed an increase of CD3 percentage after the initial decline, whereas in stimulated EGFP only mice this percentage remained low until the end of the experiment. The percentage of transgene/EGFP expressing cells within the CD3$^+$ population of these two cohorts rose almost to up to 100% in TCL1A recipients and to 80% in EGFP control mice. Surprisingly, unstimulated TCL1A showed a comparable increase in EGFP percentage as OVA stimulated EGFP mice. Although the initial transplant mainly consisted out of transgenic CD8 T cells, TCL1A cohorts also showed a significant decline of EGFP$^+$ CD8 T cells and an increase of EGFP$^+$ CD4 T cells instead (Figure 3-23). The percentage of CD19$^+$ B cells in the PB was less than 5% throughout the entire observation time in all cohorts (data not shown). The blood analysis of TCL1A mice shown in Figure 3-23 is representative for its two variants myr-TCL1A and nls-TCL1A, as these groups show similar expression patterns in the PB during the experiment.

To characterize the functional phenotype of OT-1 T cells in recipient mice, blood samples were further analyzed for the T-cell markers CD69, CCR7, CD62L and CD44 (see section 1.1.2). Most TCL1A transduced T cells in OVA stimulated recipient mice showed a typical T$_{EM}$ profile as they expressed CD44, but lacked expression of CD69, CCR7, and CD62L (Figure 3-24). Only small subpopulations showed expression of CCR7, CD62L and CD69. Stimulated EGFP only transduced T cells showed the same expression pattern with the exception to CD62L, which was detected on almost half of the cells (Figure 3-24). The T cells of unstimulated EGFP only and TCL1A cohorts showed mostly a high expression of CD62L and CD44, while only a small population expressed CCR7 and CD69 expression was completely absent. Again, myr-TCL1A and nls-TCL1A expressing T cells showed a similar functional phenotype as TCL1A$^+$ T cells shown in Figure 3-24.
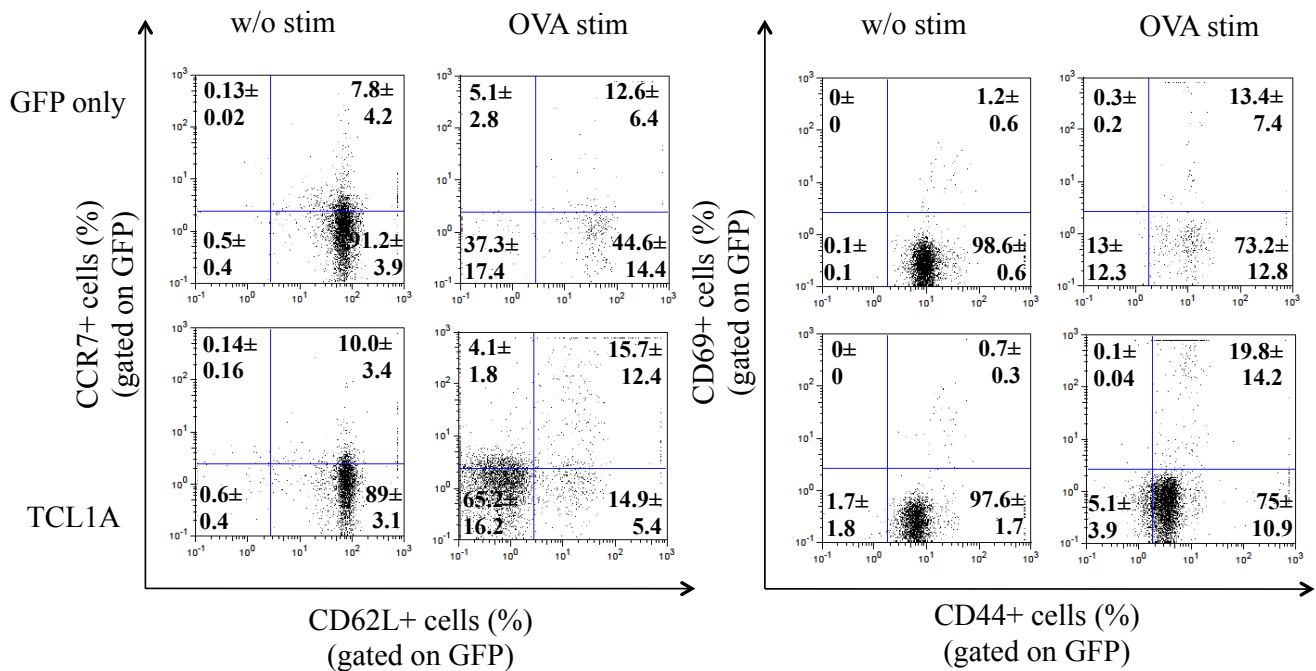
Figure 3-24: Functional phenotype of transduced OT-1 T cells in the PB
Flow cytometric analysis of EGFP+ cells in the PB of PBS/IFA (w/o stim) and OVA/IFA (OVA stim)
injected OT-1 T-cell recipient mice 36 weeks after transplantation. Cells were gated on EGFP$^+$ cells
and analyzed for the expression of CCR7 and CD62L (left panel), and CD69 and CD44 (right panel)
in EGFP only (top row) and TCL1A (bottom row) cohorts. FACS plots show mean percentage and SD
of sub-gates of five analyzed animals.

3.3.2 Stimulated TCL1A T cells accumulate in spleen and other abdominal regions

Analysis of the PB showed that the percentage of CD3+ cells decreased upon TCR stimulation with OVA. Without sacrificing the mice, it was not possible to determine the localization of the transplanted T cells in other organs. Thus, a retroviral vector with a luciferase reporter was utilized to visualize T-cell localization by in vivo imaging (Figure 3-1). The control vector contained a T-Sapphire reporter gene in addition to the luciferase reporter. The control vector and TCL1A vector were both transduced into OT-1 T cells with a comparable transduction efficiency of around 20% (data not shown). Twelve weeks after the first PBS or OVA injection, mice were analyzed by bioluminescence imaging (Figure 3-25). This analysis was done 10 days after the last injection.

A

Control (w/o stim) (n=4) Control (OVA stim) (n=5)

TCL1A (w/o stim) (n=3) TCL1A (OVA stim) (n=5)

B
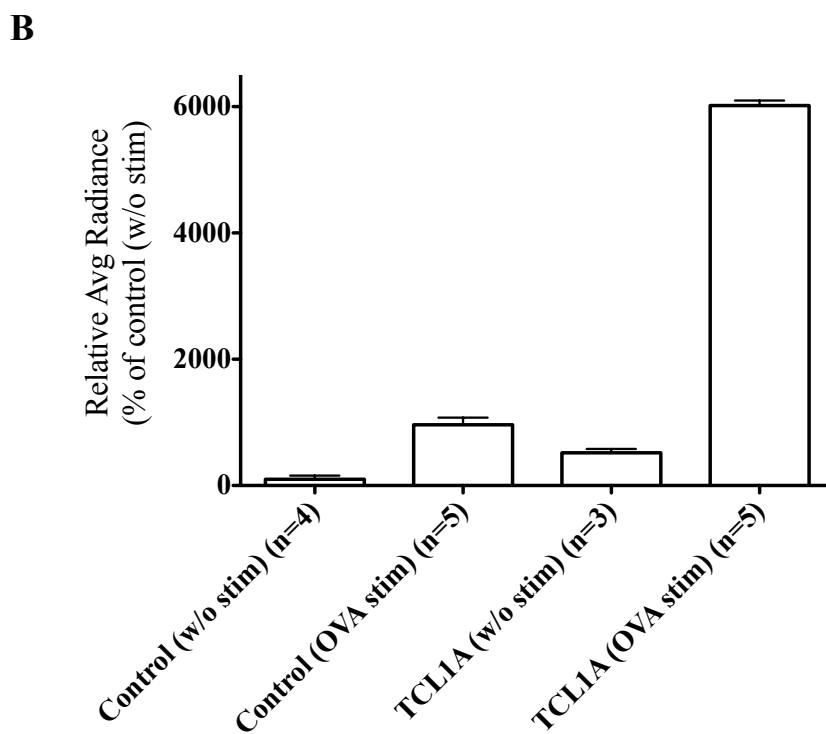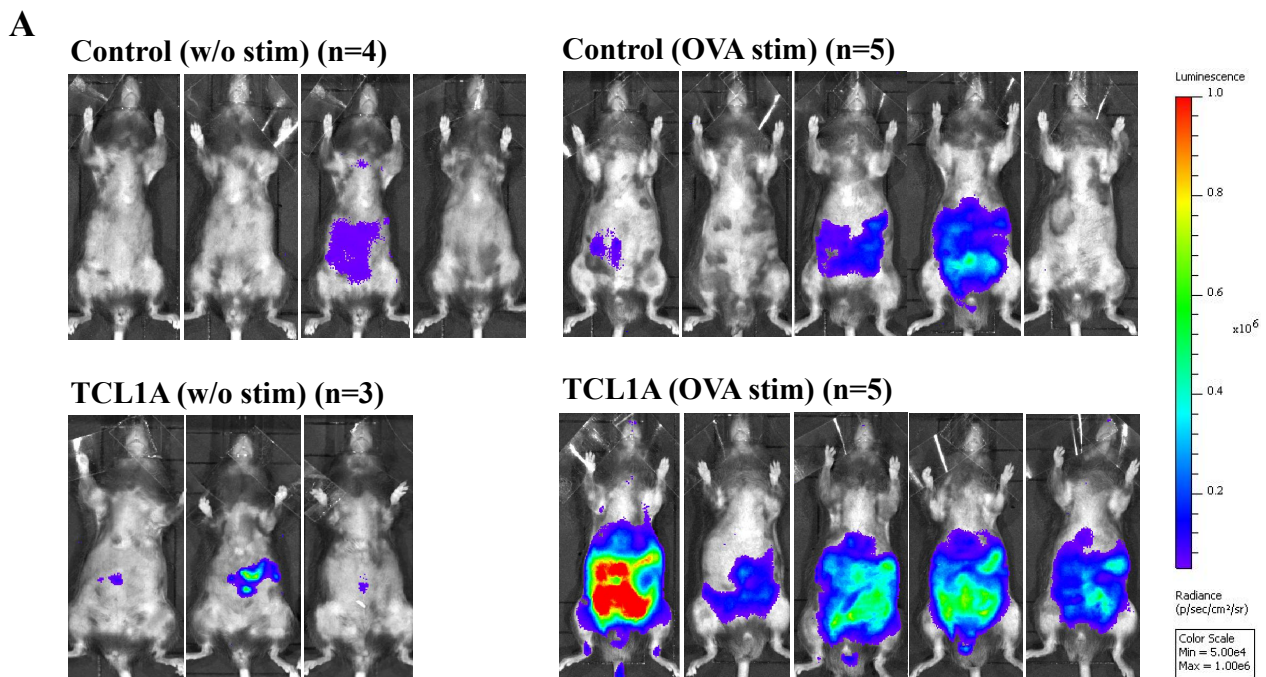
Figure 3-25: Bioluminescence imaging of OT-1 T-cell mice
Bioluminescence imaging of unstimulated (w/o stim) and stimulated (OVA stim) control and TCL1A OT-1 T-cell recipient mice. (A) For all images shown, the color scale for bioluminescence displayed as average radiance ranges from $5x10^4$ (blue) to $1x10^6$ (red) photons/s/cm^2/sr. (B) For each group of mice, whole body bioluminescence signals were determined and shown as mean values of average radiance relative to the unstimulated control group. Error bars represent RSD.

The strongest whole body bioluminescence signals, expressed as average radiance, were detected in OVA stimulated mice (Figure 3-25). Relative to unstimulated control mice, this signal was approximately 60 times higher for stimulated TCL1A mice, 10 times higher for stimulated control mice, and 5 times higher for unstimulated TCL1A mice (Figure 3-25B). To narrow down the localization of transplanted cells, signals were determined for selected regions of interest (ROI) (Figure 3-26A). Average radiance for each ROI relative to the cervical LN of each cohort is shown in Figure 3-26B. In unstimulated control and TCL1A mice, the strongest signal was found in the abdominal regions and the spleen (Figure 3-26B). Based on the strong signal in the abdominal regions, it was not possible to narrow down the exact tissues involved; and an intestinal origin is a rather speculated site. Cervival, axillary, and inguinal LN showed an evenly distributed signal in these mice. In OVA stimulated cohorts, the signal was low in cervical and axillary LNs, but high in regions of the inguinal LNs, abdominal regions, and spleen (Figure 3-26B).
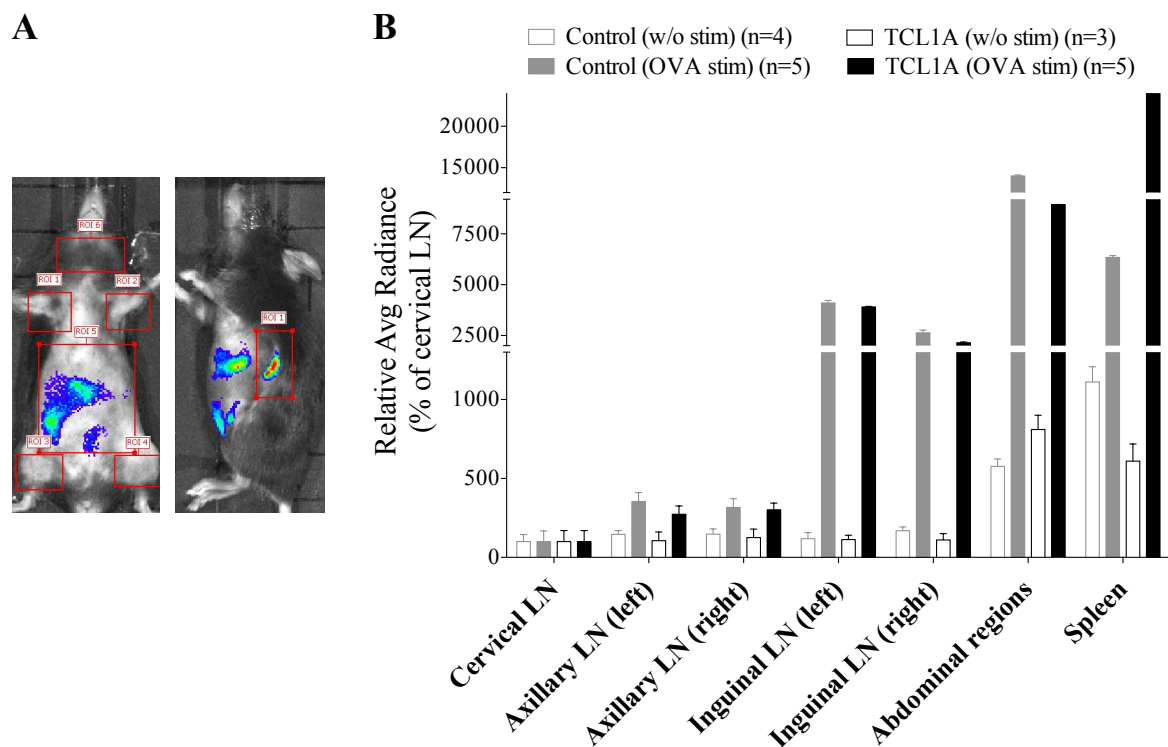
Figure 3-26: Bioluminescence signals in selected regions of interest
Bioluminescence imaging of unstimulated (w/o stim) and stimulated (OVA stim) control and TCL1A OT-1 T-cell recipient mice. (A) In ventro-dorsal position of the mouse, regions of interest (ROI) were drawn for the abdominal regions and cervical, axillary and inguinal LNs (left). In latero-lateral position, a ROI was drawn for the spleen (right). (B) For each group of mice, bioluminescence signals were determined for each ROI and shown as mean values of average radiance relative to its own cervival LN ROI. Error bars represent RSD.

3.3.3 Constant TCR stimulation facilitates TCL1A-driven transformation

After transplantation of TCL1A, myr-TCL1A and nls-TCL1A transduced OT-1 T cells, PBS/IFA injected recipients developed lymphoid malignancies after latencies between 7 and 20 months, whereas mice receiving OVA/IFA injections showed a significantly reduced survival between 6.5 and 13.5 months (Figure 3-27).
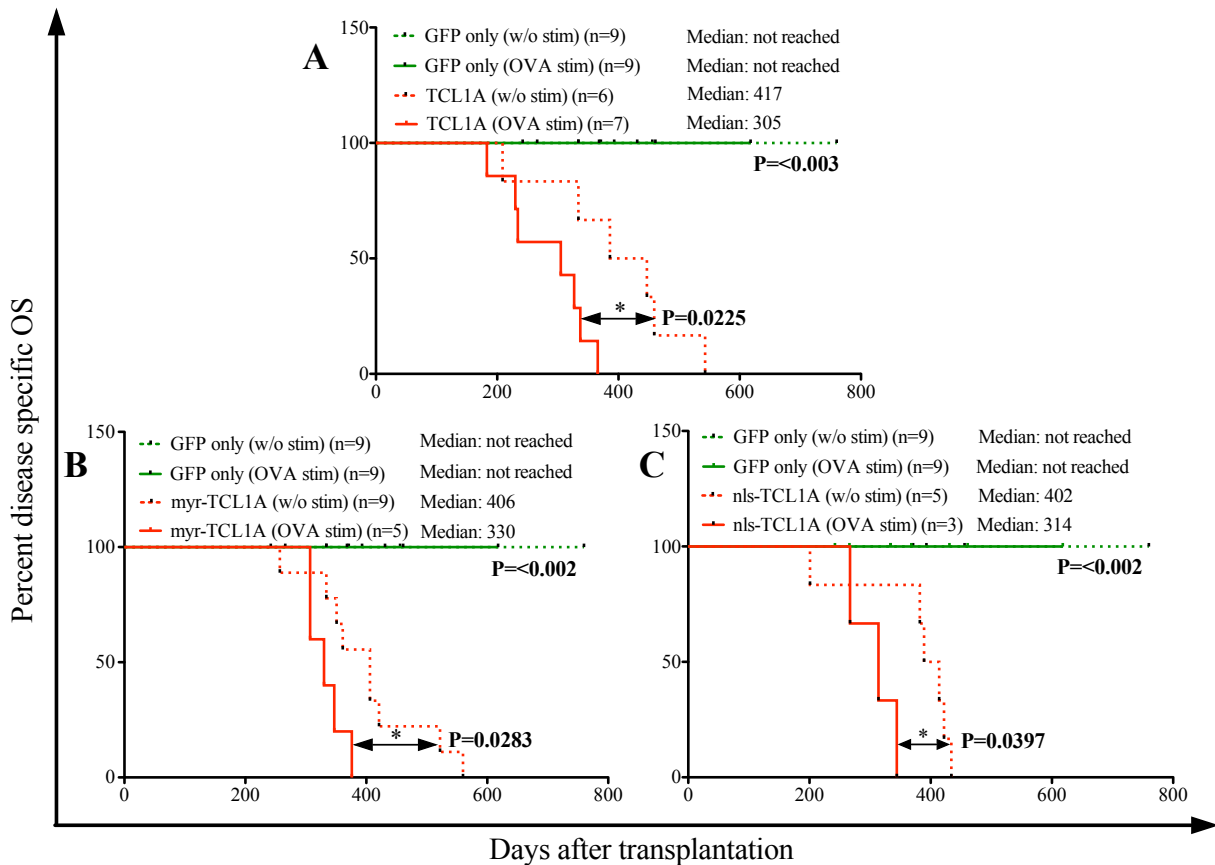
Figure 3-27: Survival of OT-1 T-cell recipient mice
Recipient mice of TCL1A (A), myr-TCL1A (B) and nls-TCL1A (C) transduced OT-1 T cells were injected with IFA/PBS (w/o stim, red dotted line) or IFA/OVA (OVA stim, red solid line) every two weeks and developed lymphoma/leukemia after significant different latencies. Control animals (EGFP only) that were treated with IFA/PBS (w/o stim, green dotted line) or IFA/OVA (OVA stim, green solid line) did not show any signs of disease during the observation time (A-C).

Recipient mice of TCL1A transduced OT-1 T cells that were injected with PBS had a median survival of 417 days. Repeated stimulation of the OT-1 TCR through OVA injections, led to a significant reduction of the median survival to 305 days (Figure 3-27). The same was observed for stimulated and unstimulated recipient mice of myr-TCL1A and nls-TCL1A

variants. All groups presented with splenomegaly, variable enlargement of mesenteric, inguinal and/or axillary LNs, as well as leukemic WBC higher than 15×10^6 cells per µl blood (Table 3-5). The phenotype of these tumors was determined by flow cytometric analysis, staining for CD3, CD4, CD8, and CD19 (Table 3-5). Recipient mice of OT-1 T cells transduced with TCL1A variants developed mostly T-cell malignancies. Interestingly, a few mice of the unstimulated cohorts developed B-cell tumors.

Oncogene		Gross-anatomic features	Elevated PB leukocyte count (15×10^6 cells/µl)	CD4/8 DP	CD4 SP	CD8 SP	CD19
TCL1A	+	Splenomegaly, Lymphadenopathy	7/7	0/7	3/7	4/7	0/7
	-	Splenomegaly, Lymphadenopathy	6/6	1/6	3/6	0/6	2/6
myr-TCL1A	+	Splenomegaly, Lymphadenopathy	3/5	0/5	4/5	1/5	0/5
	-	Splenomegaly, Lymphadenopathy	3/9	1/9	4/9	2/9	2/9
nls-TCL1A	+	Splenomegaly, Lymphadenopathy	2/3	0/3	3/3	0/3	0/3
	-	Splenomegaly, Lymphadenopathy	5/6	1/6	3/6	0/6	2/6

Table 3-5: Phenotype of tumors induced by TCL1A variants in OT-1 transplantation model
+ = OVA stimulation, - = w/o stimulation
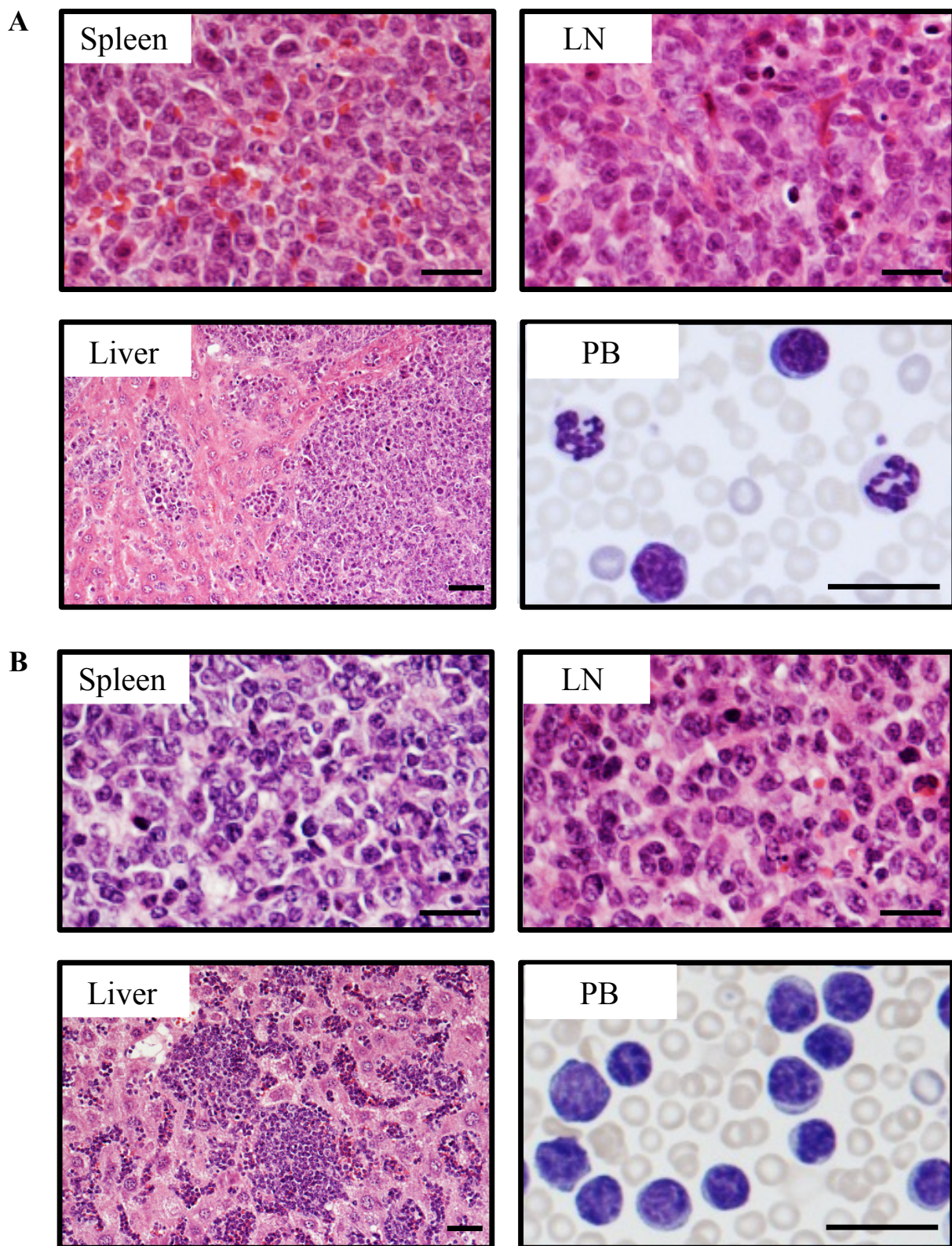
Figure 3-28: Histological and cytomorphological features of T- and B-cell malignancies induced by TCL1 family genes in OT-1 transplantation model

Representative H&E stained histological sections of animals with T-cell (A) and B-cell (B) malignancies showing enlarged spleens and LNs (original magnification 20x), infiltrations in the liver (original magnification 10x) and PB. Scale bar: 20µm.

Clinically apparent mice with T- and B-cell malignancies presented with variable splenomegaly and lymphadenopathy. Cytological analysis showed medium-sized lymphoid cells with scant basophilic cytoplasm in the blood of mice that developed tumors with a T-cell phenotype (Figure 3-28A). These tumor cells also infiltrated the spleen, LNs, and liver (Figure 3-28A). B-cell tumors in this model showed round medium-sized lymphoid cells with a high nucleo-cytoplasmic ratio in the blood that appeared more mature than the ones seen in the HSC/HPC model (Figure 3-28B). These cells were also found in spleen, LNs, and liver (Figure 3-28B). Infiltrations in lung and kidney were often observed for both T- and B-cell tumor types (data not shown)

LM-PCR analyses were performed using genomic DNA from tumor tissue to determine clonality of the T-cell tumors and to identify integration sites of retroviral vectors within the host cell genome. Tumors were classified based on the number of identified clones into monoclonal, oligoclonal, and polyclonal tumors. Figure 3-29 shows a typical pattern of monoclonal (1 band), oligoclonal (more than 1 band), and polyclonal samples (smear). The internal control for gammaretroviral vectors is visible as a 200bp band. Tumors of all cohorts showed a monoclonal or oligoclonal pattern, summarized in Table 3-6.
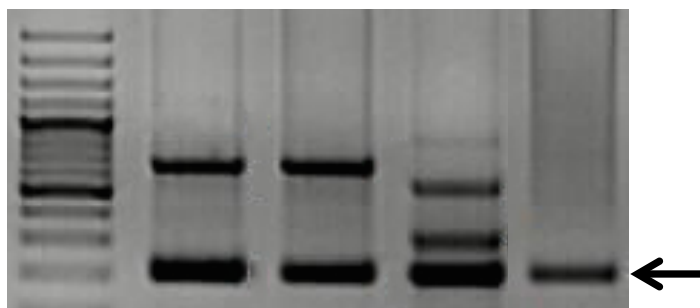
Figure 3-29: LM-PCR Analysis of tumors
Representative gel image for monoclonal (Lane 1 and 2), oligoclonal (Lane 3) and polyclonal (Lane 4, "smear") band patterns. Tissue from EGFP control mice was used as an example for a polyclonal pattern. The 200bp band represents internal control (◄).

Retroviral integration sites were further analyzed based on the genes that are found within a 250kb distance up- and downstream of the integration site. Affected genes in tumors of unstimulated mice (Table 3-7) and OVA stimulated mice (Table 3-8) were functionally characterized using the PANTHER pathway classification system. Generally, there was no statistical overrepresentation of flanking genes involved in signaling pathways. However, similar signaling pathways were affected in the different tumor cohorts, e.g. CCKR signaling,

inflammation mediated by chemokine and cytokine signaling pathway, PI3 Kinase pathway, etc. A complete list of identified genes can be found in section 5.4.

		Monoclonal	**Oligoclonal**
TCL1A	OVA stim	3/7	4/7
	w/o OVA	2/6	4/6
myr-TCL1A	OVA stim	2/5	3/5
	w/o OVA	4/9	5/9
nls-TCL1A	OVA stim	1/3	2/3
	w/o OVA	3/6	3/6

Table 3-6: Number of identified clones in T-cell tumors induced by TCL1 variants
OVA stim: OVA/IFA injection, w/o stim: PBS/IFA injection.

w/o stim	TCL1		myr-TCL1A		nls-TCL1A	
Distance to integration site	**250kb (n=115)**	**C (n=7)**	**250kb (n=83)**	**C (n=8)**	**250kb (n=59)**	**C (n=5)**
Alzheimer disease-presenilin pathway	-	-	1 (1.2)	-	-	-
Angiogenesis	2 (1.7)	-	1 (1.2)	-	-	-
Blood coagulation	3 (2.6)	-	-	-	-	-
Cadherin signaling pathway	-	-	1 (1.2)	-	-	-
Cell cycle	-	-	1 (1.2)	1 (12.5)	-	-
CCKR signaling map	3 (2.6)	-	1 (1.2)	-	1 (1.7)	-
Cortocotropin signaling pathway	1 (0.9)	-	-	-	-	-
Cytoskeletal regulation by Rho GTPase	1 (0.9)	-	2 (2.4)	-	1 (1.7)	-
EGF receptor signaling pathway	2 (1.7)	-	1 (1.2)	-	-	-
FAS signaling pathway	1 (0.9)	-	-	-	-	-
FGF signaling pathway	1 (0.9)	-	1 (1.2)	-	-	-
Gonadotropin releasing hormone receptor pathway	2 (1.7)	1 (14.3)	-	-	-	-

Pathway						
Heterotrimeric G-protein signaling pathway	7 (6.3)	-	-	-	6 (10.2)	-
Huntington disease	-	-	1 (1.2)	-	1 (1.7)	-
MAPK pathway	1 (0.9)	-	-	-	-	-
Inflammation mediated by chemokine and cytokine signaling pathway	3 (2.6)	-	9 (10.8)	1 (12.5)	1 (1.7)	-
Insulin/IGF pathway	-	-	1 (1.2)	-	1 (1.7)	-
Integrin signaling pathway	1 (0.9)	-	-	-	1 (1.7)	-
Interleukin signaling pathway	2 (1.7)	-	-	-	-	-
Ionotropic glutamate receptor pathway	-	-	-	-	1 (1.7)	-
JAK/STAT signaling pathway	-	1 (14.3)	-	-	-	-
Metabotropic glutamate receptor pathway	-	-	-	-	2 (3.4)	-
Methylmalonyl pathway	-	-	1 (1.2)	-	-	-
Muscarinic acetylcholine receptor 1 and 3 signaling pathway	-	-	-	-	1 (1.7)	-
Nicotinic acetylcholine receptor signaling pathways	-	1 (14.3)	1 (1.2)	-	1 (1.7)	-
Nicotine pharmacodyn. pathway	1 (0.9)	-	-	-	-	-
Notch signaling pathway	-	-	1 (1.2)	-	-	-
Parkinson disease	2 (1.7)	-	1 (1.2)	-	-	-
PDGF signaling pathway	2 (1.7)	-	-	-	1 (1.7)	-
PI3 kinase pathway	1 (0.9)	-	1 (1.2)	1 (12.5)	1 (1.7)	-
p53 pathway	1 (0.9)	-	3 (3.6)	-	2 (3.4)	-
Ras Pathway	1 (0.9)	-	-	-	-	-
TGF-beta signaling pathway	1 (0.9)	-	-	-	-	-
Toll receptor signaling pathway	1 (0.9)	-	-	-	1 (1.7)	-
Transcription regulation	-	-	-	-	-	2 (40)
Ubiquitin proteasome pathway	-	-	2 (2.4)	-	-	-
VEGF signaling pathway	1 (0.9)	-	-	-	-	-
Wnt signaling pathway	1 (0.9)	-	1 (1.2)	-	-	-

Table 3-7: PANTHER pathway classification of retroviral integrations sites in T-cell tumors induced by TCL1A variants in unstimulated mice

N=Number of genes within a 250kb distance up- and downstream of the integration site, recognized by PANTHER. C= closest genes to integration site. In brackets: %-ages of genes within gene set.

OVA stim	TCL1		myr-TCL1A		nls-TCL1A	
Distance to integration site	**250kb (n=71)**	**C (n=7)**	**250kb (n=43)**	**C (n=4)**	**250kb (n=50)**	**C (n=2)**
Alzheimer disease-amyloid secretase pathway	1 (1.4)	-	-	-	-	-
Alzheimer disease-presenilin pathway	1 (1.4)	-	-	-	-	-
Angiogenesis	-	-	1 (2.0)	-	1 (2.0)	-
Angiotensin II-stimulated signaling	-	-	1 (2.0)	-	-	-
Apoptosis signaling pathway	1 (1.4)	-	-	-	-	-
Axon guidance mediated by netrin	1 (1.4)	-	-	-	-	-
Cadherin signaling pathway	1 (1.4)	-	-	-	-	-
CCKR signaling map	1 (1.4)	-	1 (2.0)	-	1 (2.0)	-
Cell cycle	-	-	-	-	-	-
Cholesterol biosynthesis	-	-	-	-	1 (2.0)	-
Cortocotropin signaling pathway	-	-	1 (2.0)	-	-	-
Cytoskeletal regulation by Rho GTPase	1 (1.4)	-	-	-	1 (2.0)	-
De novo purine biosynthesis	1 (1.4)	-	-	-	-	-
Dopamine receptor mediated signaling pathway	-	-	1 (2.0)	-	-	-
EGF receptor signaling pathway	-	-	2 (4.1)	-	1 (2.0)	-
Endogenous cannabinoid signaling	-	-	1 (2.0)	-	-	-
5HT2 type receptor mediated signaling pathway	1 (1.4)	-	-	-	-	-
Flavin biosynthesis	-	-	-	-	1 (2.0)	-
FGF signaling pathway	1 (1.4)	-	1 (2.0)	-	1 (2.0)	-
GABA-B receptor II signaling	-	-	1 (2.0)	-	-	-
Glycolysis	-	-	-	-	1 (2.0)	-
Gonadotropin releasing hormone receptor pathway	2 (2.8)	-	1 (2.0)	-	-	-
Heterotrimeric G-protein signaling pathway	-	-	3 (6.2)	-	-	-
Histamine H1 receptor mediated signaling pathway	1 (1.4)	-	-	-	-	-
Inflammation mediated by chemokine and cytokine signaling pathway	4 (5.6)	1 (14.3)	1 (2.0)	-	2 (4.0)	-
Integrin signaling pathway	1 (1.4)	-	-	-	1 (2.0)	-
Interleukin signaling pathway	-	-	1 (2.0)	-	1 (2.0)	-

Methylmalonyl pathway	-	-	1 (2.0)	-	-	-
N-acetylglucosamine metabolism	-	-	-	-	1 (2.0)	-
Oxytocin receptor mediated signaling pathway	1 (1.4)	-	-	-	-	-
PDGF signaling pathway	1 (1.4)	-	-	-	1 (2.0)	-
PI3 kinase pathway	-	-	-	-	-	-
p53 pathway	-	-	3 (6.2)	-	-	-
Pyruvate metabolism	-	-	-	-	1 (2.0)	-
Ras Pathway	-	-	-	-	1 (2.0)	-
Serine glycine biosynthesis	-	-	-	-	1 (2.0)	-
Thyrotropin receptor signaling pathway	1 (1.4)	-	-	-	-	-
Toll receptor signaling pathway	-	-	-	-	2 (4.0)	-
Ubiquitin proteasome pathway	-	-	1 (2.0)	-	-	-
VEGF signaling pathway	-	-	1 (2.0)	-	-	-
Wnt signaling pathway	2 (2.8)	-	2 (4.1)	1 (25.0)	1 (2.0)	-

Table 3-8: PANTHER pathway classification of retroviral integrations sites in T-cell tumors induced by TCL1A variants in stimulated mice
N=Number of genes within a 250kb distance up- and downstream of the integration site, recognized by PANTHER. C= closest genes to integration site. In brackets: %-ages of genes within gene set.

3.3.4   TCL1A functions as a signaling enhancer in vitro

In vitro studies with OT-1 T cells are challenging, as these primary cells do not survive long enough in culture to study the effect of TCL1A expression on cellular properties. Thus, the murine IL-2 dependent T-cell line CTLL-2 was used instead (138). Although this cell line showed TCR expression, it did not respond to stimulation with CD3/28 beads (data not shown). Instead, these cells responded well to activation through IL-2. As this cytokine activates similar downstream pathways as the TCR (see section 1.1.3), it was used to analyze the cooperation of TCL1A and downstream signaling.

First, survival and proliferation of EGFP only or TCL1A expressing CTLL-2 cells at different IL-2 concentrations was analyzed. CTLL-2 cells were normally maintained at an IL-2 concentration of 300 units (U) per ml. Cell numbers were determined every two days in

cultures with IL-2 concentrations ranging from 0 to 300U per ml over a period of 16 days (Figure 3-30A). Cell numbers dropped with decreasing IL-2 concentrations in both groups and did not show a significant difference. Next, cell numbers were determined in cultures with IL-2 concentrations ranging from 300 to 1000U per ml after two days in culture. Higher IL-2 concentrations showed an effect on cell number in TCL1A transduced CTLL-2 (Figure 3-30B). While the EGFP only group maintained the same cell number at different concentrations, cell numbers of TCL1A expressing CTLL-2 increased with rising IL-2 concentrations.

A

B
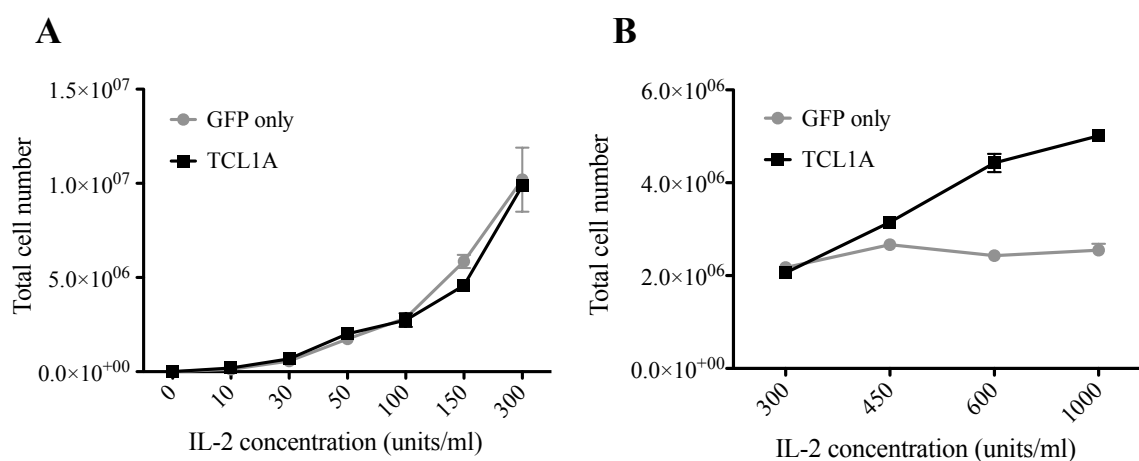
Figure 3-30: Cell numbers of TCL1A transduced CTLL-2 at different IL-2 concentrations
CTLL-2 cells were transduced with EGFP only and TCL1A and maintained at different IL-2 concentrations. CTLL-2 cells are normally cultured at a concentration of 300U IL-2 per ml. (A) At lower IL-2 concentrations, cell numbers of CTLL-2 decreased over a period of 16 days. (B) At higher IL-2 concentrations, cell numbers increased in TCL1A transduced over a period of two days.

Next, protein phosphorylation of downstream signaling molecules was evaluated in these cells by PhosFlow analysis of pSTAT5, pAKT and pERK1/2, 24 hours after adding fresh IL-2 to the cultures (Figure 3-31). TCL1A CTLL-2 cells showed increased phosphorylation of AKT (Figure 3-31A) and ERK1/2 (Figure 3-31B) compared to EGFP control cells, whereas no difference was observed in phosphorylation of the key IL-2 signaling protein STAT5 (Figure 3-31C).
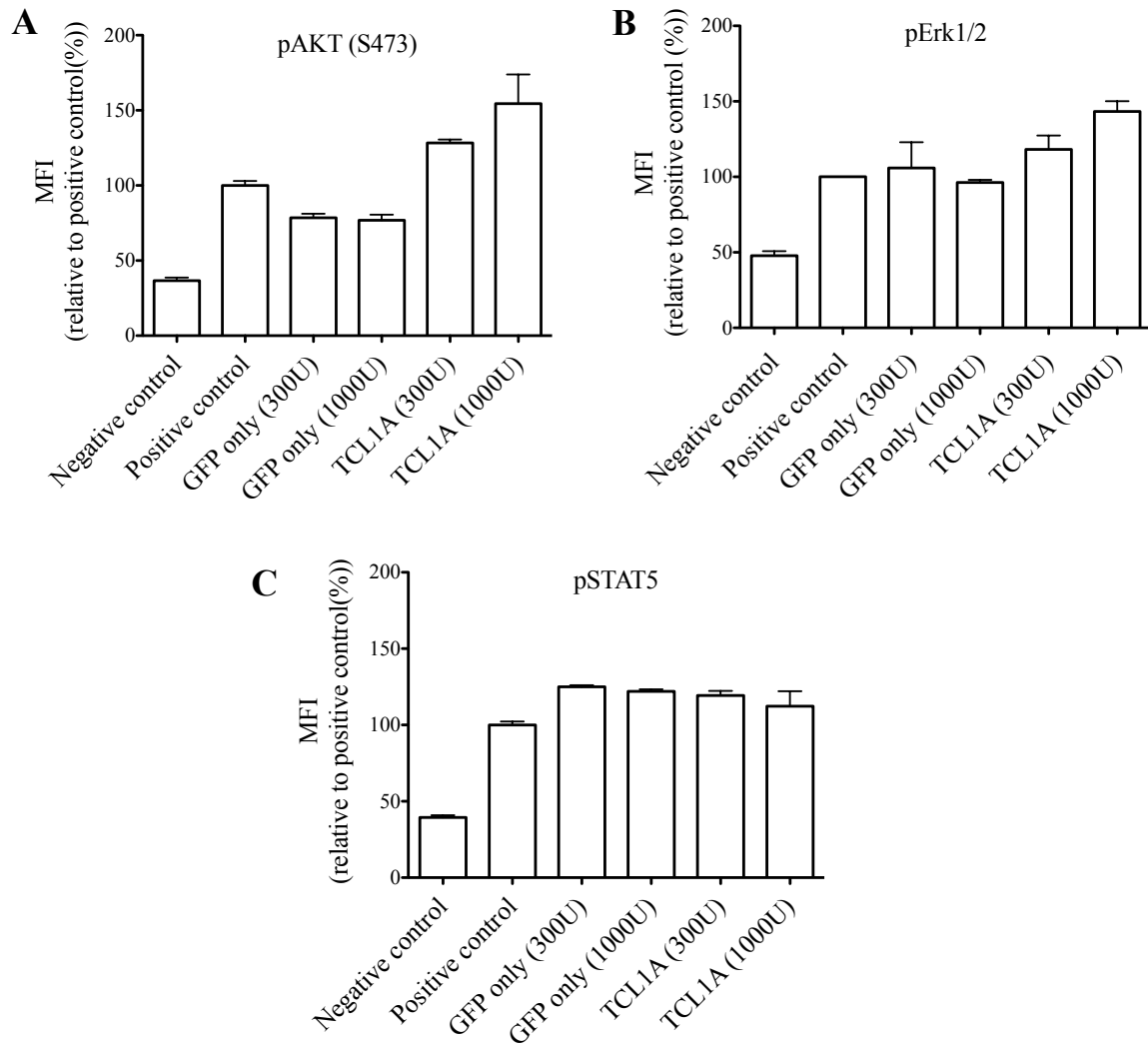
Figure 3-31: Protein phosphorylation in TCL1A transduced CTLL-2 at high IL-2 concentrations
CTLL-2 cells transduced with EGFP only and TCL1A were cultured with 300U and 1000U IL-2 for 24hours and then analyzed for phosphorylation of AKT (S473)(A), ERK1/2 (B) and STAT5 (C). Serum starved CTLL-2 cells were used as negative control and CTLL-2 stimulated with H_2O_2 served as positive control.

4. Discussion

In this thesis, the oncogenic mechanisms of the TCL1 family have been studied using two murine transplantation models. These genes were introduced into HSCs/HPCs for comparative analyses of their oncogenic potential in general (see section 4.1) or upon targeted expression to cellular compartments (see section 4.2). Additionally, TCL1A variants were introduced into monoclonal T cells to study the cooperation of TCR signaling and TCL1A in mature T-cell transformation (see section 4.3). Both transplantation systems proved to be useful to study different aspects of the TCL1 family and its role in B- and T-cell malignization (see section 4.4).

4.1 Comparative analysis of TCL1 family members

The oncogenic potential of the TCL1 family members TCL1A and MTCP1 in lymphocytes has been described in different transgenic mouse models (see section 1.2.2.3). However, the use of different promoters that drive TCL1 family gene expression in these models, does not allow a direct comparison of the different family members in their oncogenic potential. Additionally, no transgenic model has been described for the third TCL1 family member TML1. The establishment of transgenic mouse models is laborious and hardly feasible for the three family members at once. As syngeneic mouse models offer a good alternative, retroviral vectors were used in this thesis to introduce the TCL1 family genes TCL1A, MTCP1, and TML1 into HSCs/HPCs that were then transplanted into lethally irradiated WT mice (see section 3.2.2). Transduced HSCs/HPCs were not sorted before transplantation to recapitulate a more 'natural' pathogenesis, where not all cells carry the same genetic hit. TCL1A and MTCP1 mice predominantly developed B-cell lymphomas after comparable latencies (Figure 3-5). Based on the expression of the mature B-cell markers B220, CD19, and IgM (Table 3-2), a lymphoblastoid morphology (Figure 3-7) and leukemic presentation (Figure 3-8), these tumors were classified as Burkitt-like lymphomas according to the proposed classification of lymphoid neoplasms in mice (140). Thus, TCL1A and MTCP1 are oncogenes with comparable oncogenic potential. Although the exact oncogenic mechanisms of TCL1A remain incompletely resolved, it is known to interact with various key signaling molecules (see section 1.3.1.3). Less is known about the functional aspects of MTCP1, except that it binds AKT. This interaction is approximately 100-fold weaker than the interaction between

TCL1A and AKT (132). TCL1 is thought to enhance AKT activity by dimerization and oligomerization, thereby facilitating AKT transphosphorylation (141). The low affinity for AKT and the lack of a MTCP1 dimerization domain suggests that MTCP1 has a distinct mechanism for AKT activation and/or induces transformation of lymphocytes through separate mechanisms.

Although originally described as T-cell oncogenes, most TCL1A and MTCP1 recipient mice developed B-cell malignancies in the presented model. For TCL1A, this is in accordance with a study of transgenic mice expressing TCL1A in T- and B-cell populations at equal levels that predominantly developed Burkitt-like lymphomas as well (110). However, the only published MTCP1 transgenic model was T cell-specific (81). Therefore, the presented data showed for the first time that MTCP1 is capable of B-cell transformation. The predominant transformation of B cells by TCL1A and MTCP1 is most likely due to accumulation of secondary mutations during B cell-specific diversification processes. Upon activation, peripheral B cells undergo secondary diversification processes, such as somatic hypermutation and class switch recombination, to further enhance antigen binding (60). Somatic hypermutation is achieved by introducing point mutations into the variable regions of immunoglobins resulting in the expression of mutant BCRs. During immunoglobulin class switching the constant region of the immunoglobulin heavy chain is replaced with an alternate region through a process called class switch recombination, a intrachromosomal deletional recombination event requiring double strand breaks. Both processes are known to contribute of deregulated gene expression resulting in transformation of B cells (61). Mature T cells lack similar error-prone mechanisms. It is therefore likely that TCL1/MTCP1-induced T-cell transformation requires more time and is outcompeted by transformation of B cells in the presented model.

The third TCL1 family member TML1 is activated in human T-PLL together with TCL1A. However, it is unknown whether TML1 itself has oncogenic properties. Although TML1 appears to be a weaker oncogene than its two other family members, the presented data provided the first proof for the oncogenic function of TML1 (Figure 3-5). Moreover, it's oncogenic function was restricted to T cells (Table 3-1). There is little information on the functional aspects of TML1. Unlike TCL1A, it lacks a dimerization domain and binds AKT with low affinity (141). As it has a weak T cell-specific oncogenic function, TML1 most likely has mechanisms that are different from TCL1A and MTCP1. Interesting is also a 14aa stretch insertion in TML1 as compared to TCL1A, which may point to a phylogenetic evolution from TML1 to the proto-oncogene TCL1 after duplication and deletion of the14aa

stretch in higher mammals, where TCL1A expression is restricted to. Moreover, retroviral vector-mediated gene transfer bears the risk for insertional mutagenesis that might have contributed to induction or acceleration of tumor development in this model.

4.2   Targeting TCL1A to cellular compartments

In the next part of this thesis, the focus was laid on one of the family members, namely TCL1A, to learn more about the molecular basis of its oncogenic properties. It has been described that TCL1A interacts with different signaling molecules in different cellular compartments (see section 1.3.1.3). However, these studies did not reveal how localization of TCL1A relates to its oncogenic potential. Therefore, expression of TCL1A was targeted to the membrane and the nucleus using a myristoylated variant of TCL1A (myr-TCL1A) and a variant containing a nuclear localization signal (nls-TCL1A), respectively (see section 3.2.4). Interestingly, restricted localization of TCL1A did not impair its oncogenic potential. Similar to the generic TCL1A and MTCP1, both variants predominantly induced Burkitt-like lymphomas (Table 3-4). Survival of myr-TCL1A mice was comparable to the generic TCL1A cohort, whereas nls-TCL1A mice showed a significant reduction in survival (Figure 3-11). Gene expression analyses of these tumors revealed higher similarities between TCL1A and its nuclear variant (Figure 3-14, Figure 3-15). Together this data implicates that TCL1A's predominant oncogenic function relies on its nuclear presence.

Nevertheless, the oncogenic properties of the membrane-bound variant of TCL1A are not impaired compared to the generic TCL1A. Gene expression analyses of TCL1A-, myr-TCL1A- and nls-TCL1-induced tumors also showed that several signaling pathways are always affected in these tumors, including PI3K/AKT signaling, cell cycle, MAPK signaling, p53 signaling and GPCR signaling pathways (Figure 3-13). These pathways either share pathway components (Table 5-1) or are known to regulate each other. Together these data suggest, that TCL1A has a wide range of molecular mechanisms and is able to ultimately deregulate the same pathways regardless of its cellular localization.

Tumor cells usually show highly deregulated gene expression making it impossible to pinpoint the genetic alteration leading to deregulation of these pathways and ultimately to cellular transformation. Therefore, pre-leukemic B and T cells were sorted from TCL1A, myr-TCL1A and nls-TCL1A HSC/HPC recipient mice 100 days after transplantation to identify early changes in gene expression. Generally, B cells expressing TCL1A variants

showed a significant higher number of deregulated genes than the respective T cells at this time point (Figure 3-16). Moreover, similar pathways were affected in B and T cells (Figure 3-17, Figure 3-18), suggesting that transformation of both cell types is due to deregulation of the same signaling pathways. This data supports the hypothesis that predominant transformation of B cells is due to accumulation of secondary mutations during error-prone, B cell-specific diversification processes, thereby leading to earlier deregulation of cellular pathways.

Interestingly, cell cycle and p53-signaling pathway genes were both affected in B cells and B-cell tumors (Figure 3-13, Figure 3-17), but not in T cells. These pathways might therefore play an important role in the transformation of B cells in the presented model. DNA damage induces the p53-signaling pathway resulting in cell cycle checkpoint activation, thereby promoting either cell survival or death. Deregulation of these pathways has been associated with cellular transformation in general, but has also been detected specifically in B-cell lymphomas as a common feature (142). Cell cycle/p53 pathway genes up-regulated in analyzed B cells and B-cell tumors are Bub1b, Ccna2, Ccnb1, Ccnb2, Mpeg1 and Rrm2 (Table 5-1, Table 5-2). The cyclin genes Ccna2, Ccnb1 and Ccnb2 play an essential role in G2/M cell cycle transition. Overexpression is associated with chromosomal instability and double-strand breaks (143,144). The mitotic checkpoint gene Bub1b normally inhibits cell cycle progression and is more associated with tumor suppressive properties as heterozygous mice display chromosome instability and increased tumor susceptibility (145,146). The observed up-regulation might therefore be a compensatory effect for deregulation of other cell cycle components. The ribonucleotide reductase Rrm2 is important for DNA synthesis in dividing cells and overexpression in mice induces tumor development (147). There is no information on Mpeg1 and its role in cell cycle regulation. Based on this data it is not possible to determine which gene is responsible for cell cycle/p53 signaling deregulation as most of the up-regulated genes have been associated with cellular transformation. TCL1A has been associated with cell cycle interaction through ATM (see section 1.3.1.3). However, this gene is only down-regulated in TCL1A B cells and TCL1A tumors, but not in other cohorts (data not shown). This suggests that TCL1A might interfere with the cell cycle through other components besides ATM. The presented data does not allow drawing similar conclusions about the role of this pathway in the transformation of T cells, as this pathway is not affected in pre-leukemic T cells at the selected time point. This is most likely due to the general lack of early changes in T cells and analyses at later time points might reveal more about the involvement of this pathway. Nevertheless, a few genes were already deregulated in these

cells and they affect the same pathways as the ones seen in pre-leukemic and leukemic B cells, including PI3K/AKT signaling, MAPK signaling pathways and chemokine signaling (Figure 3-13, Figure 3-17, Figure 3-18). Remarkably, one gene is found in five out of the six affected pathways in pre-leukemic T cells, namely AKT1 (Table 5-3). It has been described that TCL1A enhances the kinase activity of AKT by forming hetero-oligomers at the plasma membrane (141). AKT has numerous substrates, thereby regulating survival, growth, cell cycle, proliferation, migration, etc (148). It is therefore likely that it plays a central role in deregulating these pathways in pre-leukemic T cells. However, it seems that the TCL1A-induced activation of AKT is not solely based on the interaction at the plasma membrane, as nls-TCL1A expressing T cells show the same up-regulation of AKT1 (Table 5-3). So far, it has only been described that TCL1A mediates nuclear translocation of AKT (74,119). This data suggests that TCL1A has additional mechanisms for activation of AKT besides oligomerization at the plasma membrane.

Interestingly, the murine TCL1 family members Mtcp1 and Tcl1b4 were down-regulated in TCL1A tumors and pre-leukemic TCL1A B-cells, respectively. This might be due cellular compensation of TCL1A overexpression by reducing endogenous expression of TCL1 family members that does not affect expression of the transgene.

4.3   Cooperation of TCL1A and TCR signaling

In a previously described HSC/HPC transplantation model, overexpression of TCL1A variants resulted predominantly in the transformation of B cells, which makes this model unsuitable to study the role of TCL1A in T cells. TCL1A interacts with different signaling molecules along the TCR signaling cascade, suggesting a role of TCR signaling in TCL1A-induced T-cell transformation (see section 1.3.1.3). Newrzela et al showed that T cells can be transformed in a TCR mono-/oligoclonal setting by certain T-cell oncogenes (45), but not in a TCR polyclonal environment (44). This OT-1 TCR monoclonal T-cell model was utilized to study the cooperation between TCL1A and TCR signaling by specifically stimulating the TCR of TCL1A transduced OT-1 T cells in vivo with an OVA peptide. Therefore, mice received transplants of TCL1A transduced OT-1 T cells and were then repeatedly injected with OVA peptide every two weeks. Blood sampling revealed early differences between OVA stimulated TCL1A mice and control mice. In stimulated control mice, the percentage of transplanted T cells decreased in the PB, whereas in TCL1A mice this percentage increased

after an initial decline (Figure 3-23). In vivo imaging showed that these cells are not lost in control mice and rather accumulate in inguinal LNs, abdominal regions and spleen, which was the same for stimlated TCL1A recipient mice (Figure 3-25, Figure 3-26). Thus, this data suggests that T cells retreat to secondary lymphoid organs in a 'chronically' stimulated environment. These organs provide pro-survival signals, including cytokines and spMHC peptides that might be essential for maintenance of repeatedly stimulated memory T cells.

The higher percentage of TCL1A expressing T cells in the PB was most likely due to enhanced accumulation of T cells in the presence of TCL1. This is supported by several observations: 1.) Generally higher bioluminescence signals in TCL1A cohorts compared to their unstimulated/stimulated control counterparts (Figure 3-25), 2.) Enrichment of transgene/EGFP expressing T cells in unstimulated TCL1 recipient mice, but not in unstimulated EGFP control mice (Figure 3-23), and 3.) Accelerated enrichment of TCL1A$^+$ T cells in OVA stimulated TCL1 recipient mice (Figure 3-23). Together this data implicates that enhanced accumulation of TCL1A$^+$ T cells in these mice is due to increased proliferative activity of these T cells, which is further enhanced by TCR stimulation. More importantly, the presence of TCL1A seemed to be enough to compensate for a TCR signal, as a similar enrichment of EGFP$^+$ T cells was only observed in stimulated and not unstimulated EGFP only control mice (Figure 3-23). In stimulated control EGFP recipient mice, this enrichment is most likely due to the viral integration that gives these cells an advantage over non-transduced cells, but only in the presence of a TCR stimulus.

The primary aim of this model was to establish, if chronic TCR stimulation has an effect on TCL1A's oncogenic potential. A significant reduction of survival of stimulated TCL1A mice compared to their unstimulated counterpart clearly demonstrated that chronic TCR engagement facilitated TCL1A-driven transformation (Figure 3-27). The same was observed for the two variants of TCL1A, namely myr-TCL1A and nls-TCL1A (Figure 3-27). This data provides functional proof for the role of TCR stimulation in augmenting the oncogenic properties of TCL1A, most likely by enhancing proliferation of TCL1A expressing T cells. Notable is also the difference in tumor phenotype between unstimulated and stimulated TCL1A mice (Table 3-5). Although a T-cell based transplantation model was used, B-cell tumors arose in a few unstimulated mice. This can be explained by a low percentage of B-cell contamination in the initial transplant (Figure 3-22). However, these tumors did not develop in stimulated mice, thereby suggesting that TCR stimulation drives specific transformation of T cells (or helps in outcompeting the B-cell tumors that would develop at a "basal" rate).

T-cell tumors in these mice often had a CD4 phenotype. This was unexpected as the initial transplant mainly consisted out CD8$^+$ T cells that specifically recognize the injected OVA peptide. The transgenic OT-1 TCR is MHC class I-restricted thereby limiting OT-1 TCR expression to CD8 T cells. The transgenic TCR is primarily selected in these mice, which leads to preferential outgrowth of transgenic OT-1 TCR expressing CD8 T cells. However, it has been shown that OT-1 thymocytes contain endogenous α chains that are able to undergo rearrangement and pair with the transgenic β chain, thereby producing CD4 and CD8 T cells with a chimeric TCR (149). These cells usually remain at a very low percentage in the initial transplant, but are not able to recognize the injected OVA peptide (Figure 3-22). A different explanation for the outgrowth of CD4 T-cell malignancies in the presented model is offered by a recent study that has shown that CD8 T cells in OT-1 mice have the capability of differentiating into CD4 T cells that express a functional OT-1 TCR (150). These cells were mostly detected in the large-intestine lamina propria of RAG1$^{-/-}$ OT-1 TCR transgenic mice that lack T cells with chimeric TCRs. Adoptively transferred CD4 T cells into WT mice responded to stimulation with OVA peptide. Interestingly, the CD4 tumor phenotype observed in the presented mouse model resembles the T-PLL phenotype in humans (see section 1.2.2.1). Cytologically, these cells resemble medium-sized T lymphocytes seen in T-PLL as well.

Studying OT-1 stimulation in vitro over a long period of time was not feasible. Therefore, for in vitro studies an IL-2 dependent murine T-cell line was used instead. These cells did not respond to TCR stimulation, but to IL-2 stimulation. The IL-2 pathway initiates the same downstream pathways as TCR engagement. In accordance with the data collected in vivo, TCL1A enhanced proliferation of T cells upon activation (Figure 3-30B). At low IL-2 concentrations, TCL1A did not have an anti-apoptotic effect that conferred a survival advantage (Figure 3-30A). The phosphorylation status of the two key signaling molecules AKT1 and ERK1/2 increased with higher IL-2 concentrations in stimulated TCL1A-carrying cells (Figure 3-31). STAT5 is one of the key mediators of IL-2-induced signaling and did not show any difference in its phosphorylation status. Thus, augmented proliferation of TCL1A expressing cells was associated with an enhanced activation of specific signaling molecules. TCL1A enhanced signaling pathways involved in activation and proliferation of T cells in the presented study, but only in the presence of an external stimulus. IL-2 or any other cytokine or co-stimulus would not be sufficient to induce a functional immune response in vivo. Therefore, the TCR plays most likely an important role in mediating / enhancing TCL1A's oncogenic properties by initiating downstream signaling pathways.

The involvement of the TCR in TCL1-driven transformation of T cells suggests the presence of a specific (auto)antigenic drive in T-PLL patients. For some PTCL entities, it has been shown that chronic inflammations often precede lymphoma / leukemia development, e.g. dermatitis prior to cutaneous T-cell lymphomas or expansions of autoimmune cytotoxic T cells prior to T-cell large granular lymphocyte leukemia (77). Inflammatory lesions or a bias in TCR gene usage has not been observed for T-PLL (78,79). This might hint at alternative mechanisms of TCR activation, such as intrinsically autonomous activation.

Retroviral vectors are commonly used for stable integration of genes into the genome of target cells. Despite the initial success in gene therapy, the further use of these vectors in clinical trials has been limited by severe side effects caused by insertional mutagenesis. In our studies, this clinical disadvantage is used to recapitulate secondary genetic hits that often drive the development of cancer. Integration of viral vectors into the host's genome can alter expression of genes around the site of integration that might favor malignant outgrowth. Control mice in these studies did not develop tumors, proving that this side effect is rare. Additionally, integration site analysis of tumors showed that only low numbers of genes are affected and classified in pathways, indicating that the introduced oncogene alone is responsible for cellular transformation (Table 3-7, Table 3-8). Although similar pathways are affected, there is no statistical overrepresentation that would allow drawing sound conclusions.

Besides the generic TCL1A, its variants myr-TCL1A and nls-TCL1A were also used in the described T-cell model. The effect of stimulation on survival was comparable to the generic TCL1A (Figure 3-27). There was no significant difference in survival between the different variants in the T-cell model, although nls-TCL1A showed reduced survival in the HSC/HPC model compared to the other variants (Figure 3-11). This suggests that TCL1A's nuclear presence might be more important for transformation of B cells than for T cells.

It should be noted that mice often developed ascites in this model as a side effect of repeated i.p. injections over a long period of time and had to be sacrificed before tumor development. This was not cohort-related as it was observed for stimulated and unstimulated control and TCL1A mice. To prevent this side effect and improve the system, it might be necessary to lower the frequency of injections.

4.4 General considerations for the use of HSCs/HPCs or TCR monoclonal T cells as target cells in syngeneic mouse models for lymphoma/leukemia studies

In the presented syngeneic mouse models, grafts from mice with the same genetic background were genetically manipulated using retroviral vectors. Most studies that work with these models use BM-derived HSCs/HPCs as donor cells. Retroviral transduction and transplantation of HSCs/HPCs is an efficient method to introduce transgenes into lymphocytes without altering these cells directly. Additionally, this has the advantage that the hematopoietic system is fully developed and functional, recapitulating a more "natural" tumorigenesis in immunocompetent hosts. This model is highly suitable for comparative analyses of oncogenic properties. In the case of TCL1A and its family members, B cells are predominantly transformed, making this a useful model for B-cell studies, but not for studying T-cell transformation. Interestingly, histological and cytological analysis showed that B-cell tumors induced in the HSC/HPC model had a larger and more immature morphology than the ones that developed in the T-cell model. This difference was not observed based on the flow cytometric analysis alone. Thus, using HSCs/HPCs or mature lymphocytes made a difference for the phenotype of the induced B-cell tumors.

Studying mature T-cell malignancies in mice has been challenging, as there is no promoter available that targets transgene expression specifically to mature T cells (151). In the presented HSC/HPC model, only immature T-cell tumors developed and were mostly outcompeted by the outgrowth of B-cell malignancies. Using mature T cells as target cells for retroviral transduction has been limited by their resistance to transformation by oncogenes, including TCL1A (44). However, using TCR monoclonal instead of TCR polyclonal T cells circumvented this effect (45). The TCR monoclonal system offers the possibility to study the role of the TCR in cellular transformation. There are several different transgenic TCR models that allow specific stimulation of CD4 and CD8 T cells, such as OT-1, OT-2 or P14. Similarly, this could be done for B cells and BCR stimulation, e.g. using MD4 transgenic B cells that specifically recognize hen egg lysozyme. However, these models represent rather simplified approaches to study the pathogenesis of mature T- or B-cell tumors. Immunodeficient hosts and TCR monoclonal lymphocytes do not represent a "natural" environment, but they offer a good starting point to dissect the complex course of cellular transformation. Next, this model can be further adapted by mixing TCR polyclonal T cells to

the TCR monoclonal transplant or by using Nude mice as recipients that have functional B cells and only lack T cells.

4.5   Conclusions and Outlook

The presented study covers different aspects on the function of TCL1 oncogene family members. First, it was shown that TCL1A and MTCP1 share a similar oncogenic capacity, whereas TML1 is a weak oncogene with low penetrance in our systems. Currently, primary T-PLL cases are analyzed for expression frequency of these three oncogenes in our laboratory.

Next, it was shown that nuclear localization of TCL1A reduced survival of recipient mice compared to the generic TCL1A protein and a membrane-localizing variant. Gene expression data revealed an important role of p53 signaling and cell cycle genes in the transformation of B cells. Gene expression data collected from this study is currently compared to gene expression data from TCL1A transgenic mice at different time points before tumor development.

In the last part of this thesis a new in vivo model was established to specifically stimulate the TCR of TCR monoclonal T cells in vivo. The data clearly show that TCL1A-driven transformation is facilitated by repeated TCR stimulation, thereby demonstrating that there likely is a pro-leukemogenic cooperation between TCL1A and TCR signaling. To further analyze this synergy, signaling dosages of TCL1A and TCR are currently analyzed in human CTCL cell lines by titrating TCL1A levels in a Tet-ON TCL1A-inducible system and by titrating TCR activation through blocking antibodies (OKT3 or 15E8). The aim of this experiment is to determine how these signals compensate for each other, e.g. if a higher expression of TCL1A can compensate for high-avidity TCR engagement. For further in vivo studies polyclonal T cells are added to the OT-1 T cell transplant to test if the additional TCR stimulus allows TCL1A transduced T cells to overcome clonal competition. Furthermore, TCL1 transgenic mice are crossbred with CD3-deficient and MHC-deficient mice to address the requirement of TCR signaling input in TCL1-mediated oncogenesis.

The antigen receptor plays a central role in T- and B-cell development, function and survival. The clinical and therapeutic importance of the BCR has been well described for B-cell malignancies (152). In the recent years, specific inhibitors of BCR signaling molecules, such as PI3K or Bruton's tyrosine kinase (BTK), have been approved for the treatment of B-cell

lymphomas / leukemias and have shown promising clinical results (153,154). For the treatment of PTCL, an inhibitor of the TCR signaling kinase mTOR showed successful results in ongoing clinical trials as well (155). The suitability of interleukin-2-inducible T-cell Kinase (ITK) as an effective drug target for PTCL is currently investigated, but likely its role in T cells is not congruently reflected by BTK in B-cells and the derived tumors (156). These studies emphasize the potential of treatment approaches targeting antigen receptor signaling and the demand for a detailed understanding of TCR involvement in PTCL pathobiology.

References

1. Godfrey DI, Kennedy J, Suda T, Zlotnik A. A developmental pathway involving four phenotypically and functionally distinct subsets of CD3-CD4-CD8- triple-negative adult mouse thymocytes defined by CD44 and CD25 expression. J Immunol. 1993;150(10):4244–52.

2. Oettinger MA, Schatz DG, Gorka C, Baltimore D. RAG-1 and RAG-2, adjacent genes that synergistically activate V(D)J recombination. Science (80). 1990;248(4962):1517–23.

3. Capone M, Hockett RD, Zlotnik A. Kinetics of T cell receptor beta, gamma, and delta rearrangements during adult thymic development: T cell receptor rearrangements are present in CD44(+)CD25(+) Pro-T thymocytes. Proc Natl Acad Sci U S A. 1998;95(21):12522–7.

4. von Boehmer H, Fehling HJ. Structure and function of the pre-T cell receptor. Annu Rev Immunol. 1997;15:433–52.

5. Falk I, Nerz G, Haidl I, Krotkova A, Eichmann K. Immature thymocytes that fail to express TCRbeta and/or TCRgamma delta proteins die by apoptotic cell death in the CD44-CD25- (DN4) subset. Eur J Immunol. 2001;31(11):3308–17.

6. Germain RN. T-cell development and the CD4-CD8 lineage decision. Nat Rev Immunol. 2002;2(5):309–22.

7. Teh HS, Kisielow P, Scott B, Kishi H, Uematsu Y, Blüthmann H, et al. Thymic major histocompatibility complex antigens and the alpha beta T-cell receptor determine the CD4/CD8 phenotype of T cells. Nature. 1988;335(6187):229–33.

8. Singer A, Adoro S, Park J-H. Lineage fate and intense debate: myths, models and mechanisms of CD4- versus CD8-lineage choice. Nat Rev Immunol. 2008;8(10):788–801.

9. Broere F, Apasov SG, Sitkovsky M V., van Eden W. T cell subsets and T cell-mediated immunity. Principles of Immunopharmacology. Basel: Birkhäuser Basel; 2011. p. 15–27.

10. Mueller SN, Gebhardt T, Carbone FR, Heath WR. Memory T Cell Subsets, Migration Patterns, and Tissue Residence. Annu Rev Immunol. 2013 Mar 21;31(1):137–61.

11. Appay V, Van Lier RAW, Sallusto F, Roederer M. Phenotype and function of human T lymphocyte subsets: Consensus and issues. Cytom A. 2008;73(11):975–83.

12. Hamann D, Baars PA, Rep MH, Hooibrink B, Kerkhof-Garde SR, Klein MR, et al. Phenotypic and functional separation of memory and effector human CD8+ T cells. J Exp Med. 1997;186(9):1407–18.

13.   Alari-Pahissa E, Notario L, Lorente E, Vega-Ramos J, Justel A, López D, et al. CD69 Does Not Affect the Extent of T Cell Priming. Hasenkrug KJ, editor. PLoS One. 2012 Oct 30;7(10):e48593.

14.   Hernandez MGH, Shen L, Rock KL. CD40-CD40 Ligand Interaction between Dendritic Cells and CD8+ T Cells Is Needed to Stimulate Maximal T Cell Responses in the Absence of CD4+ T Cell Help. J Immunol. 2007 Mar 1;178(5):2844–52.

15.   Wambre E, James EA, Kwok WW. Characterization of CD4+ T cell subsets in allergy. Curr Opin Immunol. 2012;24(6):700–6.

16.   Sallusto F, Lenig D, Förster R, Lipp M, Lanzavecchia A. Two subsets of memory T lymphocytes with distinct homing potentials and effector functions. Nature. 1999;401(6754):708–12.

17.   Masopust D, Vezys V, Marzo AL, Lefrançois L. Preferential localization of effector memory cells in nonlymphoid tissue. Science (80-). 2001;291(5512):2413–7.

18.   Venturi V, Price DA, Douek DC, Davenport MP. The molecular basis for public T-cell responses? Nat Rev Immunol. 2008 Mar;8(3):231–8.

19.   Meydan C, Otu HH, Sezerman O. Prediction of peptides binding to MHC class I and II alleles by temporal motif mining. BMC Bioinformatics. 2013;14(Suppl 2):S13.

20.   Weiss A. Molecular and genetic insights into T cell antigen receptor structure and function. Annu Rev Genet. 1991;25:487–510.

21.   Murphy K. Antigen Recognition by B-cell and T-cell Receptors. Janeway's Immunobiology. 8th ed. New York: Garland Science; 2011. p. 127–56.

22.   Gascoigne NRJ. Do T cells need endogenous peptides for activation? Nat Rev Immunol. 2008 Nov;8(11):895–900.

23.   Zhang W, Sloan-Lancaster J, Kitchen J, Trible RP, Samelson LE. LAT: The ZAP-70 Tyrosine Kinase Substrate that Links T Cell Receptor to Cellular Activation. Cell. 1998 Jan;92(1):83–92.

24.   Sue Goo Rhee, Choi KD. Regulation of inositol phospholipid-specific phospholipase C isozymes. J Biol Chem. 1992;267(18):12393–6.

25.   Pollizzi KN, Powell JD. Integrating canonical and metabolic signalling programmes in the regulation of T cell responses. Nat Rev Immunol. 2014 Jun 25;14(7):435–46.

26.   Masuda ES, Imamura R, Amasaki Y, Arai K, Arai N. Signalling into the T-Cell Nucleus: NFAT regulation. Cell Signal. 1998 Oct;10(9):599–611.

27.   Teixeira C, Stang SL, Zheng Y, Beswick NS, Stone JC. Integration of DAG signaling systems mediated by PKC-dependent phosphorylation of RasGRP3. Blood. 2003;102(4):1414–20.

28. Chang F, Steelman LS, Lee JT, Shelton JG, Navolanic PM, Blalock WL, et al. Signal transduction mediated by the Ras/Raf/MEK/ERK pathway from cytokine receptors to transcription factors: potential targeting for therapeutic intervention. Leukemia. 2003 Jul;17(7):1263–93.

29. Lin X, O'Mahony A, Mu Y, Geleziunas R, Greene WC. Protein kinase C-theta participates in NF-kappaB activation induced by CD3-CD28 costimulation through selective activation of IkappaB kinase beta. Mol Cell Biol. 2000;20(8):2933–40.

30. Israël A. The IKK complex, a central regulator of NF-kappaB activation. Cold Spring Harb Perspect Biol. 2010;2(3).

31. Takeda K, Harada Y, Watanabe R, Inutake Y, Ogawa S, Onuki K, et al. CD28 stimulation triggers NF-kappaB activation through the CARMA1-PKCtheta-Grb2/Gads axis. Int Immunol. 2008;20(12):1507–15.

32. Nunès JA, Collette Y, Truneh A, Olive D, Cantrell DA. The role of p21ras in CD28 signal transduction: triggering of CD28 with antibodies, but not the ligand B7-1, activates p21ras. J Exp Med. 1994;180(3):1067–76.

33. Alegre M-L, Frauwirth KA, Thompson CB. T-cell regulation by CD28 and CTLA-4. Nat Rev Immunol. 2001 Dec;1(3):220–8.

34. Okkenhaug K, Vanhaesebroeck B. PI3K in lymphocyte development, differentiation and activation. Nat Rev Immunol. 2003 Apr 25;3(4):317–30.

35. Manning BD, Cantley LC. AKT/PKB Signaling: Navigating Downstream. Cell. 2007 Jun;129(7):1261–74.

36. Ozes ON, Mayo LD, Gustin JA, Pfeffer SR, Pfeffer LM, Donner DB. NF-kappaB activation by tumour necrosis factor requires the Akt serine-threonine kinase. Nature. 1999;401(6748):82–5.

37. Liao W, Lin J-X, Leonard WJ. Interleukin-2 at the Crossroads of Effector Responses, Tolerance, and Immunotherapy. Immunity. 2013 Jan;38(1):13–25.

38. Sprent J, Surh CD. Normal T cell homeostasis: the conversion of naive cells into memory-phenotype cells. Nat Immunol. 2011;12(6):478–84.

39. Moses CT, Thorstenson KM, Jameson SC, Khoruts A. Competition for self ligands restrains homeostatic proliferation of naive CD4 T cells. Proc Natl Acad Sci U S A. 2003 Feb 4;100(3):1185–90.

40. Troy AE, Shen H. Cutting Edge: Homeostatic Proliferation of Peripheral T Lymphocytes Is Regulated by Clonal Competition. J Immunol. 2003 Jan 15;170(2):672–6.

41. Kieper WC, Burghardt JT, Surh CD. A role for TCR affinity in regulating naive T cell

homeostasis. J Immunol. 2004 Jan 1;172(1):40–4.

42.   Hao Y, Legrand N, Freitas AA. The clone size of peripheral CD8 T cells is regulated by TCR promiscuity. J Exp Med. 2006 Jul 10;203(7):1643–9.

43.   Agenès F, Dangy J-P, Kirberg J. T cell receptor contact to restricting MHC molecules is a prerequisite for peripheral interclonal T cell competition. J Exp Med. 2008 Nov 24;205(12):2735–43.

44.   Newrzela S, Cornils K, Li Z, Baum C, Brugman MH, Hartmann M, et al. Resistance of mature T cells to oncogene transformation. Blood. 2008;112(6):2278–86.

45.   Newrzela S, Al-Ghaili N, Heinrich T, Petkova M, Hartmann S, Rengstl B, et al. T-cell receptor diversity prevents T-cell lymphoma development. Leukemia. 2012 Dec 30;26(12):2499–507.

46.   Akbar AN, Borthwick NJ, Wickremasinghe RG, Panayoitidis P, Pilling D, Bofill M, et al. Interleukin-2 receptor common gamma-chain signaling cytokines regulate activated T cell apoptosis in response to growth factor withdrawal: selective induction of anti-apoptotic (bcl-2, bcl-xL) but not pro-apoptotic (bax, bcl-xS) gene expression. Eur J Immunol. 1996;26(2):294–9.

47.   Boise LH, Minn AJ, Noel PJ, June CH, Accavitti MA, Lindsten T, et al. CD28 costimulation can promote T cell survival by enhancing the expression of Bcl-XL. Immunity. 1995;3(1):87–98.

48.   Nagata S, Suda T. Fas and Fas ligand: lpr and gld mutations. Immunol Today. 1995;16(1):39–43.

49.   Calvo CR, Amsen D, Kruisbeek AM. Cytotoxic T lymphocyte antigen 4 (CTLA-4) interferes with extracellular signal-regulated kinase (ERK) and Jun NH2-terminal kinase (JNK) activation, but does not affect phosphorylation of T cell receptor zeta and ZAP70. J Exp Med. 1997;186(10):1645–53.

50.   von Boehmer H. Mechanisms of suppression by suppressor T cells. Nat Immunol. 2005;6(4):338–44.

51.   Van Parijs L, Abbas AK. Homeostasis and self-tolerance in the immune system: turning lymphocytes off. Science (80-). 1998;280(5361):243–8.

52.   Schluns KS, Kieper WC, Jameson SC, Lefrançois L. Interleukin-7 mediates the homeostasis of naïve and memory CD8 T cells in vivo. Nat Immunol. 2000 Nov;1(5):426–32.

53.   Kondrack RM, Harbertson J, Tan JT, McBreen ME, Surh CD, Bradley LM. Interleukin 7 regulates the survival and generation of memory CD4 cells. J Exp Med. 2003 Dec 15;198(12):1797–806.

54. Goldrath AW, Sivakumar P V, Glaccum M, Kennedy MK, Bevan MJ, Benoist C, et al. Cytokine requirements for acute and Basal homeostatic proliferation of naive and memory CD8+ T cells. J Exp Med. 2002 Jun 17;195(12):1515–22.

55. Swain SL, Hu H, Huston G. Class II-independent generation of CD4 memory T cells from effectors. Science (80-). 1999 Nov 12;286(5443):1381–3.

56. Murali-Krishna K, Lau LL, Sambhara S, Lemonnier F, Altman J, Ahmed R. Persistence of memory CD8 T cells in MHC class I-deficient mice. Science (80-). 1999 Nov 12;286(5443):1377–81.

57. Tanchot C, Lemonnier FA, Pérarnau B, Freitas AA, Rocha B. Differential requirements for survival and proliferation of CD8 naïve or memory T cells. Science (80-). 1997 Jun 27;276(5321):2057–62.

58. Markiewicz MA, Girao C, Opferman JT, Sun J, Hu Q, Agulnik AA, et al. Long-term T cell memory requires the surface expression of self-peptide/major histocompatibility complex molecules. Proc Natl Acad Sci U S A. 1998 Mar 17;95(6):3065–70.

59. Swerdlow SH, Campo E, Harris NL, Jaffe ES, Pileri SA, Stein H, et al. Tumours of Hematopoietic and Lymphoid Tissues. Fourth Edi. World Health Organization Classification of Tumours. Lyon, France: IARC Press; 2008.

60. Li Z, Woo CJ, Iglesias-Ussel MD, Ronai D, Scharff MD. The generation of antibody diversity through somatic hypermutation and class switch recombination. Genes Dev. 2004;18(1):1–11.

61. Küppers R, Dalla-Favera R. Mechanisms of chromosomal translocations in B cell lymphomas. Oncogene. 2001 Sep 10;20(40):5580–94.

62. Vose J, Armitage J, Weisenburger D. International peripheral T-cell and natural killer/T-cell lymphoma study: pathology findings and clinical outcomes. J Clin Oncol. 2008;26(25):4124–30.

63. Savage KJ. Therapies for Peripheral T-Cell Lymphomas. ASH Educ B. 2011;2011(1):515–24.

64. Herling M, Jones D. Mature T-cell Leukemias - Current Challenges in Diagnosis and Therapy. Am J Clin Oncol. 2004;10(3):608–17.

65. Herling M, Khoury JD, Washington LT, Duvic M, Keating MJ, Jones D. A systematic approach to diagnosis of mature T-cell leukemias reveals heterogeneity among WHO categories. Blood. 2004;104(2):328–35.

66. Ravandi F, O'Brien S, Jones D, Lerner S, Faderl S, Ferrajoli A, et al. T-cell prolymphocytic leukemia: a single-institution experience. Clin Lymphoma Myeloma. 2005;6(3):234–9.

67. Matutes E, Brito-Babapulle V, Swansbury J, Ellis J, Morilla R, Dearden C, et al. Clinical and laboratory features of 78 cases of T-prolymphocytic leukemia. Blood. 1991;78(12):3269–74.

68. Grey-Davies E, Dearden C. The T-Cell Leukaemias. In: Foss F, editor. T-Cell Lymphomas. New York: Humana Press; 2013. p. 137–53.

69. Brito-Babapulle V, Catovsky D. Inversions and tandem translocations involving chromosome 14q11 and 14q32 in T-prolymphocytic leukemia and T-cell leukemias in patients with ataxia telangiectasia. Cancer Genet Cytogenet. 1991;55(1):1–9.

70. Virgilio L, Narducci MG, Isobe M, Billips LG, Cooper MD, Croce CM, et al. Identification of the TCL1 gene involved in T-cell malignancies. Proc Natl Acad Sci U S A. 1994;91(26):12530–4.

71. Hoyer KK, Herling M, Bagrintseva K, Dawson DW, French SW, Renard M, et al. T cell leukemia-1 modulates TCR signal strength and IFN-gamma levels through phosphatidylinositol 3-kinase and protein kinase C pathway activation. J Immunol. 2005;175(2):864–73.

72. Soulier J, Pierron G, Vecchione D, Garand R, Brizard F, Sigaux F, et al. A complex pattern of recurrent chromosomal losses and gains in T-cell prolymphocytic leukemia. Genes Chromosom Cancer. 2001;31(3):248–54.

73. Maljaei SH, Brito-Babapulle V, Hiorns LR, Catovsky D. Abnormalities of chromosomes 8, 11, 14, and X in T-prolymphocytic leukemia studied by fluorescence in situ hybridization. Cancer Genet Cytogenet. 1998 Jun;103(2):110–6.

74. Herling M, Patel KA, Teitell MA, Konopleva M, Ravandi F, Kobayashi R, et al. High TCL1 expression and intact T-cell receptor signaling define a hyperproliferative subset of T-cell prolymphocytic leukemia. Blood. American Society of Hematology; 2008;111(1):328–37.

75. Costa D, Queralt R, Aymerich M, Carrio A, Rozman M, Vallespi T, et al. High levels of chromosomal imbalances in typical and small-cell variants of T-cell prolymphocytic leukemia. Cancer Genet Cytogenet. 2003;147(1):36–43.

76. Stilgenbauer S, Schaffner C, Litterst A, Liebisch P, Gilad S, BarShira A, et al. Biallelic mutations in the ATM gene in T-prolymphocytic leukemia. Nat Med. 1997;3(10):1155–9.

77. Warner K, Weit N, Crispatzu G, Admirand J, Jones D, Herling M. T-Cell Receptor Signaling in Peripheral T-Cell Lymphoma – A Review of Patterns of Alterations in a Central Growth Regulatory Pathway. Curr Hematol Malig Rep. 2013 Sep 27;8(3):163–72.

78. Hodges E, Edwards SE, Howell WM, Smith JL. Polymerase chain reaction amplification analyses of clonality in T-cell malignancy including peripheral T-cell

lymphoma. Leukemia. 1994;8(2):295–8.

79.   Tembhare P, Yuan CM, Xi L, Morris JC, Liewehr D, Venzon D, et al. Flow Cytometric Immunophenotypic Assessment of T-Cell Clonality by Vβ Repertoire Analysis . Am J Clin Pathol. 2011 Jun 1;135 (6):890–900.

80.   Virgilio L, Lazzeri C, Bichi R, Nibu K, Narducci MG, Russo G, et al. Deregulated expression of TCL1 causes T cell leukemia in mice. Proc Natl Acad Sci U S A. 1998;95(7):3885–9.

81.   Gritti C, Dastot H, Soulier J, Janin A, Daniel MT, Madani A, et al. Transgenic mice for MTCP1 develop T-cell prolymphocytic leukemia. Blood. 1998;92(2):368–73.

82.   Stern MH, Soulier J, Rosenzwajg M, Nakahara K, Canki-Klain N, Aurias A, et al. MTCP-1: a novel gene on the human chromosome Xq28 translocated to the T cell receptor alpha/delta locus in mature T cell proliferations. Oncogene. 1993;8(9):2475–83.

83.   Sugimoto J, Hatakeyama T, Narducci MG, Russo G, Isobe M. Identification of the TCL1/MTCP1-like 1 (TML1) gene from the region next to the TCL1 locus. Cancer Res. 1999;59(10):2313–7.

84.   Hallas C, Pekarsky Y, Itoyama T, Varnum J, Bichi R, Rothstein JL, et al. Genomic analysis of human and mouse TCL1 loci reveals a complex of tightly clustered genes. Proc Natl Acad Sci U S A. 1999 Dec 7;96(25):14418–23.

85.   Croce CM, Isobe M, Palumbo A, Puck J, Ming J, Tweardy D, et al. Gene for alpha-chain of human T-cell receptor: location on chromosome 14 region involved in T-cell neoplasms. Science (80-). 1985 Mar 1;227(4690):1044–7.

86.   Fu TB, Virgilio L, Narducci MG, Facchiano A, Russo G, Croce CM. Characterization and localization of the TCL-1 oncogene product. Cancer Res. 1994;54(24):6297–301.

87.   Hoh F, Yang YS, Guignard L, Padilla A, Stern MH, Lhoste JM, et al. Crystal structure of p14TCL1, an oncogene product involved in T-cell prolymphocytic leukemia, reveals a novel beta-barrel topology. Structure. 1998;6(2):147–55.

88.   Narducci MG, Virgilio L, Engiles JB, Buchberg AM, Billips L, Facchiano A, et al. The murine Tcl1 oncogene: embryonic and lymphoid cell expression. Oncogene. 1997;15(8):919–26.

89.   Ivanova N, Dobrin R, Lu R, Kotenko I, Levorse J, DeCoste C, et al. Dissecting self-renewal in stem cells with RNA interference. Nature. 2006 Aug 3;442(7102):533–8.

90.   Kang SM, Narducci MG, Lazzeri C, Mongiovi AM, Caprini E, Bresin A, et al. Impaired T- and B-cell development in Tcl1-deficient mice. Blood. 2005;105(3):1288–94.

91. Pekarsky Y, Hallas C, Isobe M, Russo G, Croce CM. Abnormalities at 14q32.1 in T cell malignancies involve two oncogenes. Proc Natl Acad Sci U S A. 1999;96(6):2949–51.

92. Seifert M, Sellmann L, Bloehdorn J, Wein F, Stilgenbauer S, Durig J, et al. Cellular origin and pathophysiology of chronic lymphocytic leukemia. J Exp Med. 2012 Nov 19;209(12):2183–98.

93. Herling M, Teitell MA, Shen RR, Medeiros LJ, Jones D. TCL1 expression in plasmacytoid dendritic cells (DC2s) and the related CD4+ CD56+ blastic tumors of skin. Blood. 2003;101(12):5007–9.

94. Thick J, Metcalfe JA, Mak YF, Beatty D, Minegishi M, Dyer MJS, et al. Expression of either the TCL1 oncogene, or transcripts from its homologue MTCP1/c6.1B, in leukaemic and non-leukaemic T cells from ataxia telangiectasia patients. Oncogene. 1996;12(2):379–86.

95. Narducci MG, Fiorenza MT, Kang SM, Bevilacqua A, Di Giacomo M, Remotti D, et al. TCL1 participates in early embryonic development and is overexpressed in human seminomas. Proc Natl Acad Sci U S A. 2002;99(18):11712–7.

96. Roos J, Hennig I, Schwaller J, Zbaren J, Dummer R, Burg G, et al. Expression of TCL1 in hematologic disorders. Pathobiology. 2001;69(2):59–66.

97. Wang X, Yang S, Zhao X, Guo H, Ling X, Wang L, et al. OCT3 and SOX2 promote the transformation of Barrett's esophagus to adenocarcinoma by regulating the formation of tumor stem cells. Oncol Rep. 2014 Apr;31(4):1745–53.

98. Hong X, Song R, Song H, Zheng T, Wang J, Liang Y, et al. PTEN antagonises Tcl1/hnRNPK-mediated G6PD pre-mRNA splicing which contributes to hepatocarcinogenesis. Gut. 2014 Oct;63(10):1635–47.

99. Lau SK, Weiss LM, Chu PG. TCL1 protein expression in testicular germ cell tumors. Am J Clin Pathol. 2010/04/17 ed. 2010;133(5):762–6.

100. Liu A, Cheng L, Du J, Peng Y, Allan RW, Wei L, et al. Diagnostic utility of novel stem cell markers SALL4, OCT4, NANOG, SOX2, UTF1, and TCL1 in primary mediastinal germ cell tumors. Am J Surg Pathol. 2010/04/23 ed. 2010;34(5):697–706.

101. Virgilio L, Isobe M, Narducci MG, Carotenuto P, Camerini B, Kurosawa N, et al. Chromosome walking on the TCL1 locus involved in T-cell neoplasia. Proc Natl Acad Sci U S A. 1993;90(20):9275–9.

102. Pekarsky Y, Hallas C, Croce CM. Molecular basis of mature T-cell leukemia. Jama. 2001;286(18):2308–14.

103. Herling M, Patel KA, Khalili J, Schlette E, Kobayashi R, Medeiros LJ, et al. TCL1 shows a regulated expression pattern in chronic lymphocytic leukemia that correlates

with molecular subtypes and proliferative state. Leukemia. Nature Publishing Group; 2006;20(2):280–5.

104. Fink SR, Paternoster SF, Smoley SA, Flynn HC, Geyer SM, Shanafelt TD, et al. Fluorescent-labeled DNA probes applied to novel biological aspects of B-cell chronic lymphocytic leukemia. Leuk Res. 2005;29(3):253–62.

105. Yuille MR, Condie A, Stone EM, Wilsher J, Bradshaw PS, Brooks L, et al. TCL1 is activated by chromosomal rearrangement or by hypomethylation. Genes Chromosom Cancer. 2001;30(4):336–41.

106. French SW, Malone CS, Shen RR, Renard M, Henson SE, Miner MD, et al. Sp1 transactivation of the TCL1 oncogene. J Biol Chem. 2003;278(2):948–55.

107. Sivina M, Hartmann E, Vasyutina E, Boucas JM, Breuer A, Keating MJ, et al. Stromal cells modulate TCL1 expression, interacting AP-1 components and TCL1-targeting micro-RNAs in chronic lymphocytic leukemia. Leukemia. 2012/03/31 ed. 2012 Aug;26(8):1812–20.

108. Herling M, Patel KA, Hsi ED, Chang KC, Rassidakis GZ, Ford R, et al. TCL1 in B-cell tumors retains its normal B-cell pattern of regulation and is a marker of differentiation stage. Am J Surg Pathol. 2007;31(7):1123–9.

109. Vasyutina E, Boucas JM, Bloehdorn J, Aszyk C, Crispatzu G, Stiefelhagen M, et al. The regulatory interaction of EVI1 with the TCL1A oncogene impacts cell survival and clinical outcome in CLL. Leukemia. 2015 Oct;29(10):2003–14.

110. Hoyer KK, French SW, Turner DE, Nguyen MTN, Renard M, Malone CS, et al. Dysregulated TCL1 promotes multiple classes of mature B cell lymphoma. Proc Natl Acad Sci U S A. National Academy of Sciences; 2002;99(22):14392–7.

111. Bichi R, Shinton SA, Martin ES, Koval A, Calin GA, Cesari R, et al. Human chronic lymphocytic leukemia modeled in mouse by targeted TCL1 expression. Proc Natl Acad Sci U S A. 2002;99(10):6955–60.

112. Simonetti G, Bertilaccio MTS, Ghia P, Klein U. Mouse models in the study of chronic lymphocytic leukemia pathogenesis and therapy. Blood. 2014 Aug 14;124(7):1010–9.

113. Matoba R, Niwa H, Masui S, Ohtsuka S, Carter MG, Sharov AA, et al. Dissecting Oct3/4-regulated gene networks in embryonic stem cells by expression profiling. PLoS One. 2006;1:e26.

114. Ema M, Mori D, Niwa H, Hasegawa Y, Yamanaka Y, Hitoshi S, et al. Krüppel-like factor 5 is essential for blastocyst development and the normal self-renewal of mouse ESCs. Cell Stem Cell. 2008;3(5):555–67.

115. Miyazaki T, Miyazaki S, Ashida M, Tanaka T, Tashiro F, Miyazaki J. Functional Analysis of Tcl1 Using Tcl1-Deficient Mouse Embryonic Stem Cells. Wutz A, editor.

PLoS One. 2013 Aug 5;8(8):e71645.

116. Ragone G, Bresin A, Piermarini F, Lazzeri C, Picchio MC, Remotti D, et al. The Tcl1 oncogene defines secondary hair germ cells differentiation at catagen-telogen transition and affects stem-cell marker CD34 expression. Oncogene. 2009;

117. Laine J, Kunstle G, Obata T, Sha M, Noguchi M. The protooncogene TCL1 is an Akt kinase coactivator. Mol Cell. 2000;6(2):395–407.

118. French SW, Shen RR, Koh PJ, Malone CS, Mallick P, Teitell MA. A modeled hydrophobic domain on the TCL1 oncoprotein mediates association with AKT at the cytoplasmic membrane. Biochemistry. 2002;41(20):6376–82.

119. Pekarsky Y, Koval A, Hallas C, Bichi R, Tresini M, Malstrom S, et al. Tcl1 enhances Akt kinase activity and mediates its nuclear translocation. Proc Natl Acad Sci U S A. 2000;97(7):3028–33.

120. Kunstle G, Laine J, Pierron G, Kagami Si S, Nakajima H, Hoh F, et al. Identification of Akt association and oligomerization domains of the Akt kinase coactivator TCL1. Mol Cell Biol. 2002;22(5):1513–25.

121. Pekarsky Y, Palamarchuk A, Maximov V, Efanov A, Nazaryan N, Santanam U, et al. Tcl1 functions as a transcriptional regulator and is directly involved in the pathogenesis of CLL. Proc Natl Acad Sci U S A. 2008;105(50):19643–8.

122. Colotta F, Polentarutti N, Sironi M, Mantovani A. Expression and involvement of c-fos and c-jun protooncogenes in programmed cell death induced by growth factor deprivation in lymphoid cell lines. J Biol Chem. 1992;267(26):18278–83.

123. Gaudio E, Spizzo R, Paduano F, Luo Z, Efanov A, Palamarchuk A, et al. Tcl1 interacts with Atm and enhances NF-kappaB activation in hematologic malignancies. Blood. 2011/11/09 ed. 2012;119(1):180–7.

124. Kastan MB, Lim DS. The many substrates and functions of ATM. Nat Rev Mol Cell Biol. 2000;1(3):179–86.

125. Fan Y, Dutta J, Gupta N, Fan G, Gélinas C. Regulation of programmed cell death by NF-kappaB and its role in tumorigenesis and therapy. Adv Exp Med Biol. 2008;615:223–50.

126. Malstrom S, Tili E, Kappes D, Ceci JD, Tsichlis PN. Tumor induction by an Lck-MyrAkt transgene is delayed by mechanisms controlling the size of the thymus. Proc Natl Acad Sci U S A. The National Academy of Sciences; 2001;98(26):14967–72.

127. Barlow C, Hirotsune S, Paylor R, Liyanage M, Eckhaus M, Collins F, et al. Atm-deficient mice: a paradigm of ataxia telangiectasia. Cell. 1996 Jul 12;86(1):159–71.

128. Herling M, Patel KA, Weit N, Lilienthal N, Hallek M, Keating MJ, et al. High TCL1 levels are a marker of B-cell receptor pathway responsiveness and adverse outcome in chronic lymphocytic leukemia. Blood. American Society of Hematology; 2009;114(21):4675–86.

129. Despouy G, Joiner M, Le Toriellec E, Weil R, Stern MH. The TCL1 oncoprotein inhibits activation-induced cell death by impairing PKC theta and ERK pathways. Blood. 2007;110(13):4406–16.

130. Soulier J, Madani A, Cacheux V, Rosenzwajg M, Sigaux F, Stern MH. The MTCP-1/c6.1B gene encodes for a cytoplasmic 8 kD protein overexpressed in T cell leukemia bearing a t(X;14) translocation. Oncogene. 1994;9(12):3565–70.

131. Madani A, Choukroun V, Soulier J, Cacheux V, Claisse JF, Valensi F, et al. Expression of p13MTCP1 is restricted to mature T-cell proliferations with t(X;14) translocations. Blood. 1996;87(5):1923–7.

132. Auguin D, Barthe P, Royer C, Stern MH, Noguchi M, Arold ST, et al. Structural basis for the co-activation of protein kinase B by T-cell leukemia-1 (TCL1) family proto-oncoproteins. J Biol Chem. 2004;279(34):35890–902.

133. Teague TK, Hildeman D, Kedl RM, Mitchell T, Rees W, Schaefer BC, et al. Activation changes the spectrum but not the diversity of genes expressed by T cells. Proc Natl Acad Sci U S A. 1999;96(22):12691–6.

134. Stitz J, Buchholz CJ, Engelstädter M, Uckert W, Bloemer U, Schmitt I, et al. Lentiviral vectors pseudotyped with envelope glycoproteins derived from gibbon ape leukemia virus and murine leukemia virus 10A1. Virology. 2000;273(1):16–20.

135. Schambach A, Wodrich H, Hildinger M, Bohne J, Kräusslich HG, Baum C. Context dependence of different modules for posttranscriptional enhancement of gene expression from retroviral vectors. Mol Ther. 2000;2(5):435–45.

136. Pear WS, Nolan GP, Scott ML, Baltimore D. Production of high-titer helper-free retroviruses by transient transfection. Proc Natl Acad Sci U S A. 1993;90(18):8392–6.

137. Hartley JW, Rowe WP. Clonal cells lines from a feral mouse embryo which lack host-range restrictions for murine leukemia viruses. Virology. 1975;65(1):128–34.

138. Gillis S, Smith KA. Long term culture of tumour-specific cytotoxic T cells. Nature. 1977;268(5616):154–6.

139. Thomas PD. PANTHER: A Library of Protein Families and Subfamilies Indexed by Function. Genome Res. 2003 Sep 1;13(9):2129–41.

140. Morse 3rd HC, Anver MR, Fredrickson TN, Haines DC, Harris AW, Harris NL, et al. Bethesda proposals for classification of lymphoid neoplasms in mice. Blood. 2002;100(1):246–58.

141. Noguchi M, Ropars V, Roumestand C, Suizu F. Proto-oncogene TCL1: more than just a coactivator for Akt. Faseb J. 2007/03/16 ed. 2007;21(10):2273–84.

142. Sanchez-Beato M. Cell cycle deregulation in B-cell lymphomas. Blood. 2003 Feb 15;101(4):1220–35.

143. Tane S, Chibazakura T. Cyclin A overexpression induces chromosomal double-strand breaks in mammalian cells. Cell cycle. 2009;8(23):3900–3.

144. Sarafan-Vasseur N, Lamy A, Bourguignon J, Le Pessot F, Hieter P, Sesboüé R, et al. Overexpression of B-type cyclins alters chromosomal segregation. Oncogene. 2002;21(13):2051–7.

145. Baker DJ, Jeganathan KB, Cameron JD, Thompson M, Juneja S, Kopecka A, et al. BubR1 insufficiency causes early onset of aging-associated phenotypes and infertility in mice. Nat Genet. 2004;36(7):744–9.

146. Dai W, Wang Q, Liu T, Swamy M, Fang Y, Xie S, et al. Slippage of mitotic arrest and enhanced tumor development in mice with BubR1 haploinsufficiency. Cancer Res. 2004;64(2):440–5.

147. Xu X, Page JL, Surtees JA, Liu H, Lagedrost S, Lu Y, et al. Broad overexpression of ribonucleotide reductase genes in mice specifically induces lung neoplasms. Cancer Res. 2008;68(8):2652–60.

148. Martelli AM, Tabellini G, Bressanin D, Ognibene A, Goto K, Cocco L, et al. The emerging multiple roles of nuclear Akt. Biochim Biophys Acta. 2012 Dec;1823(12):2168–78.

149. Ge Q, Holler PD, Mahajan VS, Nuygen T, Eisen HN, Chen J. Development of CD4+ T cells expressing a nominally MHC class I-restricted T cell receptor by two different mechanisms. Proc Natl Acad Sci U S A. 2006 Feb 7;103(6):1822–7.

150. Lui JB, Devarajan P, Teplicki SA, Chen Z. Cross-Differentiation from the CD8 Lineage to CD4 T Cells in the Gut-Associated Microenvironment with a Nonessential Role of Microbiota. Cell Rep. 2015 Feb;10(4):574–85.

151. Warner K, Crispatzu G, Al-Ghaili N, Weit N, Florou V, You MJ, et al. Models for mature T-cell lymphomas-A critical appraisal of experimental systems and their contribution to current T-cell tumorigenic concepts. Crit Rev Oncol Hematol. 2013;88(3):680–95.

152. Young RM, Staudt LM. Targeting pathological B cell receptor signalling in lymphoid malignancies. Nat Rev Drug Discov. 2013 Mar 1;12(3):229–43.

153. Shah A, Mangaonkar A. Idelalisib: A Novel PI3Kδ Inhibitor for Chronic Lymphocytic Leukemia. Ann Pharmacother. 2015 Oct;49(10):1162–70.

154. Forconi F. Three years of ibrutinib in CLL. Blood. 2015 Apr 16;125(16):2455–6.

155. Witzig TE, Reeder C, Han JJ, LaPlant B, Stenson M, Tun HW, et al. The mTORC1 inhibitor everolimus has antitumor activity in vitro and produces tumor responses in patients with relapsed T-cell lymphoma. Blood. 2015 Jul 16;126(3):328–35.

156. Dondorf S, Schrader A, Herling M. Interleukin-2-inducible T-cell Kinase (ITK) Targeting by BMS-509744 Does Not Affect Cell Viability in T-cell Prolymphocytic Leukemia (T-PLL): FIGURE 1. J Biol Chem. 2015 Apr 17;290(16):10568–9.

5.   Appendices

5.1   Abbreviations

AICD   Activation-induced cell death
AITL   Angioimmunoblastic T-cell lymphoma
APC   Antigen presenting cell
ALCL   Anaplastic large cell lymphoma
ATM   Ataxia telangiectasia mutated
BM   Bone marrow
BSA   Bovine serum albumin
CAR   Chimeric antigen receptor
CCL   Chemokine with C-C motive
CD   Cluster of differentiation
CDR   Complementarity determining region
CLL   Chronic lymphocytic leukemia
CLP   Common lymphoid progenitor
CTL   Cytotoxic T-lymphocyte
DMEM   Dulbecco's modified eagle medium
DMSO   Dimethyl sulfoxide
DN   Double negative
DNA   Deoxyribonucleic acid
DP   Double positive
E.coli   Escherichia coli
EDTA   Ethylenediaminetetraacetic acid
EGFP   Enhanced green fluorescent protein
ER   Endoplasmic reticulum
FACS   Fluorescence activated cell sorting
FBS   Fetal bovine serum
FC   Flow cytometry
FELASA   Federation of European Laboratory Animal Science Associations
GPCR   G protein–coupled receptor
HBSS   Hanks balanced salt solution
HE   Hematoxylin/eosin
HEPES   Hydroxyethylpiperazineethanesulfonic acid
HPC   Hematopoietic progenitor cell
HSC   Hematopoietic stem cell
ICFC   Intracellular Flow Cytometry
IFA   Incomplete Freund's adjuvant
i.p.   Intraperitoneal
i.v.   Intravenous
IFN-γ Interferon γ

Ig	Immunoglobulin
IL	Interleukin
ITAM	Immunoreceptor tyrosine-based activation motifs
IVC	Individually ventilated cages
LN	Lymph node
LTR	Long terminal repeats
M	Molar
MACS	Magnetic activated cell sorting
MSA	Mouse Serum Albumin
MTCP1	Mature T-cell proliferation 1
MTCL	Mature T-cell leukemias/lymphomas
MHC	Major histocompatibility complex
MYC	Myelocytomatosis oncogene
NK	Natural killer
OVA	Ovalbumin
PTCL	Peripheral T-cell leukemias/lymphomas
RAG	Recombination activating gene
ROI	Region of interest
rpm	Rounds per minute
RPMI	Roswell Park Memorial Institute
RSD	Relative standard deviation
SP	Single positive
spMHC	Self-peptide/Major histocompatibility complex
STAT	Signal transducer and activator of transcription
SV40	Simian virus 40
Th	T-helper cells
TCL1A	T-cell leukemia/lymphoma 1
TCR	T-cell receptor
TGF-β1	Transforming growth factor–β1
TML1	TCL1A/MTCP1-like 1
T-PLL	T-cell prolymphocytic leukemia
v/v	Volume/Volume
WB	Western Blot
WBC	White blood count
WHO	World Health Organization

5.2 Plasmid Maps

Eco-env

Bpu1102I
Pvul
Fspl
Fsel
Nael
NgoMIV
Xhol
EcoRI
NdeI
Bst1107I
SfiI
AccIII
BamHI
SgrAI
Spel
PvuII ++
BsaBI
Pmll
Aarl
Swal
BsiWI
Sall
Rsrll
BssHII
Eco47III

Eco-env
env (Mo-MLV)

MLV gag-pol

Psil
HindIII
PmlI
Bst1107I
NdeI
SacII
HindIII
BbvCI
SV40 pA
VspI
FspI
ScaI
Bpu1102I
EcoRV
SspI
AatII
NheI
Sall
SapI
SV40 promotor
NotI
AccIII
BsgI
BsrGI
SanDI
BclI
SacI
Ecl136II
PshAI
Xcml
Van91I
NruI

MLV gag-pol
MLV gag/pol

MP91-EGFP

SspI
Ndel
NaeI
NgoMIV
BglII
BsaBI
SfiI
AMP
PstI
NotI
PshAI
AgeI
ClaI
EcoRI
MPSV LTR
MESV leader91
IRES
BlnI
SapI
PmlI
AarI
BspMI
DraIII
BtrI
XhoI
LTR
eGFP
Nhel
SphI
RsrII
StuI
EcoNI
BamHI
BsiWI
BsrGI
AccIII
Eco47III
Bst1107I
Swal

MP91-EGFP

MP91-TCL1A-EGFP

✱
SspI
NdeI
NaeI
NgoMIV
BglII
SacII
SfiI
AMP
PstI
NotI
MPSV LTR
MESV leader91
TCL1
IRES
EcoRI
SapI
BlnI
LTR
GFP
PmlI ++
BspMI
DraIII
BtrI
BstXI
wPRE
NheI
SphI
EcoNI
BamHI
BsiWI
BsrGI ++
Eco47III
SalI
Bst1107I
Swal

MP91-TCL1A-EGFP

✱Representative plasmid card for MTCP1, TML1, myr-TCL1A, and nls-TCL1A.
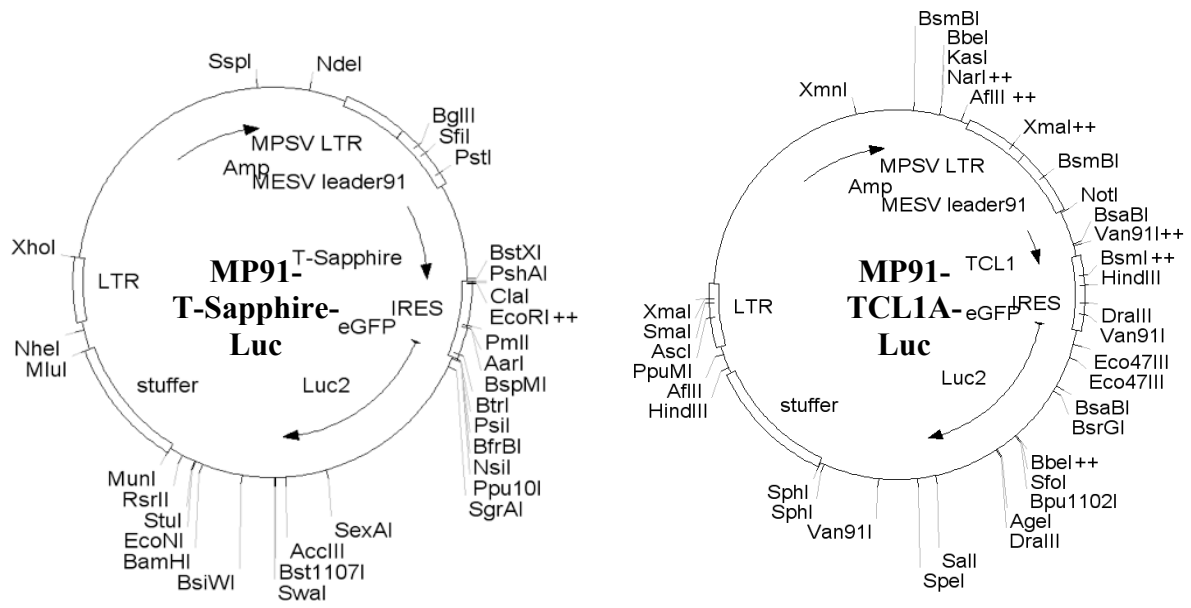
Figure 5-1: Plasmid maps.

5.3   Lists of differently expressed genes

		TCL1A	myr-TCL1A	nls-TCL1A
Chemokine Signaling Pathway	↑	Cxcl2, Gng12	Cxcl2, Gng12	Cxcl2, Gng12
	↓	Ccr7, Akt3	Ccr7, Akt3	Ccr7, Akt3
Cell Cycle	↑	Bub1b, Bub1, Ccna2, Chek1, Ccnb1, Ccnb2, Tfdp1, Cdkn1a, Cdc20, Mpeg1, Plk1, Cdc25c	Bub1b, Bub1, Wee1, Ccna2, Chek1, Ccnb1, Ccnb2, Tfdp1, Cdkn1a, Cdc20, Mpeg1, Plk1, Cdc25c	Bub1b, Wee1, Ccna2, Ccnb1, Ccnb2, Tfdp1, Cdc20, Plk1
p53 Signaling	↑	Chek1, Cdkn1a, Ccnb1, Ccnb2, Cdk1, Rrm2	Chek1, Cdkn1a, Ccnb1, Ccnb2, Cdk1, Rrm2	Ccnb1, Ccnb2, Cdk1, Rrm2
	↓	-	Ddb2	Ddb2
PI3K-AKT-mTOR Signaling Pathway	↑	Gng12, Cdkn1a	Gng12, Cdkn1a	Gng12
	↓	Itgam, Il4ra, Akt3	Itgam, Akt3	Il4ra, Akt3
miRNA regulation of DDR	↑	Cdkn1a, Ccnb1, Chek1, Cdk1, Cdc25c, H2afx, Ccnb2	Cdkn1a, Ccnb1, Chek1, Cdk1, Cdc25c, H2afx, Ccnb2	Ccnb1, Cdk1, H2afx, Ccnb2
	↓	-	Ddb2	Ddb2
MAPK Signaling Pathway	↑	Stmn1, Hspa5,	Stmn1, Hspa5	-
	↓	Tgfbr2, Ppp3cc, Akt3	Ppp3cc, Akt3	Tgfbr2, Ppp3cc, Akt3
Purine metabolism	↑	Rrm2	Rrm2, Prps2, Pde8a	Rrm2, Pde8a
	↓	Pde4d, Polr3e	Pde4d, Polr3e	Polr3e
Non-odorant GPCRs	↑	Ccrl2, Lphn2	Ccrl2	Lphn2
	↓	Ccr7, Gpr174	Ccr7, Gpr174, S1pr1	Ccr7, Gpr174, S1pr1
TGF-beta Receptor Signaling	↑	Cd44, Atf3, Tfdp1, Cdkn1a, Ccnb2	Cd44, Atf3, Tfdp1, Cdkn1a, Ccnb2	Atf3, Tfdp1, Ccnb2
	↓	Tgfbr2, Crebbp	-	Tgfbr2, Crebbp
Ca2+ Regulation	↑	Prkar2b, Gng12	Prkar2b, Gng12	Prkar2b, Gng12
	↓	-	Itpr2	Itpr2

Table 5-1: List of pathway genes up-regulated (↑) or down-regulated (↓) in at least two of three cohorts: TCL1A, myr-TCL1A and nls-TCL1A

		TCL1A	myr-TCL1A	nls-TCL1A
Cell Cycle	↑	Bub1b, Ccna2, Gadd45a, Ccnb1, Ccnb2, Mpeg1	Bub1b, Wee1, Ccna2, Gadd45a, Ccnb1, Ccnb2	Ccna2, Gadd45a, Ccnb1, Mpeg1
MAPK Signaling Pathway	↑	Gadd45a, Gna12, Mapkapk2, Il1a	Gadd45a, Gna12, Mapkapk2	Gadd45a, Gna12, Mapkapk2, Il1a
	↓	-	Ppm1b	Ppm1b
PI3K-AKT-mTOR Signaling Pathway	↑	Creb3l2	Creb3l2	Creb3l2
	↓	Itgam, Ppp2r5c	Itgam	Itgam, Ppp2r5c
Adipogenesis genes	↑	Pparg, Gadd45a, Ahr	Gadd45a, Ahr	Pparg, Gadd45a, Ahr
Regulation of Actin Cytoskeleton	↑	Gna12	Gna12, Ssh2	Gna12, Ssh2
Purine metabolism	↑	Rrm2, Entpd1	Rrm1, Rrm2	Entpd1
	↓	Pde4d, Nme2	-	Pde4d, Nme2
p53 Signaling	↑	Ccnb1, Ccnb2, Gadd45a, Rrm2	Ccnb1, Ccnb2, Gadd45a, Rrm2	Ccnb1, Gadd45a
mRNA processing	↓	Park7	-	Park7
miRNA regulation of DDR	↑	Gadd45a, Ccnb1, H2afx, Ccnb2	Gadd45a, Ccnb1, H2afx, Ccnb2	Gadd45a, Ccnb1

Table 5-2: List of pathway genes up-regulated (↑) or down-regulated (↓) in at least two of three cohorts: TCL1A, myr-TCL1A and nls-TCL1A B cells

		TCL1A	myr-TCL1A	nls-TCL1A
Chemokine Signaling Pathway	↑	Ccr8	Ccr8, Akt1	Ccr8, Akt1
MAPK Signaling Pathway	↑	-	Gna12, Akt1, Stk3, Mapkapk2	Gna12, Akt1, Stk3, Mapkapk2
Kit Receptor Signaling Pathway	↑	Grb7	Grb7, Akt1, Spred1	Grb7, Akt1, Spred1
Androgen Receptor Signaling Pathway	↑	-	Akt1	Akt1
PI3K-AKT-mTOR Signaling Pathway	↑	-	Itgax, Akt1, Ppp2r1a	Itgax, Akt1, Ppp2r1a
G1 to S cell cycle control	↑	-	Tfdp1, Mcm2, Pola2	Tfdp1, Mcm2, Pola2

Table 5-3: List of pathway genes up-regulated (↑) or down-regulated (↓) in at least two of three cohorts: TCL1A, myr-TCL1A and nls-TCL1A T cells

5.4 Lists of retroviral integration sites

Tumor	Chr	Location	Type	Gene Symbol	Distance	Start	End	OR	Hit
TCL1A	8	13214233	s	Mcf2l	340427	12873806	13020905	F	No
A1			s	Gm15349	-242492	12971826	12972029	R	No
w/o			s	Gm15352	192292	13021941	13022210	F	No
stim			s	F7	188199	13026034	13035809	F	No
			s	F10	176925	13037308	13056676	F	No
			s	Proz	153325	13060908	13075006	F	No
			s	Gm17023	138156	13076077	13082740	F	No
			s	Pcid2	-109062	13077189	13105459	R	No
			s	Gm17022	127716	13086517	13087428	F	No
			s	Cul4a	108612	13105621	13147940	F	No
			s	Lamp1	55098	13159135	13175338	F	No
			c	Grtp1	-13901	13175162	13200620	R	Yes
			s	Mir1968	-25423	13189031	13189098	R	No
			s	Adprhl1	39641	13235655	13254162	R	No
			s	Dcun1d2	73605	13255963	13288126	R	No
			s	U6	68693	13283115	13283214	R	No
			s	Tmco3	-73780	13288013	13322924	F	No
			s	Tfdp1	-124518	13338751	13378395	F	No
			s	Atp4b	182257	13386209	13396778	R	No
			s	Grk1	-190848	13405081	13421945	F	No
			s	Fam70b	-221193	13435426	13461452	F	No
	15	76736308	s	Cyhr1	-245929	76473825	76490547	R	No
			s	Kifc2	245312	76490996	76498625	F	No
			s	Foxh1	-236098	76498714	76500378	R	No
			s	Ppp1r16a	234263	76502045	76525349	F	No
			s	Gpt	209145	76527163	76530104	F	No
			s	Mfsd3	204336	76531972	76534669	F	No
			s	Recql4	-195513	76533984	76540963	R	No
			s	Lrrc14	195255	76541053	76548129	F	No
			s	Lrrc24	-183873	76545706	76552603	R	No
			s	C030006K11Rik	-182201	76551896	76554275	R	No
			s	Arhgap39	-87876	76554415	76648600	R	No
			s	Gm17271	108548	76627760	76628459	F	No
			s	Zfp251	-34611	76682578	76701865	R	No
			s	Zfp7	26619	76709689	76722822	F	No
			s	Commd5	5968	76730340	76731735	F	No
			c	Rpl8	1807	76734501	76736748	F	Yes
			s	Zfp647	11964	76741281	76748440	R	No
			s	1110038F14Rik	-42661	76778969	76781159	F	No
			s	Mb	144624	76845919	76881100	R	No
			s	Apol6	-138851	76875159	76887537	F	No
			s	U6	-161913	76898221	76898327	F	No
			s	Rbfox2	401007	76909420	77137483	R	No
			s	1700109K24Rik	-178565	76914873	76926744	F	No
TCL1A	1	132948239	s	Fcamr	250760	132697479	132711317	F	No
A2			s	Gm15848	-227883	132706554	132720661	R	No
w/o			s	Pigr	224978	132723261	132748826	F	No
stim			s	Faim3	185993	132762246	132777367	F	No
			s	Il24	-164513	132778651	132784031	R	No
			s	Il20	-140671	132803769	132807873	R	No
			s	Il19	-111894	132829235	132836650	R	No
			s	Il10	31817	132916422	132921551	F	No
			s	Mapkapk2	45600	132950281	132994144	R	No
			c	U6	21784	132970235	132970328	R	Yes
			s	7SK	50778	132998970	132999322	R	No
			s	Dyrk3	86267	133025018	133034811	R	No
			s	Eif2d	-101519	133049758	133084235	F	No
			s	Rassf5	193291	133072987	133141835	R	No
			s	Ikbke	227639	133150920	133176183	R	No
			s	Srgap2	475394	133181828	133423938	R	No
	14	21036013	s	Gng2	-239276	20691781	20796849	R	No
			s	1810063B07Rik	-133731	20894868	20902394	R	No
			s	Kcnk5	-35121	20959280	21001004	R	No
			c	SNORA70	-16791	21019218	21019334	R	Yes
			s	Kcnk16	52259	21081978	21088384	R	No
			s	Nudt13	-77899	21113912	21136797	F	No
			s	Ecd	131218	21139081	21167343	R	No
			s	Fam149b	-131371	21167384	21202711	F	No
			s	Dnajc9	172007	21203860	21208132	R	No
			s	Mrps16	176652	21210453	21212777	R	No
			s	Ttc18	235323	21213412	21271448	R	No
			s	7330404K18Rik	-181568	21217581	21218152	F	No
			s	Anxa7	263230	21274483	21299355	R	No

TCL1A A3 w/o stim	5	108108767	s	Ephx4	276978	107831755	107859054	F	No
			s	Gm17202	-247838	107833842	107860929	R	No
			s	Lpcat2b	248165	107860568	107864058	F	No
			s	Btbd8	241717	107867016	107920647	F	No
			s	Gm9727	-200668	107907545	107908099	R	No
			s	A830010M20Rik	183816	107924917	108009615	F	No
			s	1700028K03Rik	170770	107937963	107980568	F	No
			s	Glmn	-81860	107977986	108026907	R	No
			s	Rpap2	82341	108026392	108090857	F	No
			s	A930041C12Rik	-45898	108059269	108062869	R	No
			c	Gm17717	8267	108088116	108117034	R	Yes
			s	Gfi1	46289	108145674	108155056	R	No
			s	A430072P03Rik	-45444	108154177	108157821	F	No
			s	Evi5	195359	108173814	108304126	R	No
			s	1700013N18Rik	-150539	108259272	108260361	F	No
			s	Gm16007	-164676	108273409	108273694	F	No
			s	Rpl5	-220788	108329521	108338024	F	No
			s	Snord21	-224841	108333574	108333667	F	No
			s	SNORA66	-225463	108334196	108334327	F	No
			s	SNORA66	-227631	108336364	108336495	F	No
			s	Fam69a	307337	108337072	108416104	R	No
TCL1A A4 w/o stim	3	88255603	s	AW047730	251058	88004545	88007403	F	No
			s	Gm3764	237196	88018407	88025782	F	No
			s	Mir3093	236510	88019093	88019179	F	No
			s	AC044864.1	-236407	88019511	88019618	R	No
			s	Rhbg	-164893	88046796	88091132	R	No
			s	Gm17285	174581	88081022	88081376	F	No
			s	1700021C14Rik	-155104	88084043	88100921	R	No
			s	Cct3	154565	88101038	88125689	F	No
			s	0610031J06Rik	126658	88128945	88135235	F	No
			s	Tmem79	-117599	88132577	88138426	R	No
			s	Smg5	115421	88140182	88166259	F	No
			s	Paqr6	87097	88168506	88172463	F	No
			s	Bglap-rs1	-79360	88172538	88176665	R	No
			s	Bglap2	-73404	88181658	88182621	R	No
			s	Gm6821	70677	88184926	88186733	F	No
			s	Bglap	-67639	88187423	88188386	R	No
			s	Pmf1	-41787	88198061	88214238	R	No
			s	Slc25a44	-26964	88214420	88229061	R	No
			c	Sema4a	9079	88239881	88265104	R	Yes
			s	Lmna	57853	88285070	88313878	R	No
			s	Mex3a	-80714	88336317	88345318	F	No
			s	Mir1905	84279	88340223	88340304	R	No
			s	Rab25	96197	88345951	88352222	R	No
			s	Lamtor2	100971	88353741	88356996	R	No
			s	Ubqln4	-102035	88357638	88373647	F	No
			s	Gm10704	125038	88380329	88381063	R	No
			s	Ssr2	-127990	88383593	88392319	F	No
			s	Arhgef2	-155773	88411376	88451974	F	No
			s	RP23-398K14.3.1	168958	88420379	88424983	R	No
			s	Rxfp4	201039	88455820	88457064	R	No
			s	2810403A07Rik	-234113	88489716	88516855	F	No
			s	SCARNA15	-242250	88497853	88497979	F	No
TCL1A A5 w/o stim	14	66809027	s	Scara3	-236671	66538232	66572581	R	No
			s	Clu	221707	66587320	66600385	F	No
			s	Gulo	-181205	66605624	66628047	R	No
			s	Adam2	-112682	66646166	66696570	R	No
			s	Gm10233	145110	66663917	66664546	F	No
			s	Ephx2	-65915	66703214	66743337	R	No
			c	Chrna2	49230	66759797	66771785	F	No
			s	Ptk2b	90637	66772094	66899889	R	Yes
			s	1700001G11Rik	106714	66914171	66915966	R	No
			s	Trim35	-106841	66915868	66930261	F	No
			s	Stmn4	-154106	66963133	66980517	F	No
	11	78942302	s	Nos2	208013	78734289	78773756	F	No
			s	Lgals9	-144319	78776476	78798448	R	No
			c	Ksr1	17142	78826942	78959909	R	Yes
			s	Gm11201	105203	78837099	78844559	F	No
			s	Gm11200	-83996	79026298	79026745	F	No
			s	Wsb1	125406	79052874	79068173	R	No
			s	Gm9964	167641	79109681	79110408	R	No
			s	Nf1	-210893	79153195	79395114	F	No
			s	Gm11198	242965	79184759	79185732	R	No

Tumor	Chr	Location	Type	Gene	Distance	Start	End	OR	Hit
TCL1A	16	10778487	s	Dexi	-235823	10530300	10543147	R	No
A6			s	Clec16a	233030	10545457	10744971	F	No
w/o			s	Gm15558	-95338	10669341	10683632	R	No
stim			c	Socs1	6659	10783901	10785629	R	No
			s	Tnp2	9778	10788029	10788748	R	No
			s	Prm3	12036	10790600	10791006	R	No
			s	Prm2	13228	10791476	10792198	R	No
			s	Prm1	18009	10796419	10796979	R	No
			s	Gm10343	-22975	10801462	10801809	F	No
			s	Gm11172	-34521	10813008	10813087	F	No
			s	Gm17410	-49533	10828020	10833600	F	No
			s	A630055G03Rik	-56665	10835152	10886327	F	No
			s	Litaf	287280	10959368	11066250	R	No
			s	AC164093.1	-187330	10965817	10965942	F	No
			s	U1	-215992	10994479	10994662	F	No
			s	Gm4262	-230504	11008991	11015279	F	No
	18	35018200	s	Brd8	-234020	34758269	34784255	R	No
			s	Kif20a	233922	34784278	34792919	F	No
			s	Cdc23	-206886	34790605	34811389	R	No
			s	n-R5s25	211146	34807054	34807172	F	No
			s	Gfra3	-138234	34849557	34880041	R	No
			s	Cdc25c	-107088	34892651	34911187	R	No
			s	Gm3550	121179	34897021	34897665	F	No
			s	2010110K18Rik	106737	34911463	34918339	F	No
			s	Fam53c	99640	34918560	34933414	F	No
			s	Kdm3b	81538	34936662	34999024	F	No
			s	Gm17557	-55137	34956549	34963138	R	No
			s	Reep2	17888	35000312	35007106	F	No
			c	Egr1	-1277	35019477	35024638	F	No
			s	Gm17507	6488	35024439	35024763	R	No
			s	Etf1	73382	35062446	35091657	R	No
			s	Hspa9	95736	35097068	35114011	R	No
			s	SNORD63	82679	35100888	35100954	R	No
			s	SNORD63	84092	35102298	35102367	R	No
			s	Gm6724	112148	35129314	35130423	R	No

Table 5-4: List of retroviral integration sites of T-cell tumors induced by TCL1A in unstimulated mice

Tumor: Tumor sample. Chr: Mapped chromosome. Location: Genome location. Type: Closest (c) and surrounding (s) genes. Distance: Distance between integration and gene start. Start: Gene start. End: Gene end. OR: Relative orientation of integrated vector (F: forward, R: reverse). Hit: Hit in gene.

Tumor	Chr	Location	Type	Gene Symbol	Distance	Start	End	OR	Hit
TCL1A	13	117855843	c	Parp8	-41948	117643631	117814323	R	Yes
A1			s	Gm17509	153611	118007508	118009882	R	No
OVA			s	Emb	-153589	118009432	118062905	F	No
stim									
	11	103198572	s	Plcd3	-236177	102931618	102962972	R	No
			s	Acbd4	235576	102962996	102973514	F	No
			s	Hexim1	220933	102977639	102981039	F	No
			s	Hexim2	204829	102993743	103001190	F	No
			s	Fmnl1	166151	103032421	103060215	F	No
			s	Gm20511	-144939	103052024	103054210	R	No
			s	1700023F06Rik	-129277	103060260	103069872	R	No
			s	4933400C05Rik	-119403	103069441	103079746	R	No
			s	Map3k14	-70363	103081076	103128786	R	No
			s	1700028N14Rik	-70090	103126174	103129059	R	No
			s	Arhgap27	25857	103192811	103225006	R	No
			c	Gm11648	-7495	103206067	103211438	F	Yes
			s	Gm11647	-18443	103217015	103222406	F	No
			s	Gm11641	-25955	103224527	103225965	F	No
			s	Plekhm1	74829	103226402	103273978	R	No
			s	Lrrc37a	166762	103313269	103365911	R	No
			s	Gm884	283305	103395891	103482454	R	No
TCL1A	5	108176732	s	A830010M20Rik	251815	107924917	108009615	F	No
A2			s	1700028K03Rik	238769	107937963	107980568	F	No
OVA			s	Glmn	-149886	107977986	108026907	R	No
stim			s	Rpap2	150340	108026392	108090857	F	No
			s	A930041C12Rik	-113924	108059269	108062869	R	No
			s	Gm17717	-59759	108088116	108117034	R	No
			c	Gfi1	-21737	108145674	108155056	R	No
			s	A430072P03Rik	22555	108154177	108157821	F	No
			s	Evi5	127333	108173814	108304126	R	Yes
			s	1700013N18Rik	-82540	108259272	108260361	F	No
			s	Gm16007	-96677	108273409	108273694	F	No
			s	Rpl5	-152789	108329521	108338024	F	No
			s	Snord21	-156842	108333574	108333667	F	No
			s	SNORA66	-157464	108334196	108334327	F	No
			s	SNORA66	-159632	108336364	108336495	F	No
	7	140004122	s	Fgfr2	310854	137305965	140315033	R	No
			s	Oat	-236098	139749158	139768081	R	No
			s	Nkx1-2	-212859	139786560	139791320	R	No
			s	Gm16764	215052	139789070	139791320	F	Yes
			s	Lhpp	201801	139802321	139898103	F	No
			s	Gm15582	-152612	139849061	139851567	R	No
			c	Fam53b	1390	139903765	140005569	R	No
			s	Mettl10	40177	140019140	140044356	R	No
			s	Fam175b	-46786	140050908	140076794	F	No
			s	1500002F19Rik	118879	140081172	140123058	R	No
			s	Zranb1	-118703	140122825	140178074	F	No
			s	Gm15718	171056	140171265	140175235	R	No
			s	Ctbp2	311858	140179246	140316037	R	No
TCL1A	5	3930091	s	4930511M11Rik	244755	116938104	116940269	F	No
A3			s	Ankib1	244302	116938557	116938749	F	No
OVA			s	AC022236.1	235709	116947150	116947226	F	No
stim			s	Krit1	-224592	116956262	116958381	R	No
			s	4932412H11Rik	206377	116976482	117020582	F	No
			s	Mterf	189055	116993804	116994131	F	No
			c	Akap9	186947	116995912	116996359	F	No
			s	Cyp51	121884	117060975	117223639	F	Yes
TCL1A	7	19888968	s	Sympk	279242	19609726	19639967	F	No
A4			s	Rsph6a	248929	19640039	19659796	F	No
OVA			s	Dmwd	227370	19661598	19668125	F	No
stim			s	Dmpk	219770	19669198	19679170	F	No
			s	Mir3100	216791	19672177	19672241	F	No
			s	Six5	209025	19679943	19683898	F	No
			s	Gm4969	-185292	19686900	19703717	R	No
			s	Fbxo46	183760	19705208	19723610	F	No
			s	Qpctl	-154464	19725566	19734545	R	No
			s	Snrpd2	153897	19735071	19738084	F	No
			s	Gipr	-137533	19742474	19751476	R	No
			s	Eml2	127198	19761770	19791831	F	No
			s	Mir330	122154	19766814	19766911	F	No
			s	Gpr4	91081	19797887	19809525	F	No
			s	Opa3	75285	19813683	19841892	F	No
			s	U1	61489	19827479	19827638	F	No

Tumor	Chr	Location	Type	Gene	Distance	Start	End	OR	Hit
			s	Vasp	-31843	19842278	19857166	R	No
			s	1700058P15Rik	45127	19843841	19845088	F	No
			s	Ppm1n	-23611	19862156	19865398	R	No
			s	Rtn2	20957	19868011	19881513	F	No
			c	Gm17589	-2890	19883609	19886119	R	Yes
			s	Fosb	6385	19888070	19895394	R	No
			s	Ercc1	-41159	19930127	19941873	F	No
			s	Cd3eap	55823	19942198	19944832	R	No
			s	Ppp1r13l	-56130	19945098	19963882	F	No
			s	Ercc2	-78391	19967359	19981043	F	No
			s	Gm17574	89058	19967569	19978067	R	No
			s	Mir343	-83024	19971992	19972066	F	No
			s	Klc3	100444	19979786	19989453	R	No
			s	Ckm	-107475	19996443	20006932	F	No
			s	Gm17405	-108005	19996973	19997621	F	No
			s	A930016O22Rik	117757	20004161	20006766	R	No
			s	Mark4	154834	20010816	20043843	R	No
			s	U1	157275	20046146	20046284	R	No
			s	Exoc3l2	-185437	20074405	20082109	F	No
			s	Bloc1s3	204671	20091163	20093680	R	No
			s	Trappc6a	-205051	20094019	20101494	F	No
			s	Nkpd1	-215112	20104080	20110399	F	No
			s	Ppp1r37	258738	20116316	20147747	R	No
TCL1A A5 OVA stim	9	124060503	s	Gm4694	223643	123836860	123839608	F	No
			s	CAAA01010581	-198494	123862202	123862302	R	No
			s	Ccr1	-177271	123876959	123883525	R	No
			s	Ccr1l1	-167555	123891782	123893241	R	No
			s	Ccr3	123800	123936703	123946421	F	No
			s	Ccr2	43814	124016689	124028296	F	No
			c	Ccr5	24221	124036282	124062438	F	Yes
	6	22307449	s	A430107O13Rik	371533	21935916	22206404	F	No
			s	Wnt16	69222	22238227	22248522	F	No
			c	Fam3c	-1483	22256520	22306243	R	No
TCL1A A6 OVA stim	11	117182859	s	2810008D09Rik	244755	116938104	116940269	F	No
			s	SCARNA16	244302	116938557	116938749	F	No
			s	AL627205.1	235709	116947150	116947226	F	No
			s	Gm11730	-224592	116956262	116958381	R	No
			s	Sec14l1	206377	116976482	117020582	F	No
			s	7SK	189055	116993804	116994131	F	No
			s	Gm11745	186947	116995912	116996359	F	No
			s	Sept9	121884	117060975	117223639	F	Yes
			c	Gm16045	-58222	117118963	117124751	R	No
			s	Gm11729	-92844	117275703	117276682	F	No
			s	Gm8624	100058	117281951	117283031	R	No
			s	Gm11732	-104633	117287492	117300180	F	No
			s	Gm11733	-162823	117345682	117350328	F	No
			s	Gm11734	-202058	117384917	117393519	F	No
			s	AL672228.1	-232278	117415137	117415208	F	No
TCL1A A7 OVA stim	12	5105034	s	BC068281	254925	4850109	4863731	F	No
			s	Mfsd2b	-225000	4869246	4881165	R	No
			s	Ubxn2a	-191654	4885838	4914511	R	No
			s	Atad2b	180824	4924210	5050853	F	No
			c	U6	-99991	5006072	5006174	R	No
			s	Klhl29	276323	5084278	5382488	R	Yes
	13	37654776	s	Ly86	217562	37437214	37510905	F	No
			c	Rreb1	-215493	37870269	38043871	F	No

Table 5-5: List of retroviral integration sites in T-cell tumors induced by TCL1A in stimulated mice
Tumor: Tumor sample. Chr: Mapped chromosome. Location: Genome location. Type: Closest (c) and surrounding (s) genes. Distance: Distance between integration and gene start. Start: Gene start. End: Gene end. OR: Relative orientation of integrated vector (F: forward, R: reverse). Hit: Hit in gene.

Tumor	Chr	Location	Type	Gene Symbol	Distance	Start	End	OR	Hit
myr-TCL1A A1 w/o stim	7	29166955	s	9530053A07Rik	252470	28914485	28949830	F	No
			s	Fbl	212190	28954765	28964288	F	No
			s	Dyrk1b	202467	28964488	28972313	F	No
			s	Eid2	114055	29052900	29054184	F	No
			s	Eid2b	104230	29062725	29065148	F	No
			s	BC089491	-90882	29069671	29076205	R	No
			s	Dll3	-79830	29076673	29087257	R	No
			s	Timm50	-69996	29090535	29097091	R	No
			s	Supt5h	-43349	29099917	29123738	R	No
			s	Rps16	31284	29135671	29137715	F	No
			s	SNORA40	30428	29136527	29136651	F	No
			s	Plekhg2	-9406	29144623	29157681	R	No
			c	Zfp36	-2813	29161803	29164274	R	Yes
			s	Med29	10640	29171165	29177727	R	No
			s	Paf1	-11015	29177970	29184407	F	No
			s	Samd4b	41770	29184568	29208857	R	No
			s	Gmfg	-55511	29222466	29233252	F	No
			s	Lrfn1	-70302	29237257	29252567	F	No
			s	Il28a	128387	29293855	29295474	R	No
			s	Il28b	-140805	29307760	29309366	F	No
			s	Sycn	-158949	29325904	29327229	F	No
			s	Nccrp1	165186	29328615	29332273	R	No
			s	Pak4	216117	29343838	29383204	R	No
			s	C330005M16Rik	249264	29392653	29416351	R	No
myr-TCL1A A2 w/o stim	3	52372036	s	Foxo1	299777	52072259	52154031	F	No
			c	Gm10293	-44671	52416707	52417938	F	Yes
			s	U6	154408	52526571	52526677	R	No
	6	127103828	s	Dyrk4	-232204	126826038	126871857	R	No
			s	Rad51ap1	-214456	126873068	126889605	R	No
			s	D6Wsu163e	213844	126889984	126925722	F	No
			s	Fgf6	138268	126965560	126974736	F	No
			s	Fgf23	80908	127022920	127031426	F	No
			s	9630033F20Rik	-44493	127035134	127059568	R	No
			s	Gm17701	45421	127058407	127060485	F	No
			c	Ccnd2	-2995	127075797	127101066	R	Yes
			s	9330179D12Rik	4421	127099407	127162429	F	No
			s	Gm4968	-79946	127183774	127184637	F	No
			s	Gm7308	128466	127232081	127232527	R	No
myr-TCL1A A3 w/o stim	9	123904595	s	Ccr9	317038	123587557	123691089	F	No
			s	Gm17020	232974	123671621	123671894	F	No
			s	Gm17021	-204856	123681303	123700057	R	No
			s	Fyco1	-143893	123698628	123761020	R	No
			s	Cxcr6	189000	123715595	123720872	F	No
			s	Xcr1	-133667	123761436	123771246	R	No
			s	Gm4694	67735	123836860	123839608	F	No
			s	CAAA01010581	-42611	123862202	123862302	R	No
			s	Ccr1	-21388	123876959	123883525	R	No
			c	Ccr1l1	-11672	123891782	123893241	R	Yes
			s	Ccr3	-32108	123936703	123946421	F	No
			s	Ccr2	-112094	124016689	124028296	F	No
			s	Ccr5	-131687	124036282	124062438	F	No
	11	4435013	s	Gm11958	249550	4185463	4186942	F	No
			s	U6	-211076	4224152	4224258	R	No
			s	Hormad2	-94226	4245817	4341108	R	No
			s	Mtmr3	59532	4380871	4494866	R	No
			c	Gm11960	-28642	4463655	4464559	F	Yes
			s	Gm11032	-85057	4520070	4521701	F	No
			s	Gm11961	94680	4520278	4530014	R	No
			s	Ascc2	-102737	4537750	4585702	F	No
			s	Uqcr10	169011	4601976	4604345	R	No
			s	Zmat5	-169668	4604681	4637672	F	No
			s	Cabp7	211447	4636895	4646781	R	No
			s	Nf2	314205	4665848	4749539	R	No
myr-TCL1A A4 w/o stim	7	29166691	s	9530053A07Rik	252206	28914485	28949830	F	No
			s	Fbl	211926	28954765	28964288	F	No
			s	Dyrk1b	202203	28964488	28972313	F	No
			s	Eid2	113791	29052900	29054184	F	No
			s	Eid2b	103966	29062725	29065148	F	No
			s	BC089491	-91114	29069671	29076205	R	No
			s	Dll3	-80062	29076673	29087257	R	No

			s	Timm50	-70228	29090535	29097091	R	No
			s	Supt5h	-43581	29099917	29123738	R	No
			s	Rps16	31020	29135671	29137715	F	No
			s	SNORA40	30164	29136527	29136651	F	No
			s	Plekhg2	-9638	29144623	29157681	R	No
			c	Zfp36	-3045	29161803	29164274	R	Yes
			s	Med29	10408	29171165	29177727	R	No
			s	Paf1	-11279	29177970	29184407	F	No
			s	Samd4b	41538	29184568	29208857	R	No
			s	Gmfg	-55775	29222466	29233252	R	No
			s	Lrfn1	-70566	29237257	29252567	F	No
			s	Il28a	128155	29293855	29295474	R	No
			s	Il28b	-141069	29307760	29309366	F	No
			s	Sycn	-159213	29325904	29327229	F	No
			s	Nccrp1	164954	29328615	29332273	R	No
			s	Pak4	215885	29343838	29383204	R	No
			s	C330005M16Rik	249032	29392653	29416351	R	No
	14	123335721	s	Pcca	402175	122933546	123290322	F	No
			s	A2ld1	-22810	123215445	123312979	R	No
			s	4930594M22Rik	23469	123312252	123336691	F	No
			s	Tmtc4	47468	123318193	123383257	R	No
			c	Gm15735	-15620	123351341	123355565	F	Yes
myr-TCL1A A5 w/o stim	16	24296578	s	1110054M08Rik	96952	24391698	24393674	R	No
			c	Lpp	-96858	24393436	24992662	F	No
			s	U7	109781	24406441	24406503	R	No
	3	94938647	s	Psmb4	-247884	94688015	94690883	R	No
			s	U6	-214422	94724244	94724345	R	No
			s	Selenbp1	201669	94736978	94748680	F	No
			s	Rfx5	180650	94757997	94765483	F	No
			s	B230398E01Rik	-172797	94762956	94765970	R	No
			s	Pi4kb	159994	94778653	94810765	F	No
			s	A730011C13Rik	-137495	94798332	94801272	R	No
			s	Gm15265	-129976	94802722	94808791	R	No
			s	Zfp687	-119397	94810512	94819370	R	No
			s	4930481B07Rik	119100	94819547	94824060	F	No
			s	Psmd4	-92231	94836616	94846536	R	No
			s	Pip5k1a	-27915	94862452	94910852	R	No
			s	SNORD62	-44136	94894547	94894631	R	No
			s	U6	35225	94903422	94903528	F	No
			s	Vps72	23703	94914944	94926973	F	No
			s	Tmod4	10249	94928398	94933131	F	No
			s	Scnm1	-833	94933641	94937934	R	No
			c	Lysmd1	637	94938010	94943440	F	Yes
			s	Tnfaip8l2	7515	94943443	94946282	R	No
			s	Sema6c	-25732	94964379	94977946	F	No
			s	Gabpb2	83097	94985688	95021864	R	No
			s	Gm16740	-82732	95021379	95030580	F	No
			s	Mllt11	93832	95023057	95032599	R	No
			s	Cdc42se1	-94007	95032654	95040331	F	No
			s	Gm128	106753	95040842	95045520	R	No
			s	Bnipl	116348	95045193	95055115	R	No
			s	Prune	147231	95057596	95085998	R	No
			s	Fam63a	-146620	95085267	95100088	F	No
			s	Fam63a	-147120	95085767	95088779	F	No
			s	Anxa9	172331	95100018	95111098	R	No
			s	Gm10691	180272	95111594	95119039	R	No
			s	RP24-372P19.1.1	180282	95115298	95119049	R	No
			s	Lass2	-180067	95118714	95127510	F	No
			s	Setdb1	222357	95127447	95161124	R	No
myr-TCL1A A6 w/o stim	11	51686281	s	Nhp2	253044	51433237	51437216	F	No
			s	Rmnd5b	-237043	51437173	51449398	R	No
			s	N4bp3	-222097	51456565	51464344	R	No
			s	D930048N14Rik	221825	51464456	51471183	F	No
			s	0610009B22Rik	-184065	51498888	51502376	R	No
			s	Sec24a	-109305	51505765	51577136	R	No
			s	SNORA48	-135017	51551281	51551424	R	No
			s	Sar1b	109092	51577189	51605427	F	Yes
			c	Phf15	-15286	51626957	51671155	R	Yes
			s	Gm16953	396575	51763384	52083016	R	No
			s	AL669920.1	-91603	51777884	51777991	F	No
			s	Cdkn2aipnl	-94882	51781163	51790836	F	No
			s	Ube2b	127823	51798999	51814264	R	No
			s	Gm12204	-128074	51814355	51815413	F	No

Tumor	Chr	Location	Type	Gene	Distance	Start	End	OR	Hit
			s	Cdkl3	-131442	51817723	51903286	F	No
			s	Gm12205	166532	51852352	51852973	R	No
			s	Ppp2ca	-225902	51912183	51941280	F	No
			s	AL935177.1	226214	51912560	51912655	R	No
	7	143105549	s	Ptpre	376042	142729507	142877977	F	No
			c	Mki67	-198034	142881471	142908062	R	Yes
myr-TCL1A A7 w/o stim	7	113380878	s	RP23-466I14.1.1	330796	113050082	113236851	F	No
			s	Gm8979	-159541	113219246	113221378	R	No
			c	Gvin1	-22065	113300049	113358854	R	Yes
			s	Gm8989	87123	113465910	113468042	R	No
			s	Gm4759	203668	113565064	113584587	R	No
			s	SNORA17	-189348	113570226	113570361	F	No
myr-TCL1A A8 w/o stim	10	4620468	s	Rgs17	196327	4424141	4520878	F	No
			s	Mtrf1l	97837	4522631	4534654	F	No
			s	Fbxo5	79527	4540941	4547381	F	No
			c	AC162387.1	-38694	4659162	4659257	F	Yes
			s	Vip	86673	4698927	4707323	R	No
			s	Myct1	132163	4739754	4752813	R	No
			s	Syne1	-175381	4795849	5326338	F	No
myr-TCL1A A9 w/o stim	5	43607358	c	Cpeb2	-17344	43624702	43680963	F	Yes
			s	Gm7854	19052	43626241	43626591	R	No
			s	U7	-245066	43852424	43852479	F	No

Table 5-6: List of retroviral integration sites in T-cell tumors induced by myr-TCL1A in unstimulated mice

Tumor: Tumor sample. Chr: Mapped chromosome. Location: Genome location. Type: Closest (c) and surrounding (s) genes. Distance: Distance between integration and gene start. Start: Gene start. End: Gene end. OR: Relative orientation of integrated vector (F: forward, R: reverse). Hit: Hit in gene.

Tumor	Chr	Location	Type	Gene Symbol	Distance	Start	End	OR	Hit
myr-TCL1A A1 OVA stim	17	28393489	s	Anks1	347204	28046285	28199545	F	No
			s	Gm15598	-248388	28124973	28145377	R	No
			s	Tcp11	-176181	28203692	28217584	R	No
			s	4930526A20Rik	-180143	28211995	28213622	R	No
			s	Scube3	114228	28279261	28311797	F	No
			s	Zfp523	79337	28314152	28342831	F	No
			s	Def6	48766	28344723	28365553	F	No
			c	Ppard	23790	28369699	28438414	F	Yes
			s	Fance	-56986	28450475	28463513	F	No
			s	Rpl10a	-71927	28465416	28467977	F	No
			s	Tead3	93985	28468616	28487750	R	No
			s	Tulp1	108362	28488460	28502127	R	No
			s	Fkbp5	260704	28536040	28654469	R	No
			s	7SK	-190317	28583806	28584093	F	No
	5	111606075	s	Ttc28	297253	111308822	111718800	F	No
			s	Mir701	172912	111433163	111433271	F	No
			s	Gm15988	-168836	111437499	111437865	R	No
			c	Pitpnb	-153708	111759783	111817379	F	Yes
			s	Mn1	-240307	111846382	111886053	F	No
myr-TCL1A A2 OVA stim	7	71302183	s	Klf13	-218460	71031237	71083801	R	No
			s	U3	-195277	71106787	71106984	R	No
			s	RP24-292K9.1.1	99695	71202488	71207844	F	No
			c	Trpm1	3462	71298721	71414661	F	Yes
			s	AC139849.1	-42059	71344242	71368861	F	No
			s	Mir211	-48509	71350692	71350797	F	No
			s	Mtmr10	-130356	71432539	71485293	F	No
			s	Gm20457	188589	71482436	71490850	R	No
			s	Fan1	216720	71491644	71518981	R	No
			s	Mphosph10	234893	71521427	71537154	R	No
			s	Mcee	-235348	71537531	71557007	F	No
myr-TCL1A A3 OVA stim	9	45105648	s	Mpzl2	255140	44850508	44862098	F	No
			s	Mpzl3	242379	44863269	44885519	F	No
			s	Amica1	218382	44887266	44916613	F	No
			s	Gm10684	-162055	44915259	44943689	R	No
			s	Scn2b	179689	44925959	44938153	F	No
			s	Scn4b	159128	44946520	44962235	F	No
			c	Tmprss4	-93569	44980809	45012175	R	No
			s	Gm17099	124568	44981080	44983244	F	No
			s	BC049352	115558	44990090	45058103	F	No
			s	Il10ra	-28512	45061920	45077232	R	No
			s	RP24-166B2.4.1	36510	45069138	45069373	F	No
			s	1700003G13Rik	24418	45126348	45130162	R	No
			s	Tmprss13	-21535	45127183	45155664	F	No
			s	Fxyd6	-72620	45178268	45204241	F	No
			s	Fxyd2	-102309	45207957	45218361	F	No
			s	4833428L15Rik	133571	45224709	45239315	R	No
			s	Dscaml1	-129640	45235288	45561343	F	No
myr-TCL1A A4 OVA stim	7	17265909	s	Zc3h4	279679	16986230	17023043	F	No
			s	Tmem160	227781	17038128	17040838	F	No
			s	Npas1	-203988	17041070	17062129	R	No
			s	n-R5s151	208747	17057162	17057280	F	No
			s	Grlf1	-65775	17079822	17200342	R	No
			s	U6	-56091	17209924	17210026	R	No
			c	Ceacam15	-5063	17256680	17261054	R	Yes
			s	AC150681.1	29919	17295966	17296036	R	No
			s	Ceacam9	-41369	17307278	17311459	F	No
			s	Ap2s1	-57850	17323759	17334643	F	No
			s	Slc1a5	-100786	17366695	17383623	F	No
			s	Fkrp	134361	17394619	17400478	R	No
			s	Strn4	-135329	17401238	17426280	F	No
			s	Prkd2	-162374	17428283	17455810	F	No
			s	9330104G04Rik	194118	17456703	17460235	R	No
			s	Dact3	-194757	17460666	17472650	F	No
			s	Gng8	-211226	17477135	17480784	F	No
			s	Ptgir	-225930	17491839	17496254	F	No
			s	Calm3	243346	17500728	17509463	R	No
	11	51686281	s	Nhp2	253044	51433237	51437216	F	No
			s	Rmnd5b	-237043	51437173	51449398	R	No
			s	N4bp3	-222097	51456565	51464344	R	No
			s	D930048N14Rik	221825	51464456	51471183	F	No
			s	0610009B22Rik	-184065	51498888	51502376	R	No
			s	Sec24a	-109305	51505765	51577136	R	No

Tumor	Chr	Location	Type	Gene	Distance	Start	End	OR	Hit
			s	SNORA48	-135017	51551281	51551424	R	No
			s	Sar1b	109092	51577189	51605427	F	No
			c	Phf15	-15286	51626957	51671155	R	Yes
			s	Gm16953	396575	51763384	52083016	R	No
			s	AL669920.1	-91603	51777884	51777991	F	No
			s	Cdkn2aipnl	-94882	51781163	51790836	F	No
			s	Ube2b	127823	51798999	51814264	R	No
			s	Gm12204	-128074	51814355	51815413	F	No
			s	Cdkl3	-131442	51817723	51903286	F	No
			s	Gm12205	166532	51852352	51852973	R	No
			s	Ppp2ca	-225902	51912183	51941280	F	No
			s	AL935177.1	226214	51912560	51912655	R	No
myr-TCL1A A5 OVA stim	15	96539134	s	Scafl1	-247925	96242129	96291274	R	No
			s	Slc38a1	-65855	96401849	96473344	R	No
			s	U6	36910	96502224	96502331	F	No
			c	Slc38a2	-9070	96517825	96530129	R	Yes
	X	103210461	s	Fgf16	250843	102959618	102970278	F	No
			s	Atrx	-85836	102992954	103124736	R	No
			s	U2	195239	103015222	103015404	F	No
			s	Gm14853	-170220	103039804	103040352	R	No
			s	U6	141298	103069163	103069274	F	No
			s	Magt1	-3327	103163423	103207245	R	No
			c	Cox7b	-578	103211039	103217789	F	Yes
			s	Atp7a	-12154	103222615	103320265	F	No
			s	Tlr13	-128082	103338543	103355832	F	No
			s	Gm14856	-161192	103371653	103372265	F	No
			s	Pgk1	-171978	103382439	103399038	F	No
			s	Taf9b	205925	103402222	103416497	R	No
			s	Fnd3c2	240143	103430585	103450715	R	No

Table 5-7: List of retroviral integration sites in T-cell tumors induced by myr-TCL1A in stimulated mice

Tumor: Tumor sample. Chr: Mapped chromosome. Location: Genome location. Type: Closest (c) and surrounding (s) genes. Distance: Distance between integration and gene start. Start: Gene start. End: Gene end. OR: Relative orientation of integrated vector (F: forward, R: reverse). Hit: Hit in gene.

Tumor	Chr	Location	Type	Gene Symbol	Distance	Start	End	OR	Hit
nls-	3	105733705	s	Ddx20	-243414	105481178	105490492	R	No
TCL1A			s	6530418L21Rik	226188	105507517	105523760	F	No
A1			s	Rap1a	-129658	105530185	105604248	R	No
w/o			s	Adora3	59929	105673776	105711846	F	No
stim			s	Adora3	59880	105673825	105726954	F	No
			c	I830077J02Rik	1676	105728809	105735582	R	Yes
			s	Atp5f1	29111	105745616	105763017	R	No
			s	Wdr77	-28582	105762287	105787518	F	No
			s	Ovgp1	-42924	105776629	105790341	F	No
			s	1700027A23Rik	83617	105799875	105817523	R	No
			s	Chi3l7	101907	105819837	105835813	R	No
			s	Gm4540	-103923	105837628	105837921	F	No
			s	Chia	-182442	105916147	105935038	F	No
			s	Chi3l3	288519	105950472	106022425	R	No
	1	87501588	s	Gm2666	-120162	87380827	87381717	R	No
			s	Gm16092	-78143	87407708	87423736	R	No
			s	Gm7592	78413	87423175	87465775	F	No
			s	Sp110	-6487	87473474	87495392	R	No
			s	Gm16094	5727	87495861	87496414	F	No
			c	Sp140	4635	87496953	87541612	F	Yes
			s	Gm10552	6592	87500660	87508471	R	Yes
			s	Gm17017	45281	87537797	87547160	R	No
			s	Sp100	-44975	87546563	87606573	F	No
			s	n-R5s215	-69869	87571457	87571560	F	No
			s	A630001G21Rik	173339	87613658	87675218	R	No
			s	AC161342.1	-158781	87660369	87660446	F	No
			s	AC161342.2	-179700	87681288	87681535	F	No
			s	Cab39	-188428	87690016	87748151	F	No
nls-	11	86287134	s	4632419I22Rik	272262	86014872	86117945	F	No
TCL1A			s	Ints2	-216233	86024183	86071077	R	No
A2			s	Med13	-116206	86080535	86171104	R	No
w/o			s	U3	156366	86130768	86130989	F	No
stim			s	Y_RNA	140426	86146708	86146810	F	No
			s	5S_rRNA	64806	86222328	86222447	F	No
			s	U6	-36393	86250812	86250917	R	No
			c	Rnft1	-11025	86298159	86312527	F	No
			s	Rps6kb1	70997	86312373	86358307	R	No
			s	Tubd1	-71359	86358493	86380862	F	No
			s	Vmp1	210028	86397367	86497338	R	No
			s	Mir21	110350	86397569	86397660	R	No
			s	Gm11478	157218	86443930	86444528	R	No
			s	Ptrh2	-210353	86497487	86505959	F	No
			s	Cltc	283757	86507853	86571067	R	No
	16	14082962	s	Ntan1	263618	13819344	13835544	F	No
			s	Pdxdc1	-179783	13833241	13903224	R	No
			s	Mpv17l	179708	13903254	13949712	F	No
			s	Gm15950	-161515	13919520	13921492	R	No
			s	5S_rRNA	-113457	13969441	13969550	R	No
			s	Ifitm7	-96059	13981795	13986948	R	No
			s	2900011O08Rik	96265	13986697	14101593	F	Yes
			s	Gm15806	-71198	14010855	14011809	R	No
			s	Gm15807	-44053	14037829	14038954	R	No
			c	Gm15808	15466	14067496	14068099	F	No
			s	4921513D23Rik	76360	14110626	14159367	R	No
			s	Mir484	-76757	14159719	14159785	F	No
			s	Nde1	-80406	14163368	14193021	F	No
			s	Myh11	208494	14194620	14291501	R	No
			s	0610037P05Rik	234461	14299337	14317468	R	No
			s	Gm15868	-228972	14311934	14314107	F	No
			s	Gm15869	234371	14316167	14317378	R	No
nls-	10	120926106	s	Tbc1d30	-178193	120700880	120748245	R	No
TCL1A			s	Gm4478	145778	120780328	120780714	F	No
A3			s	Gns	123960	120802146	120834301	F	No
w/o			c	Rassf3	-13132	120847406	120913306	R	No
stim			s	Tbk1	97412	120983511	121023850	R	No
			s	Xpot	136934	121024436	121063372	R	No
			s	AC124992.1	129161	121055524	121055599	R	No
			s	D930020B18Rik	-152538	121078644	121130940	F	No
nls-	14	26299776	s	Gm17716	-101942	26175287	26198121	R	No
TCL1A			c	D930049A15Rik	-19449	26275223	26280614	R	No
A4			s	Zmiz1	21105	26278671	26486229	F	Yes
w/o			s	Mir3075	-54149	26353925	26354009	F	No

Tumor	Chr	Location	Type	Gene	Distance	Start	End	OR	Hit
			s	Gm10397	-184743	26484519	26486217	F	No
			s	Ppif	-213864	26513640	26519954	F	No
			s	1700054O19Rik	226498	26525992	26526561	R	No
			s	Zcchc24	288279	26531126	26588342	R	No
nls-TCL1A A5 w/o stim	10	79494181	s	Fstl3	254164	79240017	79245375	F	No
			s	Prss57	-240822	79244219	79253706	R	No
			s	Palm	237864	79256317	79283641	F	No
			s	9130017N09Rik	210415	79283766	79293197	F	No
			s	E130317F20Rik	-176827	79314126	79317701	R	No
			s	Ptbp1	177009	79317172	79327516	F	No
			s	BC005764	-157149	79323220	79337379	R	No
			s	Gm17134	-167349	79326682	79327179	R	No
			s	Prtn3	156960	79337221	79345919	F	No
			s	Elane	145124	79349057	79350961	F	No
			s	Cfd	140583	79353598	79355401	F	No
			s	Med16	-122845	79357452	79371683	R	No
			s	U6	122241	79371940	79372046	F	No
			s	C030046I01Rik	-114777	79372798	79379751	R	No
			s	Kiss1r	114465	79379716	79385018	F	No
			s	Arid3a	104393	79389788	79417763	F	No
			s	Wdr18	71284	79422897	79431991	F	No
			s	Grin3b	60721	79433460	79439935	F	No
			s	ORF61	-47453	79437693	79447075	R	No
			s	U6	45930	79448251	79448357	F	No
			s	Cnn2	42852	79451329	79458807	F	No
			s	Abca7	34942	79459239	79478317	F	No
			s	Hmha1	14783	79479398	79494217	F	Yes
			c	Polr2e	8012	79498694	79502540	R	No
			s	Gpx4	-15730	79509911	79519184	F	No
			s	Sbno2	70915	79520161	79565443	R	No
			s	Stk11	-84367	79578548	79593427	F	No
			s	Dos	109052	79593196	79603580	R	No
			s	Atp5d	-107196	79601377	79608563	F	No
			s	Midn	-116836	79611017	79621113	F	No
			s	Cirbp	-134549	79628730	79635531	F	No
			s	1600002K03Rik	-141508	79635689	79637891	F	No
			s	Efna2	-148046	79642227	79652755	F	No
			s	Mum1	-194998	79689179	79706648	F	No
			s	Ndufs7	-217685	79711866	79719539	F	No
			s	Gamt	229229	79720896	79723757	R	No
			s	Dazap1	-230050	79724231	79751153	F	No
nls-TCL1A A6 w/o stim	15	97107287	s	Slc38a4	-221110	96825254	96886387	R	No
			s	Amigo2	-29779	97074505	97077718	R	No
			c	Fam113b	29749	97077538	97216120	F	Yes
	10	53759381	c	Man1a	35771	53624594	53795602	R	Yes
			s	Gm16998	-36347	53795728	53800887	F	No

Table 5-8: List of retroviral integration sites in T-cell tumors induced by nls-TCL1A in unstimulated mice

Tumor: Tumor sample. Chr: Mapped chromosome. Location: Genome location. Type: Closest (c) and surrounding (s) genes. Distance: Distance between integration and gene start. Start: Gene start. End: Gene end. OR: Relative orientation of integrated vector (F: forward, R: reverse). Hit: Hit in gene.

Tumor	Chr	Location	Type	Gene Symbol	Distance	Start	End	OR	Hit
nls-	5	123096660	s	Arpc3	254773	122841887	122856188	F	No
TCL1A			s	Anapc7	224958	122871702	122894921	F	No
A1			s	Gm15846	-208089	122888605	122888924	R	No
OVA			s	Atp2a2	-144830	122903531	122952183	R	No
stim			s	U6	139862	122956798	122956898	F	No
			s	Ift81	-32486	123000213	123064527	R	No
			c	P2rx7	2740	123093920	123141441	F	Yes
			s	Gm10064	50599	123147205	123147612	R	No
			s	P2rx4	-60933	123157593	123179747	F	No
			s	Camkk2	132378	123183213	123229391	R	No
			s	Anapc5	174335	123237478	123271348	R	No
			s	Rnf34	-203537	123300197	123318954	F	No
			s	Kdm2b	368076	123320677	123465089	R	No
	1	182947910	s	H3f3a	-204488	182730963	182744074	R	No
			s	Gm17275	215211	182732699	182739614	F	No
			s	Gm16067	204003	182743907	182746990	F	No
			s	U6	185010	182762900	182763007	F	No
			s	BC031781	166628	182781282	182798228	F	No
			s	Lefty2	124671	182823239	182829234	F	No
			s	Pycr2	113505	182834405	182838218	F	No
			s	Lefty1	82757	182865153	182868531	F	No
			s	Tmem63a	75435	182872475	182905243	F	No
			s	2210411M09Rik	-60282	182882195	182888280	R	No
			c	Ephx1	2473	182906286	182951035	R	Yes
			s	9130409I23Rik	-33458	182981368	182990798	F	No
			s	Nvl	125726	183023554	183074288	R	No
			s	Cnih4	-133152	183081062	183099125	F	No
			s	Wdr26	193547	183103359	183142109	R	No
			s	A430110L20Rik	-208297	183156207	183158621	F	No
			s	Rpl35a-ps2	223936	183172076	183172498	R	No
nls-	3	89193350	s	Pklr	253286	88940064	88950706	F	No
TCL1A			s	Hcn3	-229638	88949996	88964118	R	No
A2			s	Clk2	224633	88968717	88980843	F	No
OVA			s	Scamp3	211955	88981395	88986687	F	Yes
stim			s	Gm16069	-207541	88984677	88986215	R	No
			s	Fam189b	206285	88987065	88993217	F	No
			s	U6	-188561	89005089	89005195	R	No
			s	Gba	186500	89006850	89012603	F	No
			s	Mtx1	-162746	89013003	89031010	R	No
			s	Thbs3	174248	89019102	89030759	F	No
			s	Mir92b	-162636	89031038	89031120	R	No
			s	Muc1	160371	89032979	89037303	F	No
			s	Trim46	-143525	89038099	89050231	R	No
			s	Krtcap2	143462	89049888	89053644	F	No
			s	Dpm3	130070	89063280	89071001	F	No
			s	Slc50a1	-119264	89072168	89074492	R	No
			s	Efna1	-108692	89075655	89085064	R	No
			s	AC132327.1	86946	89106404	89106651	F	No
			s	Efna3	-66869	89117821	89126887	R	No
			s	Gm15998	73989	89119361	89122829	F	No
			s	Efna4	-51806	89137312	89141950	R	No
			s	4731419I09Rik	51578	89141772	89151753	F	No
			s	Adam15	-39824	89142464	89153932	R	No
			s	Dcst1	-24581	89154141	89169175	R	No
			s	Gm10702	35799	89157551	89158820	F	No
			s	Zbtb7b	4942	89181566	89198698	R	No
			c	Gm15417	-2422	89195772	89202701	F	No
			s	Lenep	12959	89204910	89206715	R	No
			s	Flad1	22036	89204926	89215792	R	No
			s	Cks1b	28549	89219394	89222305	R	No
			s	Shc1	-29015	89222365	89233937	F	No
			s	Pygo2	-40786	89234136	89239050	F	No
			s	Pbxip1	-47278	89240628	89254874	F	No
			s	Pmvk	-69690	89263040	89272935	F	No
			s	Kcnn3	-130736	89324086	89471683	F	Yes
nls-	11	60399450	s	Tom1l2	-233104	60040216	60166407	R	No
TCL1A			s	Gm12266	242703	60156747	60157708	F	No
A3			s	Lrrc48	232623	60166827	60207843	F	No
OVA			s	Atpaf2	-167552	60214128	60231959	R	No
stim			s	4933439F18Rik	168803	60230647	60264429	F	No
			s	Gm12268	139205	60260245	60260686	F	No
			s	Gm12267	-136039	60262712	60263472	R	No
			s	Drg2	131357	60268093	60282256	F	No

		s	Myo15	116609	60282841	60341871	F	No
		s	Alkbh5	49567	60349883	60372014	F	No
		s	Gm12622	-24704	60374426	60374807	R	No
		s	Gm12628	-13799	60385125	60385712	R	No
		s	Gm17423	12421	60387029	60446615	F	No
		s	Gm12623	-10460	60387069	60389051	R	No
		c	Gm12621	6093	60405223	60405604	R	Yes
		s	Gm12627	15299	60414429	60414810	R	No
		s	Gm12613	24508	60423638	60424019	R	No
		s	Gm12614	33718	60432848	60433229	R	No
		s	Gm12615	42954	60442084	60442465	R	No
		s	Gm12626	47020	60444549	60446531	R	No
		s	Gm12625	56233	60455363	60455744	R	No
		s	Gm12619	71848	60464572	60471359	R	No
		s	Gm12624	81056	60480186	60480567	R	No
		s	Gm12612	85116	60482425	60484627	R	No
		s	Gm12616	94079	60493209	60493590	R	No
		s	Gm12620	98155	60495681	60497666	R	No
		s	Gm12617	107066	60506197	60506577	R	No
		s	Llgl1	-113775	60513225	60527688	F	No
		s	Flii	141254	60527625	60540765	R	No
		s	Smcr7	-142450	60541900	60546453	F	No
		s	Mir5100	-142715	60542165	60542228	F	No
		s	U6	-149913	60549363	60549459	F	No
		s	Top3a	191356	60553560	60590867	R	No
		s	Smcr8	-191577	60591027	60601789	F	No
		s	Shmt1	225709	60601606	60625220	R	No
		s	SNORA25	-218630	60618080	60618205	F	No
		s	Gm12611	-230465	60629915	60631249	F	No
		s	Gm12618	233269	60632298	60632780	R	No
		s	Dhrs7b	-244683	60644133	60673697	F	No
2	98507281	s	Gm13806	66094	98441187	98441511	F	No
		s	Gm10801	4887	98502394	98504240	F	No
		c	Gm10800	15	98506704	98507458	R	Yes

Table 5-9: List of retroviral integration sites induced by nls-TCL1A in stimulated mice
Tumor: Tumor sample. Chr: Mapped chromosome. Location: Genome location. Type: Closest (c) and surrounding (s) genes. Distance: Distance between integration and gene start. Start: Gene start. End: Gene end. OR: Relative orientation of integrated vector (F: forward, R: reverse). Hit: Hit in gene.

Danksagung

Ich möchte mich an dieser Stelle ganz herzlich bei allen bedanken, die mich bei dieser Arbeit in jeglicher Art unterstützt haben.

Zunächst möchte ich mich bei Dr. Marco Herling bedanken, der mir die Bearbeitung dieser Arbeit ermöglicht hat. Auch möchte ich mich bei ihm für die Betreuung, Hilfestellung und engagierte Förderung bedanken. Für die nette Zusammenarbeit und Unterstützung danke ich auch der Arbeitsgruppe Herling, insbesondere Dr. Alexandra Schrader, Dr. Elena Vasyutina und Petra Mayer.

Prof. Dr. Jens Brüning danke ich für die Bereitschaft meine Doktorarbeit extern zu betreuen. Zudem möchte ich ihm und Dr. Hildegard Büning für hilfreiche Diskussionen während meiner Committee Meetings danken.

Ganz besonders möchte ich mich auch bei Dr. Sebastian Newrzela für die motivierende Betreuung bedanken und dafür, dass er stets ein offenes Ohr für mich hatte. Mein Dank geht auch an die Mitglieder der Arbeitsgruppe Newrzela: Dr. Benjamin Rengstl, Dr. Tim Heinrich, Dr. Frederike Schmid, Smaro Soworka, Robin Wistinghausen, Christian Weiser, Juliane Wannemacher, Anna Stemann und Dr. Ji-Hee Yi. Ich danke euch für die tolle Zusammenarbeit, das angenehme Arbeitsklima und eure enorme Hilfsbereitschaft!

Prof. Dr. Martin-Leo Hansmann danke ich dafür, dass er mir die Möglichkeit gegeben hat am Dr. Senckenbergischen Institut für Pathologie in Frankfurt meine Forschungsarbeit durchführen zu können. Ihm und Dr. Sylvia Hartmann danke ich auch für die Begutachtung histologischer Präparate.

A very special thanks goes to my husband Shaun. Thank you for your support, your patience, and always making me laugh!

Ein großes Dankeschön gebührt meiner Familie und Freunden, und vor allem meinen Eltern, die mir immer zur Seite standen. Besonders möchte ich mich auch bei meiner Schwester Anna bedanken, auf deren Hilfe ich mich immer verlassen konnte und die immer für mich da war.

Erklärung

Ich versichere, dass ich die von mir vorgelegte Dissertation selbständig angefertigt, die benutzten Quellen und Hilfsmittel vollständig angegeben und die Stellen der Arbeit − einschließlich Tabellen, Karten und Abbildungen −, die anderen Werken im Wortlaut oder dem Sinn nach entnommen sind, in jedem Einzelfall als Entlehnung kenntlich gemacht habe; dass diese Dissertation noch keiner anderen Fakultät oder Universität zur Prüfung vorgelegen hat; dass sie − abgesehen von unten angegebenen Teilpublikationen − noch nicht veröffentlicht worden ist sowie, dass ich eine solche Veröffentlichung vor Abschluss des Promotionsverfahrens nicht vornehmen werde. Die Bestimmungen der Promotionsordnung sind mir bekannt. Die von mir vorgelegte Dissertation ist von Prof. Dr. Jens Brüning und Dr. Marco Herling betreut worden.

....
Ort, Datum Kathrin Warner

Curriculum Vitae

Persönliche Daten

Name: Kathrin Warner
Geburtsdatum: 19.08.1985
Geburtsort: Düsseldorf
Familienstand: verheiratet
Staatsangehörigkeit: deutsch
Email: kathrin.warner@uk-koeln.de

Ausbildung

Seit 11.2015 — Wissenschaftlicher Mitarbeiter an der Uniklinik Frankfurt, verantwortlich für die Implementierung eines digitalen Pathologiesystems

07.2011-10.2015 — Promotion an der Uniklinik Köln in der Arbeitsgruppe von Dr. Marco Herling zum Thema „Proficiency and mechanisms of perturbation of mature T-cell homeostasis by the TCL1 family"

11.2009-01.2011 — Praktikum im Terry Fox Laboratory am BC Cancer Research Center in Vancouver (Kanada) zum Thema „Lymphoid progenitors in normal mouse lymph nodes"

01.2009-08.2009 — Praktikum in der Abteilung Tumorimmunologie an der Radboud Universität Nijmegen (Niederlande) zum Thema „ Knockdown of DC-STAMP to explore its function in dendritic cells"

09.2008-08.2010 — „Master of Science" Studium der medizinischen Biologie an der Radboud Universität Nijmegen (Niederlande)

04.2008-08.2008 — Praktikum in der Abteilung für Orthodontie und Orale Biologie an der Radboud Universität Nijmegen (Niederlande) zum Thema „Effects of high and low molecular weight hyaluronic acid on gel contraction"

09.2005-09.2008 — „Bachelor of Science" Studium der medizinischen Biologie an der Radboud Universität Nijmegen (Niederlande)

2000-2005   Städtisches Gymnasium Straelen, Straelen
                   Allgemeine Hochschulreife

1996-2000   Annette-von-Droste-Hülshoff Gymnasium, Düsseldorf

Publikationen

1.) **Warner K**, Weit N, Crispatzu G, Admirand J, Jones D, Herling M. T-cell receptor signaling in peripheral T-cell lymphoma – A review of patterns of alterations in a central growth regulatory pathway. **Curr Hematol Malig Rep** 2013; 8:163–172.

2.) **Warner K**, Crispatzu G, Al-Ghaili N, Weit N, Florou V, You MJ, Newrzela, Herling M. Models for mature T-cell lymphomas – A critical appraisal of experimental systems and their con-tribution to current T-cell tumorigenic concepts. **Crit Rev Oncol Hematol** 2013 Dec 21;88(3):680-95.

3.) Rengstl B, Newrzela S, Heinrich T, Weiser C, Schmid F, **Warner K**, Schroeder T, Küppers R, Rieger MA, Hansmann ML. Cell fusion leads to giant cells in Hodgkin´s Lymphoma. **Proc Natl Acad Sci U S A** 12/2013; 110(51).

4.) Heinrich T, Rengstl B, Muik A, Petkova M, Schmid F, Wistinghausen R, **Warner K**, Crispatzu G, Hansmann ML, Herling M, von Laer D, Newrzela S. Mature T-cell lymphomagenesis induced by retroviral insertional activation of janus kinase 1. **Mol Ther**. 2013 Jun;21(6):1160–8.

5.) **Warner K**, Luther C, Takei F. Lymphoid progenitors in normal mouse lymph nodes develop into NK cells and T cells in vitro and in vivo. **Exp. Hematol**. 2012;40(5):401–406.

6.) Luther C, **Warner K**, Takei F. Unique progenitors in mouse lymph node develop into CD127 + NK cells: Thymus-dependent and thymus-independent pathways. **Blood.** 2011;117(15):4012–4021.

7.) Sanecka A, Ansems M, Prosser AC, Danielski K, **Warner K**, den Brok MH, Jansen BJ, Eleveld-Trancikova D, Adema GJ. DC-STAMP knock-down deregulates cytokine production and T-cell stimulatory capacity of LPS-matured dendritic cells. **BMC Immunol**. 2011;12(1):57.